



Università degli Studi di Cagliari

PHD DEGREE

EARTH AND ENVIRONMENTAL SCIENCES AND TECHNOLOGIES

Cycle XXXII

**SELECTIVE SUSTAINABLE COBALT RECOVERING
METHODS FROM *HARDMETAL* PRODUCTION
BY-PRODUCTS**

Scientific Disciplinary Sectors

CHIM/03, CHIM/12, ICAR/03

PhD Student: AMADOU OUMAROU AMADOU

Coordinator of the PhD Programme Prof. GIORGIO GHIGLIERI

Supervisor Prof. ANGELA SERPE

Co-Supervisors Dr. GIANCARLO MARCHESELLI
Dr. AVTAR S. MATHARU

Final exam. Academic Year 2018 – 2019

Thesis defence: June - July 2020 Session

Abstract

The aim of the present work is to study new sustainable solvometallurgical routes for the selective Co-leaching from WC-Co-based "HardMetals" (HM) recovery powders, with the view to turn these hazardous by-products of the HM manufacturing process in valued secondary materials to be directly re-employed for industrial purposes.

An overview on HM, their peculiar properties as well as the criticalities related to their main constituents, W and Co, is provided in Chapter 1, besides the *green chemistry*-based approach this thesis would like to follow for pursuing the scope of a sustainable and profitable circular economy model in HM manufacturing, through the identification of *sustainable leaching systems* (PART I) and the *design of sustainable processes for industrial application* (PART II).

Bio-derived organic acids for hydrometallurgy are described in Chapter 2. They are classified on the bases of the oxidizing specie involved in leaching process (H^+ or O_2) and tested on Co-metal powder as well as on the HM test specimens. Several of them demonstrated high leaching efficiency and selectivity in Co-dissolution from WC-Co powders, preserving WC for following application. A selection of acids working in non-water solvents like alcohols were studied in Chapter 3, maleic acid ethanolic solutions showing to be the most interesting for solvometallurgy. Chapter 4 investigates *soft*- and *hard*-donor ligand-based solvometallurgy in the presence of iodine as external, recyclable and safe oxidizing agent. S-donor organic ligand/ I_2 systems demonstrated to be the most powerful with Co-leaching times significantly shorter than those found in acidic-solvometallurgy. Very promising was lactate/ I_2 system that coupled high effectiveness and sustainability being based on the use of a low cost, biodegradable and bio-derived ligand.

On the bases of the obtained results of PART I, PART II - Chapter 5 reports the scale-up of lactic, succinic and maleic acid-based leaching processes as well as the preliminary results on materials recovery for applicative HM production. Besides the confirmation of leaching efficiency and selectivity towards Co, the chapter points out the high quality of the recovered materials, prone to be used for industrial purposes. Supported by the successful experimentation, attempts of designing sustainable and profitable circular economy models in HM manufacturing, based on the use of dairy waste as source of lactic acid both for hydro- and solvo-metallurgical treatments, are proposed and discussed in Chapter 6 in the light of the idea that the greater the sustainability the greater the profitability of the model. The overall conclusions of the thesis are finally discussed in Chapter 7.

Acknowledgments

My first and most important thank you goes to Prof. Angela Serpe for her continuous and unrelenting guidance, encouragement, admirable dedication and support in this work. You have always encouraged me to be an independent researcher and for that, I will be forever grateful. It has been a privilege to be your student and to learn from you. I am also very thankful for having been allowed to work in this field which I enjoyed immensely.

I would like to thank Prof. Ing. Aldo Muntoni for always supporting me, supervising my progress and being there to answer my questions whenever I needed.

A special thanks go to Alberto Tedeschi (AD OMCD group) for the great opportunity he gave me to be part of F.I.L.M.S. family and my company supervisors Dr. Ing. Gian Pietro De Gaudenzi and Dr. Giancarlo Marcheselli for introducing me in the hard metals world and for their skilled continue advice, encouragement and support during my activity at F.I.L.M.S.

I would also like to acknowledge and appreciate the support, supervision and guidance I received from my second supervisor Dr. Avtar S. Matharu, whose advices were very important for my education and for this work, and the numerous opportunities he offered to me carrying out a part of this work at Green Chemistry Centre of Excellence (GCCE), Department of Chemistry, University of York (UK).

I extend my sincere gratitude to Prof. Giorgia De Gioannis for her valuable suggestions during the course of the work and for supervising the research on agroindustrial waste valorization. I am so grateful for the endless guidance and encouragement.

A grateful thank you to Dr. Stefano Cara, IGAG-CNR Cagliari, and Prof. Luciano Marchiò, Department of chemical sciences, life, and environmental sustainability, University of Parma, for the scientific collaboration on solid-state characterization of the samples and for their support and advice on powder and single-crystal X-ray diffraction measurements, respectively.

Many thanks go also to Dr. Martina Piredda and Ing. Daniela Spiga for their prompt and professional technical support in all the lab activities at DICAAR and their assistance with ICP-OES, CHN, GC, HPLC analysis.

For financial support, I would like to acknowledge the Italian Ministry of Instruction, University and Research - **DOTTORATI INNOVATIVI A CARATTERIZZAZIONE**

INDUSTRIALE - PON R&I 2014-2020, scholarship N. DOT1304527-3 and FILMS Corp. through the Framework Agreement and research contracts with UniCA on this project, as well as Placedoc Programme of the University of Cagliari that offered to me a financial support during my research stay at GCCE, University of York, UK.

I would like also to thank Dr. Ing. Stefano Milia and Ing. Matteo Erby for their advice and encouragement without forgetting the most fun part: "i punti".

I would also like to express my appreciation to the present and previous members of the "Laboratorio Chimico" (chemistry lab) of DICAAR for sharing the good moments and for all the dinner that we had together at the end of "Ramadan", one of the most important party for me.

I am extremely thankful to Prof. Tchakoute Kouamo Herve and Dr. Djobo Yankwa Jean-Noel for their constant motivation all along my thesis.

Many thanks go also to Sandra Tedeschi (Donna di Potere), Domenico (Moubarak), Ruggiero and Mattia (Fadil) Garabelli for their support and assistance during my stay in "Hi-Lab" at the company F.I.L.M.S. Corp.

My Ph.D. would have been a lot less fun if I did not make such good friends along the way: Andy Maneffa (Mane), Allyn Souleiman (halal boy), Jaspreet Kaur (UYork, UK); Laura Melis, Americo Rigoldi, Stefano Trudu, Martina Cera, Giulio Sogos, Carla Mercante, Davide Pintus, Fabiano Asunis, Marco Isipato, Anna Cozzolino and Giulia Puggioni (Unica, Italy). It was not always easy to support my hyperactivity and bad jokes! Anyway, I spent a great time during these 3 years and this is thanks to them.

Finally, I would like to express my profound gratitude to my parents, my brothers, and sisters for their moral and financial supports.

Table of contents

Abstract.....	3
Acknowledgements.....	4
Chapter 1. Hardmetals: features, criticality and circular economy.....	10
1.1 What are hardmetals?.....	11
1.2 Historical hardmetals evolution and production: from the beginning to date.....	11
1.3 Structure of hardmetals	16
<i>1.3.1 Carbide phase</i>	17
<i>1.3.2 Binder phase</i>	18
1.4 Mechanical properties of sintered hardmetals.....	18
1.5 Metals for HM manufacturing.....	19
<i>1.5.1 Tungsten</i>	19
<i>1.5.2 Cobalt</i>	21
<i>1.5.3 Criticality of HM and circular economy</i>	22
1.6 Recycling methods of hardmetals.....	23
<i>1.6.1 Pyrometallurgy or direct recycling</i>	24
<i>1.6.2 Chemical recycling</i>	27
<i>1.6.3 Melting Metallurgy</i>	29
1.7 Green Chemistry & Engineering.....	29
1.8 Aims and scope of the work.....	30
1.9 References.....	32
PART I: <u>Sustainable leaching systems</u>.....	38
Chapter 2. Bio-derived organic acids leaching agents for selective cobalt dissolution in water.....	39
2.1 Introduction.....	30
<i>2.1.1 Selected leaching agents for cobalt</i>	43

2.1.2 Test specimen definition.....	45
2.2 Results and Discussion.....	46
2.2.1 Leaching experiments on Co powder.....	46
2.2.2 Leaching experiments on recovery powders in water.....	51
2.3 Conclusion.....	57
2.4 Experimental.....	57
2.4.1 Synthesis of Co-complexes by acid leaching in aqueous solution.....	57
2.4.2 Characterization of cobalt complexes.....	57
2.4.3 Leaching experiments in attrition mode.....	59
2.5 References.....	59
Chapter 3. Non-water selective bio-derived organic acid lixivants for cobalt.....	63
3.1 Introduction.....	64
3.1.1 Selected leaching agents for cobalt in alcohol.....	65
3.1.2 Test specimen definition.....	66
3.2 Results and Discussion.....	66
3.2.1 Leaching experiments on Co powder in ethanol.....	66
3.2.2 Leaching experiments on Co powder with H ₂ Suc in methanol.....	68
3.2.3 Leaching experiments on recovery powders.....	68
3.2.4 Solid state characterization of the recovered WC powders after leaching.....	71
3.3 Conclusions.....	73
3.4 Experimental.....	73
3.4.1 Synthesis of Co-complexes by acid leaching in alcohol.....	73
3.4.2 Characterization of cobalt complexes.....	74
3.5 References.....	75
Chapter 4. Ligand-based leaching systems for solvometallurgy.....	77
4.1 Introduction.....	78

4.1.1 Test specimen definition.....	80
4.2 Results and discussion.....	80
4.2.1 Leaching experiments on cobalt powder by neutral ligands/I ₂ mixtures in organic solvents.....	80
4.2.2 Leaching experiments on recovery powders.....	81
4.2.3 Preliminary leaching experiments with HLat/I ₂ mixture in ethanol.....	83
4.3 Conclusion.....	84
4.4 Experimental.....	84
4.4.1 Leaching experiments on the Cobalt-powder with Tu/DTO/PhDTMA.....	84
4.5 References.....	85
PART II: <u>Designing sustainable processes for industrial application</u>.....	87
Chapter 5. Scale-up of acid-based leaching processes and materials recovery for HM production.....	88
5.1 Introduction.....	89
5.1.1 Definition of the test specimen.....	90
5.2 Results and discussion.....	90
5.2.1 Set-up of operative conditions: Liquid/Solid (L/S) ratio.....	90
5.2.2 Studying the oxygenation effect on Co leaching by aqueous HLat solutions.....	92
5.2.3 Scale-up of the solvometallurgy process.....	96
5.2.4 Scale-up of hydrometallurgy leaching process.....	98
5.2.5 Metallurgical quality control (MQC) and assessment of the WC-recovered powders.....	104
5.2.6 Cobalt recovery from the leaching solution.....	106
5.3 Conclusions.....	111
5.4 Experimental.....	112
5.4.1 Physical, mechanical and magnetic characterization.....	112
5.4.2 Electrowinning experiments.....	112

5.4.3 Thermal treatment on cobalt complexes.....	112
5.5 References.....	113
Chapter 6. Agroindustrial secondary sources of lactic acid for HM waste enhancement.....	114
6.1 Introduction.....	115
6.2 Results and discussion.....	116
6.2.1 Controlled dark fermentation processes for HLat-based hydrometallurgy.....	116
6.2.2 Hydrometallurgy with fermented cheese whey solutions.....	120
6.2.3 Circular economy model for bioderived HLat-based hydrometallurgy on HM wastes.....	120
6.2.4 Perspectives in the use of bioderived lactate salt/I ₂ solvometallurgy.....	122
6.2.5 Comparing the leaching systems in terms of green chemistry.....	125
6.3 Conclusions.....	127
6.4 References.....	128
Chapter 7. Conclusions and perspectives.....	129
7.1 Overall conclusions.....	130
7.2 Work in progress and perspectives.....	132
Appendix A1 Metallurgical Quality Control (MQC).....	135
Appendix A2 Hard-Soft acid-base theory.....	142
Appendix A3 Materials and methods.....	143
Appendix A4 Thermogravimetric Analysis of Co-complexes.....	145
Appendix A5 Single-crystal X-Ray diffraction characterization of [Co(It)(H₂O)₂]₃.....	147
Appendix A6 ICP-OES characterization of the leachates.....	153
Appendix A7 Starbon® materials.....	154
Appendix A8 Dairy waste dark fermentation procedures.....	164

Chapter 1

Hardmetals: features, criticality and circular economy

1.1 What are hardmetals?

Cemented carbides (CC), also referred to as hardmetals (HM), are liquid-phase sintered composite materials consisting of at least one hard and wear-resistant phase (WC in the majority of cases) embedded in a soft and ductile metallic one, based on one or more elements from the iron group, i.e. Co, Ni, and Fe, with Co and its alloys the most widely used, acting as a matrix binder.[1][2][3] Thanks to their composite nature, HM exhibit excellent combination of wear resistance and toughness, making them the natural choice for metal forming, cutting tools and wear parts since decades ago.[4][1][3] On the other hand, HM are mostly known as refractory composites with excellent performances in various wear conditions, especially under severe contact conditions. Moreover, HM are a very flexible group of materials: by simple changing in the chemical composition or particle size, the values of different properties can be altered multiple times and, also, as strikingly as brass and high-speed steel.[5] HM were first produced in Germany during the '20s of the past century and from that moment on, the WC–Co HM performance enhancement was continuous and some of the field of its application rapidly expanded.[1] The world HM production in 1993 was around 20,000 tons and increased from 30,000 tons in 2000 to almost 60,000 tons in 2008, with an estimated turnover worth to be more than 10 billion euros, particularly due to the entry of China on to the market. Since 2000 to date the cemented carbide production in China raised from 7000 tons in 2001 to 20,000 tons in 2011, up to 28,000 in 2017.[5][4]

1.2 Historical HM evolution and production: from the beginning to date

The history of cemented carbides dates back to the end of the 19th century and has been well described in review papers by H. Kolaska and H. Moissan. Ortner *et al.*[1b][2] The first W_2C was produced in 1896 using an electric furnace by H. Moissan, who was followed by his colleague P. Williams two years later, by synthesizing WC.[6][7] However, the material was considered too brittle, so no practical application were developed.[8] Gradually, the material was improved by introducing a hot pressing for compaction of the carbides. The first sintered tungsten carbide was produced in 1914 (see Fig 1.1) for use in drawing dies and rock drills. [5] But, it was not until 1922 that the first HM were invented by a group of researchers from Osram Company, F. Skaupy, H. Baumhauer and K. Schröter, by infiltrating the carbides with metals like Fe, Ni, and Co.[9][3]

In 1923 Schröter successfully sintered for the first time HM based on the WC–Co system [10][1] which resulted in a famous patent.[18b] Three years later, Krupp acquired the patent

and brought sintered carbides onto the market under the name of “WIDIA” (an acronym for “wie Diamant”, which means “like a diamond” in German [6]). Thus, in a short time afterward, cemented carbides started to replace high-speed steels in cutting tools due to their superior hot hardness and improved wear resistance.[6][4] The most outstanding advances of the HM industry are reflected in **Table 1.1** according to J. M. Tarago . [11]

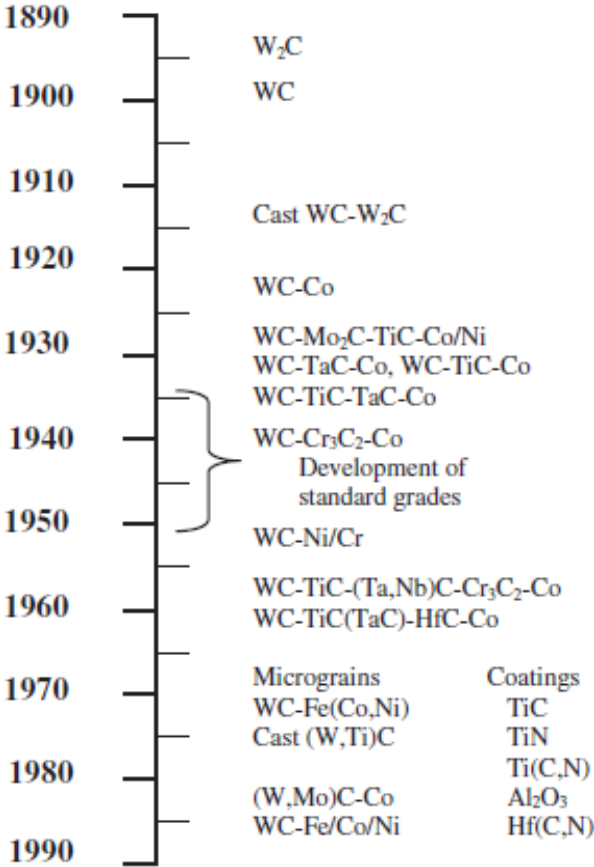


Figure 1.1: Historical development of the cemented carbides for cutting tools from 1890 to 1990 according to C. M. Fernandes and A. M. R. Senos.[6]

Nowadays, HM consist of hard refractory carbides, nitrides or carbonitrides of the transition metals (groups 4, 5 and 6 of the transition metals in the periodic table) embedded in a ductile metal binder matrix. The main phases present in cemented carbides are the hexagonal WC phase (the so called α -phase), the mixed cubic carbide/carbonitride phase (also called γ -phase or fcc-phase) and the Co-base binder phase (β -phase), which can also be Ni-based or a combination of Fe-Co-Ni metals. The carbide phases have exceptional hardness, high melting point, metallic luster, characteristic colors and simple crystal structures.[6]

Table 1.1: Principal developments in the cemented carbide industry from the invention of the first WC–Co tool.

1923-1925	The invention of the first WC–Co tool
1929-1931	Development of WC–TiC–Co and WC–TaC (VC,NbC) –Co grades
1938	WC–Cr ₃ C ₂ –Co
1948-1970	Manufacturing of submicron WC–Co HM
1965-1975	Hot Isostatic Pressing (HIP)
1965-1978	Application of CVD coatings on hard metals tools like TiC, TiN, and Al ₂ O ₃
1969-1971	Thermochemical surface hardening
1970-1990	Powders recycled by the zinc process
1974-1977	Polycrystalline diamond on WC–based HM
1981	Many thin coatings with ALON layers
1981-2015	Functionally graded cemented carbides
1983-1992	HIP sintering
1985	“CALPHAD” for phase diagram modifications
1990-2010	Fine-grained cemented carbides
1992-1995	Plasma CVD diamond coating
1993-1995	Coatings with complex carbonitride
1994	Nanocrystalline cemented carbides
2012-	Cemented carbides by additive manufacturing

High purity powders in the sub-micron and micron range size are needed, either for WC powders, metallic binder and additive carbides (TiC, TaC, NbC, ZrC, Cr₃C₂, VC). All manufacturing processes are linked, meaning that any change in any manufacturing step in the production chain will influence the subsequent process and the quality of the final product. Consequently, in the design of cemented carbide microstructures, all production steps must be taken into consideration.[6]

In the composition of WC-Co grades (the so-called HM “base system”), metallic binder can vary between 0 and 30 wt. % content: the higher the metallic binder content, the higher the toughness value. The other relevant variable in grade designing is the WC grain size, both the original powder grain size and that obtained in the microstructure after sintering. At a certain metal binder (MB) content, the lowest the WC grain size, the highest the hardness. These two

parameters allow producing HM with a wide range of mechanical properties, mainly in terms of hardness and toughness.

The manufacturing of cemented carbide tools is a complex powder metallurgical process involving many steps, such as raw powder production, mixing and milling of powders, spray drying to produce granulated ready to press powders, pressing, extruding or molding to final shape, dewaxing and pre-sintering, liquid phase sintering (i.e. vacuum sintering, sinter-HIP, gradient sintering), post-sintering treatment (i.e. grinding) and finishing operations (i.e. blasting).

The HM manufacturing process is schematized in **Fig 1.2**. The production process is divided into three main phases according to:[12][13]

- 1st step: production of tungsten carbide and/or tungsten and cobalt powders;
- 2nd step: powders mixing, drying, pressing and pre-sintering, shaping of the pre-sintered HM, and, finally, sintering of the shaped tools.
- 3rd step: finishing of the sintered products, sharpening and maintenance of cutting tools.

The powder mixing is performed in a liquid mean, usually acetone or alcohol, but more recently even water can be used. During mixing, an organic binder, usually a wax, is added for playing the role of a pressing facilitator. De-waxing and pre-sintering of pressed parts are usually performed between 500°C and 800°C. Pre-sintered parts can undergo further shaping by machining. During this phase often large amounts of waste powders are generated. The shaped products are sintered at high temperature (from 1350°C to 1550°C) under vacuum or under an inert gas (Ar) (sinter-HIPing). The last process allows to remove all the voids and porosities. The sintering mechanism is described in **Fig 1.3**. The final product can probably be coated with other materials such as titanium carbide (TiC) and/or titanium carbonitride (TiCN), alumina (Al₂O₃) and/or aluminides (e.g., TiAlN), using usually Chemical Vapor Deposition (CVD) technology.[12]

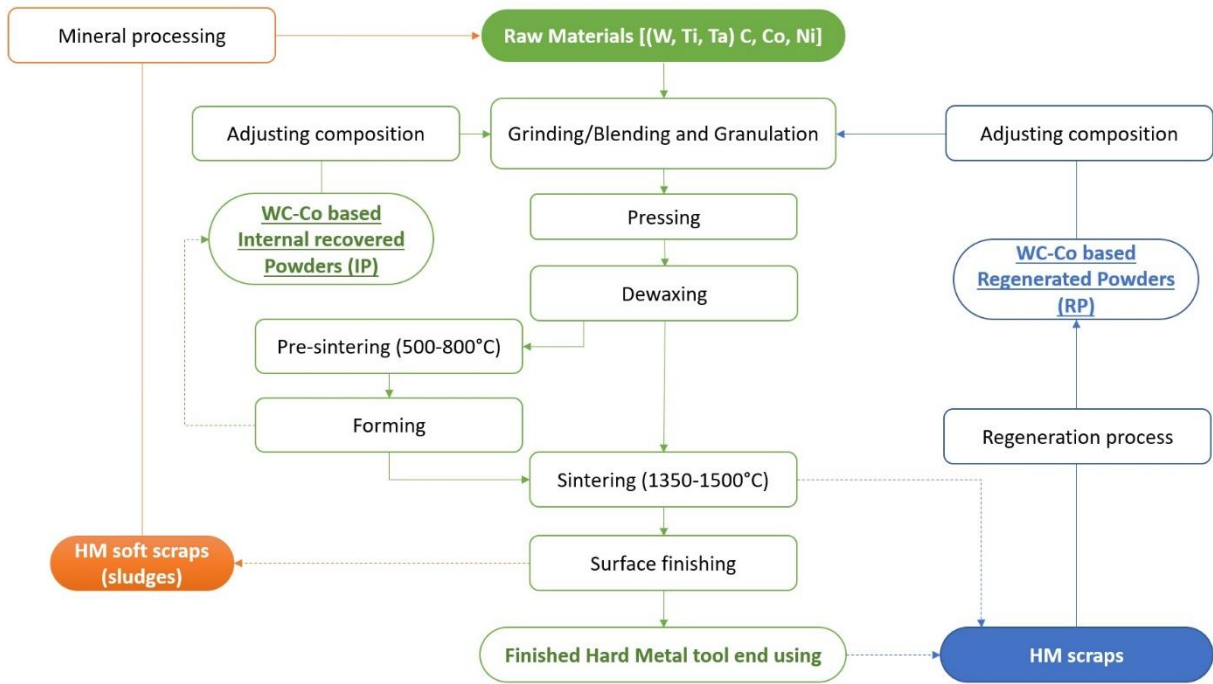


Figure 1.2: Flow sheet for HM production process and internal powders recovery (green line), external waste regeneration (blue line) and recovery (orange line).

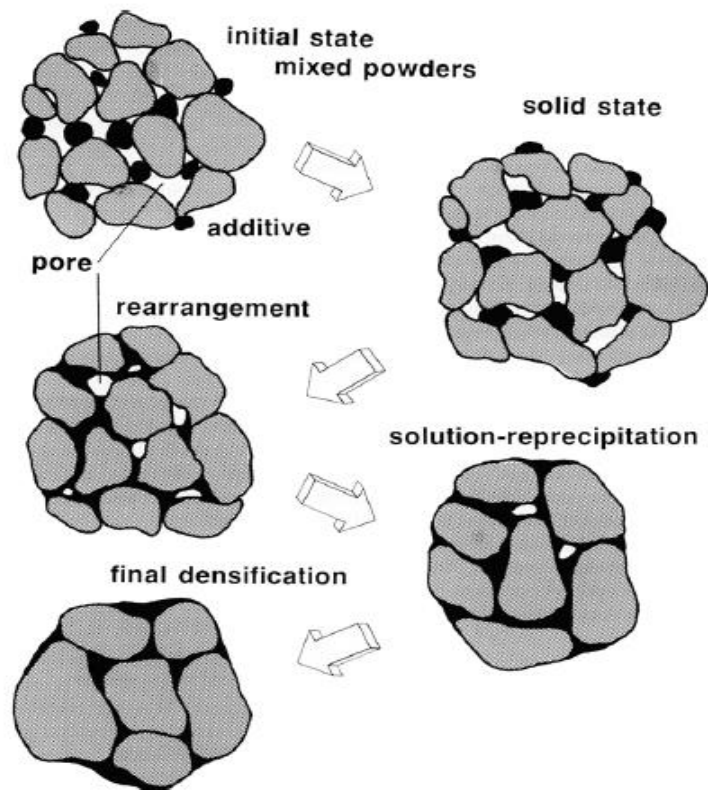


Figure 1.3: Solid state HM sintering process.

1.3 Structure of HM

Tungsten carbide-cobalt (i.e. WC–Co) is by far the most common HM system. WC–Co is considered as a pseudo-binary section in a three-component system W, C, and Co. Nevertheless, if during the manufacturing process the carbon balance is not properly controlled, additional and undesirable phases appear in the structure.[14][4] When being at low carbon contents, a sub-stoichiometric carbide phase called η -phase (M_6C or $M_{12}C$) can form.[6] The η -phase can be found also in sintered materials obtained by WC-Co powders where oxidative phenomena occurred on the material surface (consequently bearing high O% in the mixture). Indeed, the co-presence of C and O into WC-based powders obtain gaseous CO_2 formation during sintering processes, leaving the sintered material poor in C. This phase tends to decrease the toughness of cemented carbides, especially if it precipitates as large dendrites. On the contrary, high C contents result in the presence of graphite, as it can be seen in the vertical section of the W–C–Co phase diagram calculated for a WC–(10 wt.%)Co cemented carbide (**Fig 1.4**).[11][4][15][16][9] Having graphite negligible mechanical properties, graphite formations can be considered porosities that lower the mechanical properties of the material.

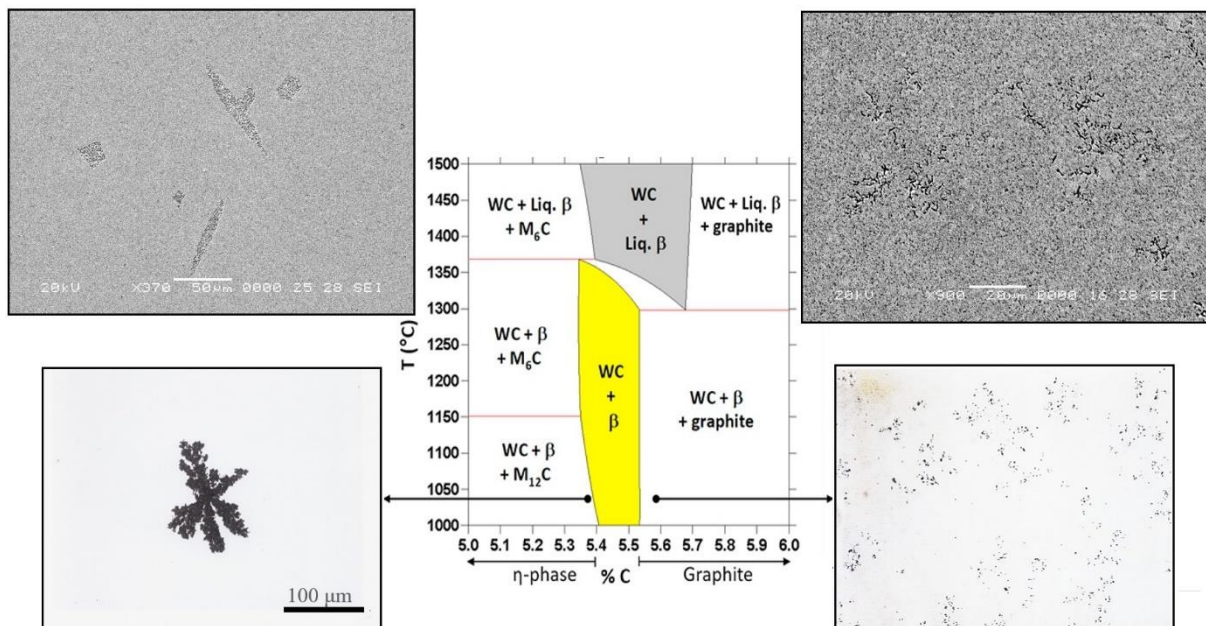


Figure 1.4: Phase diagram of the W-C-Co system showing η -phase (left), graphite (right) formation and possible phases (in the center) on a WC-(10%) Co cemented carbide.

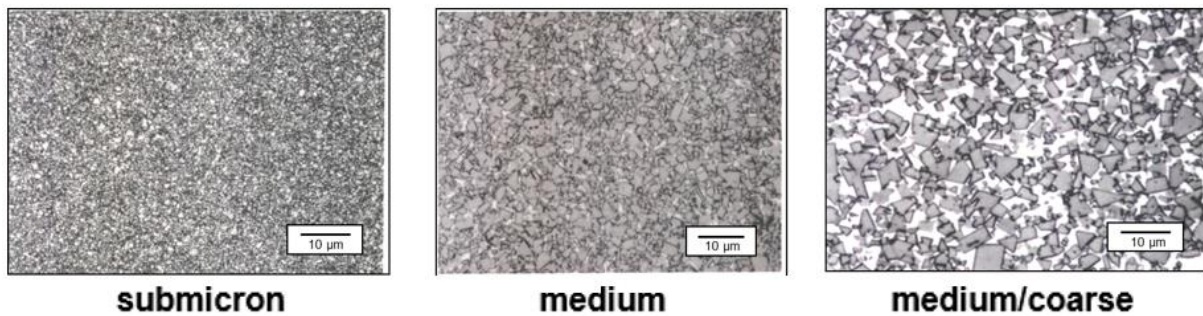
The interplay between the binder and the carbide phases determines the final microstructure. Many authors report on several different quantities related to cemented carbide microstructures, e.g., WC grain size, carbide contiguity, the volume fraction of binder and binder mean free

path. However, these variables are inter-related and most often it is sufficient to give only two of them, e.g., WC grain size and Co content, for a full description of the microstructure.

In the WC-Co based cemented carbides, the WC phase can be recognized as prismatic grains in the microstructure. The excellent wetting of Co on WC, which affects the sinterability of the final product, is the most important factor for the properties of the WC-Co system (**Fig. 1.5**).

Figure 1.5: WC-Co microstructures for different WC grain sizes. Classification according to J. Garcia et al.[6]

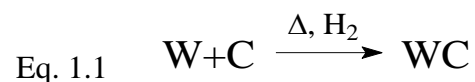
Grain size (μm)	Denomination
<0.2	nano
0.2÷0.5	ultrafine
0.5÷0.8	submicron
0.8÷1.3	fine
1.3÷2.5	medium
2.5÷6.0	coarse
>6.0	extra-coarse



1.3.1 Carbide phase

Typically, the tungsten carbide phase represents between 65 and 97% in volume of the composite material. Tungsten carbide powders are obtained by reacting tungsten (W) powders with carbon black (C) in a hydrogen atmosphere at temperatures 1400-1800°C.[17] Before carburization, the mixing of the tungsten and carbon powders is done to attain homogeneous distribution.[3] The *used* carbon is usually obtained from high purity pressed carbon lampblack, with low ash and sulfur contents.

The below equation (1.1) expresses the carburization process:



The carbon amount added to tungsten is calculated taking into account a 1:1 atomic ratio and it will respect the following C% composition (Eq. 1.2):

$$\text{Eq. 1.2} \quad \frac{\text{C}}{\text{W} + \text{C}} \times 100$$

where the W atomic weight is 184 amu and the C is 12 amu. To obtain a complete carburization, an extra amount of carbon is also added, that accounts for process losses as methane formation.

1.3.2 Binder phase

Even though it is possible to use Ni and, for low performance applications, Fe as a binder in cemented carbides, Co is the most used element, despite its relatively high price. There are several reasons behind this preferential choice. Firstly, the especially favorable chemical bonding between the WC–Co couple that leads to a very low interfacial energy, nearly perfect wetting and a very good adhesion.[18] That results in products with an outstanding compromise between hardness and toughness.[19][15] Secondly, cobalt forms an eutectic with WC at 1275-1350 °C (compared to a melting point of 1493 °C). At this temperature it can dissolve around the 22% of WC. During cooling, the tungsten carbide will precipitate according to a Ostwald ripening mechanism: to avoid re-crystallization phenomena, that can reduce mechanical properties, inhibitors elements are usually added, as Cr and V.[20] On the other hand, the binding agent must be able to be ground very finely to mix the carbide particles, as cobalt does as it can be ground to sub micrometric dimensions. Thirdly, the ferromagnetic properties of cobalt allow non-destructive quality control through the assessment of their magnetic properties, i.e. coercitivity and magnetic saturation.[21] However, Co becomes liquid during the sintering and large amounts of W, C and other elements used in the production are easily dissolved.

1.4. Mechanical properties of sintered hardmetals

Each step during powder metallurgy of cemented carbides has a significant effect on the mechanical properties of the final product. Thus, mechanical properties measurements, assessed by metallurgical quality control (MQC) procedures, are crucial for the cemented carbide manufacturing process. Those procedures usually include the assessment of:

- ***Transverse rupture strength (TRS)*** – combination of shear strength, compressive strength, and tensile strength, is used as a general measure of the strength of WC-cemented carbides;[22]
- ***Vickers and Rockwell hardness*** - resistance to plastic deformation indexes, are related to the nature of the composition and microstructure of the WC-cemented carbide since it varies with the amount and distribution of the binder, WC grain size and degree of porosity;[3][23]
- ***Density*** - determined by Archimedes' principle;

- **Magnetic properties: Coercivity (H_c) and magnetic saturation (M_s)** - measurements of the binder phase's ferromagnetic properties give information about the effectiveness of the sintering process and some information about the microstructure.[3]

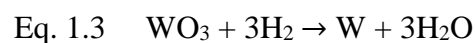
Conventional protocols and operative conditions for HM materials are defined in refs. [15][24][25] according to the specific ISO regulations, and detailed in Appendix A1.

1.5 Metals for HM manufacturing

Cobalt and tungsten, which are the main components of HM manufacturing, have strategic importance for their producers.

1.5.1 Tungsten

Tungsten is a refractory transition metal (melting point: $3423 \pm 15^\circ\text{C}$) with atomic number 74.[26][27] It is found in numerous minerals, including wolframite, scheelite, ferberite and huebnerite.[26] Ammonium paratungstate (APT, $5(\text{NH}_4)_2\text{O} \cdot 12\text{WO}_3 \cdot 5\text{H}_2\text{O}$) is a typical intermediate product of tungsten metal extraction processes. In its raw form, tungsten is a hard steel-grey metal that is often brittle and hard to work which resists attack by oxygen, acids, and alkalis.[28] The most common formal oxidation state of tungsten is +6, but it exhibits all oxidation states from -2 to +6. Tungsten typically combines with oxygen to form the lightly yellow tungstic oxide, WO_3 , which dissolves in aqueous alkaline solutions to form tungstate ions, WO_4^{2-} . WO_3 can be reduced under hydrogen to obtain W metal as shown in Equation 1.3.



Besides, WC represents one of the two tungsten carbides, the second one being W_2C (tungsten semicarbide). It is resistant to acids, except for heated HF/ HNO_3 mixtures.[29] Finely powdered WC, oxidizes readily in hydrogen peroxide aqueous solutions.[30]

About the 80% of the mine production of tungsten is made in China, the country that nowadays have a strong control of tungsten market around the world. The global flow of tungsten in 2016 is given by the ITIA (International Tungsten Industry Association) in **Fig. 1.6**.[31]

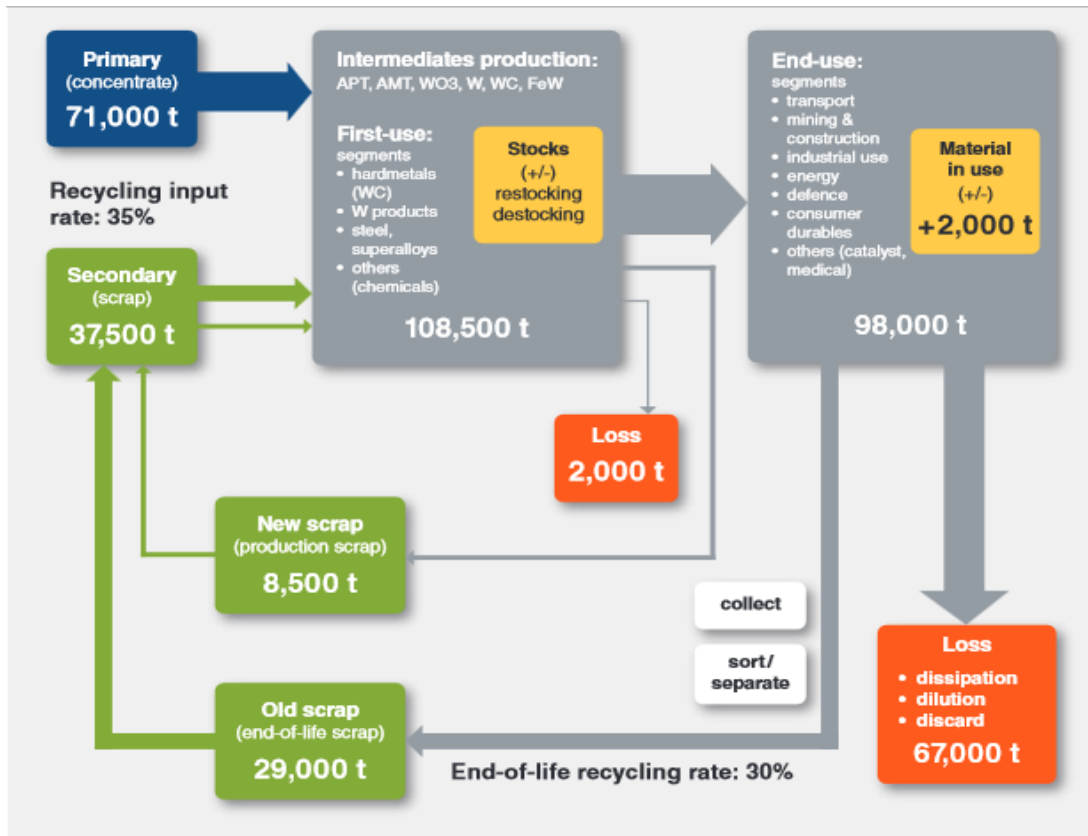


Figure 1.6: Global flow of tungsten in 2016 according to ITIA (international Tungsten Industry Association).[31]

Fig 1.7 reports the primary uses of W. As shown, the use for HM represents the greatest demand by application (>60%) of W, reaching 70,500 tons in 2016. In the same year, the total input of tungsten in the industry manufacturing (first use) was 108,500 tons, 71,000 tons of which from raw materials (primary or concentrated) and 37,500 tons from secondary materials (scraps) deriving from end-of-life (29,000 tons) and production (8,500 tons) scraps (see **Fig. 1.6**).[31]

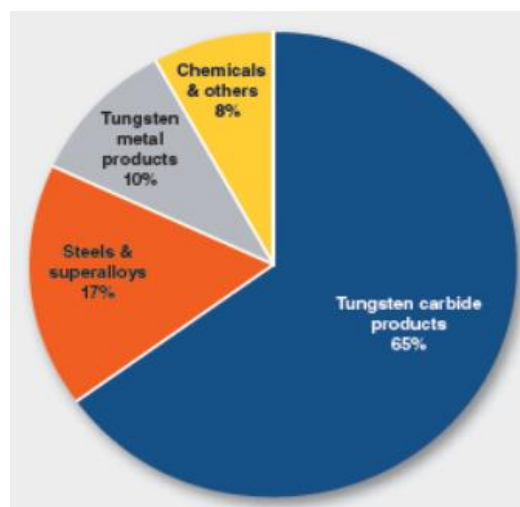
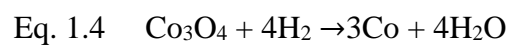


Figure 1.7: Tungsten demand by application in 2016.

1.5.2 Cobalt

The cobalt element belongs to the group 9 of the periodic table, period 4 and block d with atomic number 27 and atomic mass about 58.933 and $[Ar]3d^74s^2$ electron configuration. Cobalt is mostly mined as a byproduct of either copper or nickel. It is also the major metallic component of sulphides, arsenides, oxides and hydroxides minerals. It exists in two allotropic forms, the hcp form which is stable at temperatures below 418°C and the fcc form which is stable up to a temperature of 1495°C, melting point of pure cobalt. Initially, cobalt was produced through the reduction of cobalt oxide under hydrogen at 600-700°C, as shown in Equation 1.4.



The main cobalt mines are located in areas with severe geopolitical risks (Democratic Republic of the Congo holds over the 60% of the global Co supply) which can result in significant material disruption to cobalt output.[32] It should be noted however, that other than HM production, cobalt is also used in numerous important applicative fields such as catalysis [33][34] and batteries.[35][36][37][38] These different applications make it a critical metal of strategic importance.[39] For example, the worldwide demand in cobalt in 2016 was 93,950, but it is estimated that in 2020 it will exceed 120,000 tons, as can be seen in **Fig 1.8** (Darton Commodities, 2016).[40]

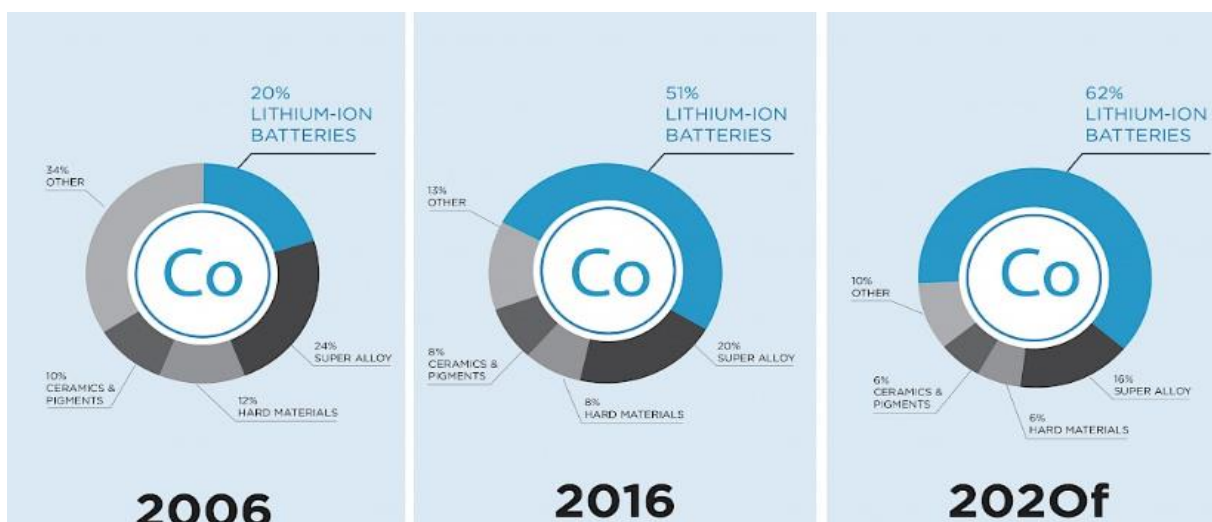


Figure 1.8: Cobalt demand evolution in 2016 according to Darton Commodities, 2016 with 2020f = forecast.[40]

1.5.3 Criticality of HM and circular economy

Current developments in the field of HM are mainly related to the high and volatile prices of W and Co due to the difficult access to raw materials. Due to their high economic relevance combined with the high risks related to the supply chain, in 2010 Co and W were included in the list of the 14 elements firstly identified as critical raw materials by European Community. [41][42][43]

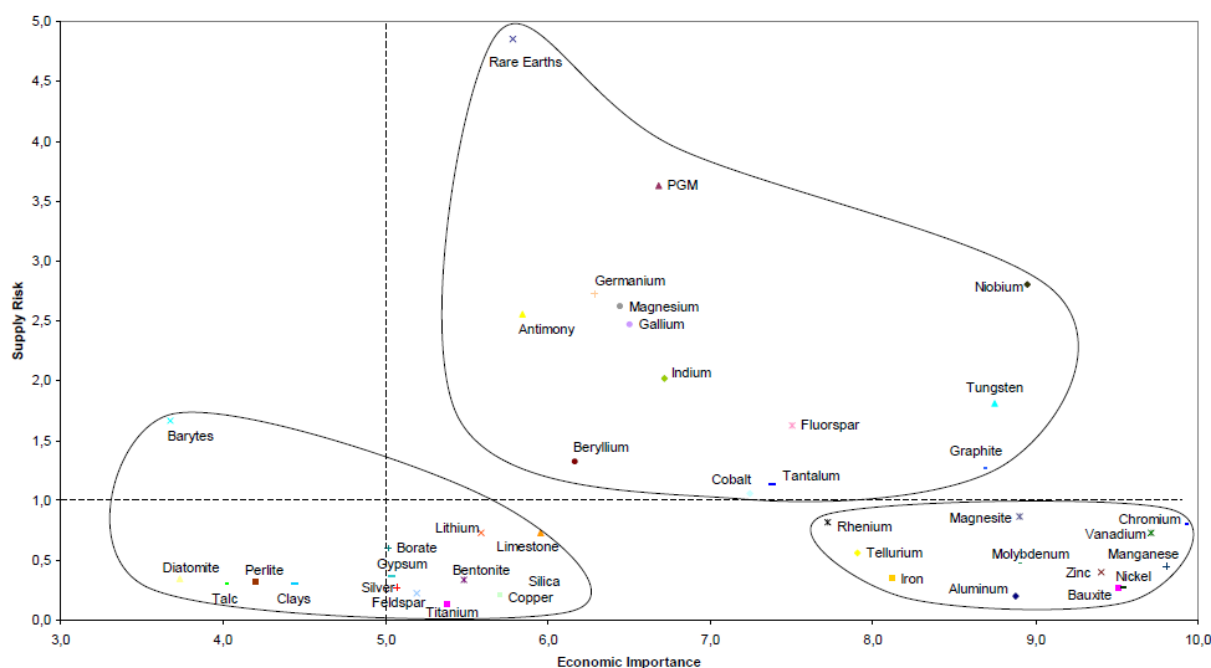


Figure 1.9: Selection of 14 EU critical raw materials as reported in refs [40][41][42].

The demand for Co and W in the production of HM and in the other important industrial fields are increasingly affecting their global criticality and their price.[44][45] Besides that, since 2011, the European program for Registration, Evaluation, Authorization, and Restriction of Chemical substances (REACH)[46] and the U.S. National Toxicology Program (NTP)[13] classified cobalt powder with particle size $<4 \mu\text{m}$ as a inhalable, toxic and carcinogenic material. For all these reasons, the use of secondary sources seems to be a more sustainable and forward-looking approach, both in terms of financial and environmental costs, in line with a circular economy model strongly encouraged by the European Directives on waste management and safeguarding of natural resources (implemented by the Waste Framework Directive),[47] where wastes are considered the new pool of secondary raw materials for production. Therefore, significant efforts are devoted to minimizing the use and/or replacing raw materials, improving the performance and enhancing the lifetime of cemented carbide tools and components, increasing the efficiency of the recycling processes. Obviously, in the case of a HM life cycle,

the circular economy concept can also be applied: *internal recovered powders (IP)* from the production process and *regenerated powders (RP)* from hard and soft scraps represent the main secondary raw materials for the production process as it is shown in **Fig 1.10**. By the way, recycling allows further savings by reducing the costs associated with waste disposal.

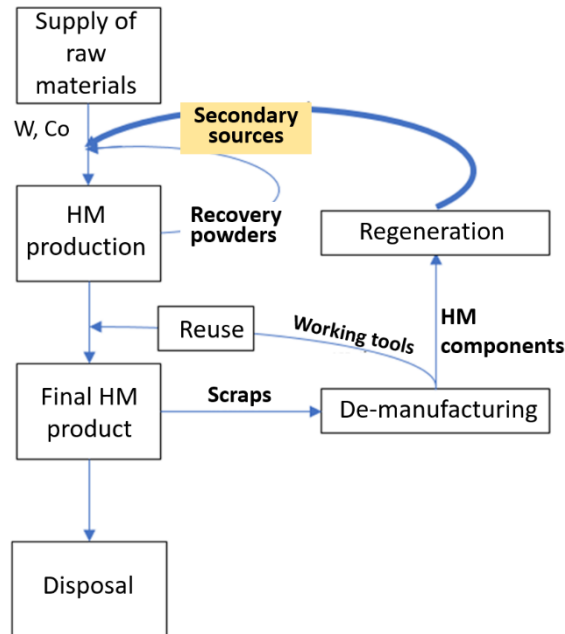


Figure 1.10: Flow sheet of circular economy applicable to HM.

Although recycling is partially applied by some of W producers and HM manufacturer, the most critical issue that limits the expansion of this practice is related to the high costs, environmental impact and, in some cases, low versatility of the recovered materials which characterize the standard recovering processes. Consequently, HM industries are seeking actively for economically and environmentally sustainable recovery methods to increase the percentage of waste sent for recycling.

1.6 Recycling methods of HM

In the HM manufacturing, recycling of tungsten is a key factor in the supply and demand of tungsten raw materials. According to A. Shemi *et al.*[48] secondary tungsten resources contribute about 34% to tungsten demand, 10% of which is from scraps generated as processing waste and about 24% from used or worn-out tungsten carbide parts from industry. This is in agreement with surveys and forecasts, which show that scraps will continue to be an increasingly important source of raw material for the tungsten industry worldwide for the foreseeable future.[49][50] In addition to this, environmental controls and resource preservation policies have led to renewed interest in the development of recycling techniques of HM which

can be economically viable and sustainable from the environmental point of view. Nowadays, pyrometallurgy and hydrometallurgy constitute the main methods in extractive metallurgy as can be seen in **Fig 1.11**. [51][52]

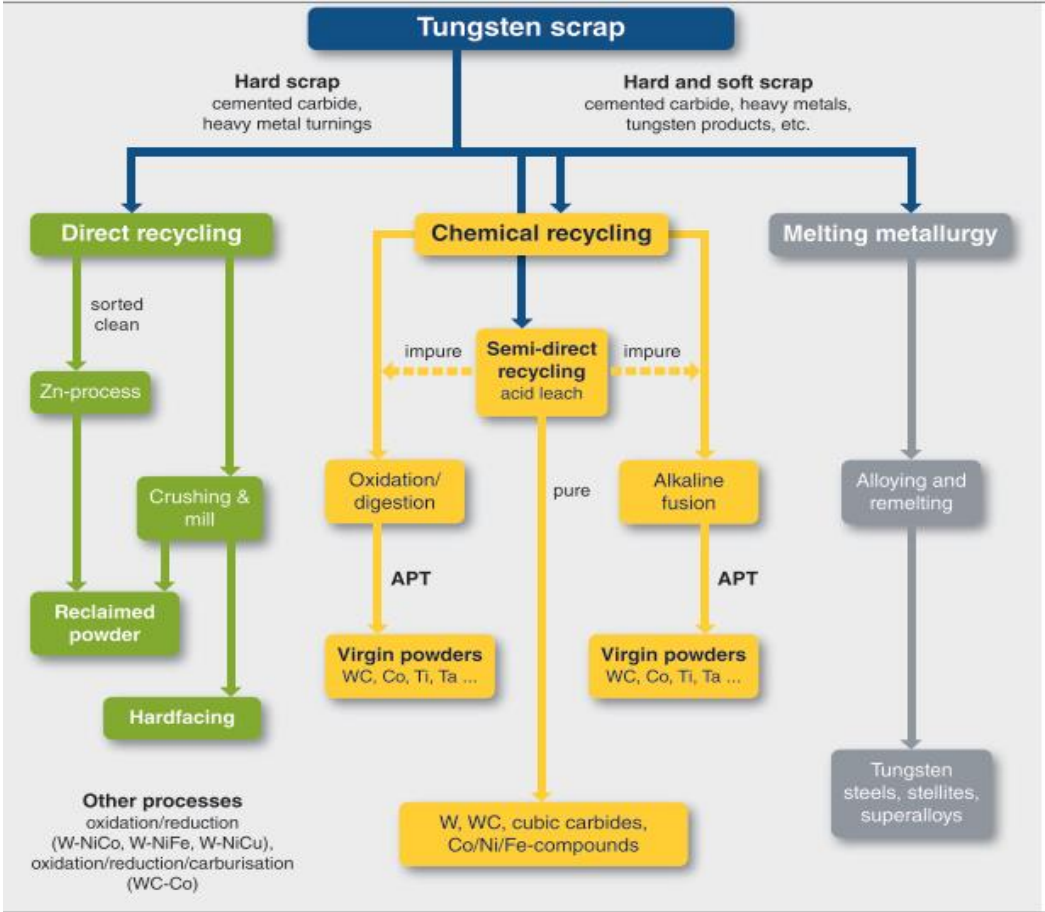


Figure 1.11: Recycling technologies for secondary tungsten according to ITIA 2019.[52]

Recycling is an important contribution to a sustainable economy. Tungsten recycling has a long history, with the first industrially used recovery technology dating back to the 1940s. Since the early days of tungsten’s industrial use, it was common practice to handle this relatively rare and expensive commodity with great care, trying to use it efficiently and not to spoil materials which could be reprocessed. However, a variety of tungsten recycling technologies were developed in the past, which today are globally used for industrial recycling. As shown in **Figure 1.11**, they can be divided into three main groups: direct recycling, chemical recycling (also called indirect recycling, including the variety of semi-direct recycling) and melting metallurgy.

Nowadays, the main HM recycler are the tungsten carbide powder producers (e.g. Wolfram BH, GTP and H.C. Starck) and the HM producers (e.g. Kennametal and Ceratizit). The former

typically use chemical recycling, the latter mainly the direct recycling approach (primarily the Zn-process), as described below.

1.6.1 Pyrometallurgy or direct recycling

Direct recycling can be defined as a process that turns a supplied waste material to a powder of the same composition by either chemical or physical treatment, or a combination of both. On the other hand, pyrometallurgy can be defined as a metallurgical process that is based on the use of heat for the treatment, including smelting and roasting.[52] It usually involves heating in a blast furnace at temperatures above 1500°C to convert waste into a form that can be refined.[53] By the way, a considerable amount of work is reported using different pyrometallurgical techniques for the direct reuse of cemented carbides, such as the zinc-melt technique, the cold stream method for reclamation of scraps, the oxidation and reduction process and the menstruum process.[48][51][54]

➤ **The zinc-melt process**

The zinc recycling process has experienced renewed interest since 2005 when tungsten prices underwent a sudden increase. The first patent on the zinc-melt process was awarded in 1946 to Trent.[52b] Later, in 1971, it was modified by Bernard *et al.*[54] The zinc process is the most widely used direct recycling process in the cemented carbide manufacturing industry. In this process, the HM scrap is first cleaned and sorted, then contacted with molten zinc at 900–1050°C in an inert atmosphere of helium/nitrogen/argon, ensuring that all pieces are completely penetrated. In the second stage, the vacuum distillation of Zn is conducted at 1000–1050°C and a pressure range of 6–13 Pa, leaving behind a friable material that can be readily disintegrated. Grinding of the cooled down material produces powder, which after stoichiometric carbon adjustments, is used as virgin material.[55] The process is dominated by the recovery of tungsten carbide WC, whereas other elements such as Co, Ta, Ti, Mo, and Cr, remain in the recovered powder. Currently, in the direct recycling, the use of Zn-reclaim for recycling of HM presents several critical aspects, as the quality of the scrap, because insufficient sorting will directly affect the quality of the RTP powder and the subsequently sintered HM part. Zn-reclaim is also limited by the size of the parts, although unreacted parts can be recycled to a new charge. Therefore, large parts have to be disintegrated into smaller parts, before processing (if at all possible). Further, high-binder grades (up to 30% binder) are not optimal candidates for this kind of processing, as significant sintering of the binder can occur during the Zn-treatment. Last, but not least, repeated recycling through Zn-processing will enrich impurities, such as iron

(picked up during ball milling) or other elements which are introduced by inaccurate sorting or insufficient separations of coatings. Thus, only a certain percentage of cemented carbide recycling will be possible by the Zn-process, and the contribution of chemically recycled scrap or the use of primary raw materials are necessary to keep trace elements below the required threshold limit for production of high quality cemented carbides.[52][56]

➤ **The cold stream process**

The cold stream process is a technique that involves a mechanical comminution method, where the WC-scrap is heated around 600–700°C and hit by a stream of cold air with a high velocity of 1000km/h.[51] The main advantages of this process reside in its high purity retention, its easily controllable particle size, as well as the low temperature range that can prevent oxidation of the tungsten carbide materials and makes the metal brittle for easier size reduction.[52] It is important to note that, in the manufacturing of HM materials, slight oxidation of tungsten carbide may cause porosity in the final product due to reduced sintering surface tension and the consequent degradation of the mechanical properties. As well as for the Zinc process, a drawback of the cold stream process is the incomplete separation of the tungsten carbide from the metallic binder. The complete extraction requires a specialized expensive equipment.

➤ **The menstruum process**

The menstruum process is one of the most important pyrometallurgy methods for the direct recycling of metallic tungsten scraps. In this process, very high temperatures, in the 1550 to 1660°C range, are reached in an induction furnace where the HM scraps are being dissolved in Fe-C or Co-C melts.[51] For this, HM reacts with the carbon of the melt to form WC, which settles at the bottom of the melt because of its higher density. Once the excess liquid is collected, the material floating above WC is removed.

➤ **The oxidation-reduction process**

This process requires oxidation pre-treatment around 800°C to transform the HM scrap to oxidic materials which can easily undergo a gas-solid reaction.[48][52] The oxidized product is subsequently milled, screened and finally reduced to tungsten powder in a hydrogen atmosphere at 900–1000°C in a push-type furnace.[51][52]

As was described previously, the pyrometallurgical processes, despite being well established, require a high amount of energy necessary to reach the high temperatures. Therefore, as an alternative method for recycling HM, various hydrometallurgical processes have been

developed which seem more selective, more predictable and easily controlled, although they can lead also to the use of dangerous reagents and the production of large amount of acid wastewater.

1.6.2 Chemical recycling

Chemical recycling implies that the scrap is converted chemically into “virgin” APT (ammonium paratungstate), the major high-purity intermediate for most tungsten products, except melting metallurgy. It is done in a similar way to that used for the processing of tungsten concentrates. However, tungsten as W metal or WC must be first oxidized by thermal treatment in air, chemicals or electric energy, in order to transform to the hexavalent state (W^{+6}), which is then soluble in an alkaline leach process. Chemical modification is the more versatile approach being applicable to all sort of W-based materials and achieving high-purity raw materials which can be applied in all the desired fields. On the other hand, they are an energy- and chemicals-intensive class of treatments which require expensive equipment, complex plants and skilled workers. It is typically applied for mineral processing and is the approach of election for impure or unsorted waste materials (e.g. sludges). Sometimes only a part of the scrap is converted chemically (“semi-direct” recycling) leaving the respective tungsten material (W, WC) intact in powder form for subsequent re-use. [52]

➤ Semi-direct recycling

Hydrometallurgical processes can be also exploited for the treatment of binary- and ternary-phase tungsten materials, e.g. WC-Co-based powders (like IP and RP) and scraps by a more selective acidic leaching able to dissolve just one phase, primarily the binder, leaving W-based phases unreacted. The process advantages over pyrometallurgical reclamation include low energy-demanding processes, the treatment of more impurities and the achieving of a wide range of products with a variety of industrial applications.[51] Hydrometallurgical processes typically involve several phases, among them:

- mechanical pretreatments which can concentrate and expose the elements of interest to chemical treatment;
- leaching of metal values;
- separation of the metals transferred in aqueous solution through precipitation, liquid-liquid extraction (solvent) and liquid-solid extraction for solid materials, or

- recovery of the metal from the leaching solution through chemical or electrochemical reduction.

The leaching phase is the core of the process where one or more components of the composite material are dissolved by the action of a chemical agent through metal complex formation, leaving the other phase(s) at the solid state. The efficacy of the process is heavily affected by the stability, selectivity and rapidity of metal complex formation. In the case of HM materials, a selective leaching would provide the binder metal(s) dissolution while leaving the WC phase unaffected, due to its (their) richer redox and coordination chemistry. The use of strong inorganic acids (phosphoric, sulfuric, nitric or hydrochloric acids), despite its effectiveness in Co dissolution, can lead to W transformation to tungstic acid which is deposited in the pores of the leached zones requiring further treatments for recycling and heavily threatens the environment and operators due to the harmfulness of reagents and gaseous by-products.[57][58][59][58] Thus, a promising alternative is related to the use of safer and easily available organic acids which can work as selective leaching agents for Co. Their employment seems attractive due to their complexing/chelating properties which can favor metal oxidation.

Edtmaier *et al.* described a method in which they used 3.6 M acetic acid solution to solubilize up to 85% of cobalt binder from hard metal scrap if reacted within a temperature range of 40–80°C, at an air pressure of 1–5 KPa and a time of 2.6–6.5 days.[60] Under these conditions, W, Cr, V and Fe were co-extracted with cobalt but WC and other metal carbides such as NbC, TaC and TiC remained unreacted. The dissolved metal species, if required, may be recovered through known chemical means.[60] Besides, several interesting experiments on the use of organic acids, such as acetic or formic acids, in the presence of H₂O₂ as an oxidant, were investigated with promising results.[61] Several examples for hydrometallurgy for Co recovery from oxidized HM scraps were also proposed, as in the case of the use of malic acid/H₂O₂ for Co leaching from CoWO₄. [62] In some cases, leaching can be mediated by current. In a combined hydrometallurgical/electrochemical method, the oxidation of the HM scrap is performed at the anode under controlled conditions in order to dissolve cobalt into an acidic solution, leaving a skeleton of WC particles.[63] Lin and co-researchers investigated the anodic current density for WC-scrap in different mineral acids at an active state of 200 mV.[63][51] They demonstrated that the selective dissolution of cobalt from the WC–Co scrap was efficient when it was electrolyzed at 200–600 mV in a 1M HCl solution containing 0.1 M citric acid. Besides, Wongsia *et al.* investigated an electrolysis process combined with the hydrothermal pre-leaching of cemented WC–Co scraps, showing that around 60% of binder metal was

dissolved after 24h.[51][64] It is also highlighted that in the electrolytic leaching the temperature has a remarkable effect on cobalt dissolution. However, this process requires additional complexing agents and cell design.[51]

1.6.3 Melting Metallurgy

Melting Metallurgy is the process route for tungsten steels and super alloys. Tungsten-bearing scrap can substitute ferrotungsten in steels and high purity tungsten metal scrap can be directly used for addition to super alloys.

1.7 Green Chemistry & Engineering

Currently approach adopted by the scientific community is to design and develop chemical products and processes, which can reduce or eliminate the use of harmful substances to the environment and human health. “Green chemistry” is a relatively new way of doing chemistry, pursuing sustainability at the *molecular level* by all aspects of the process life-cycle (raw materials selection, toxicity and production; toxicity of products and by-products; efficiency, energy consumption, waste production and safety of the chemical process).[65][66] The 12 Principles of Green Chemistry have been established as a guide to the general aims of green chemistry and how they can be achieved, as in **Fig. 1.12**. [66][67][68]

In the context of HM waste valorization, selective and effective leaching processes promise to be more tunable, exact and predictable with respect to energy-intensive thermal treatments currently in use for metals recycling. For this reason, a further effort in finding better leaching agents for Co from these secondary sources, capable to meet all the features required for sustainability in agreement with the green chemistry principles, seems worthy to be done to overcome the environmental issues related to the use of the hazardous and/or ineffective reagents currently in use by hydrometallurgy. The design of new chemical processes able to meet these requirements should take into account the reactivity of the elements contained in the complex material, specifically Co (and other iron family metals) and W redox and coordination chemistry, in order to play on the differences among them for pursuing selectivity, and on their affinity towards complexing agents, for pursuing efficiency in mild conditions.

The selection of the best reagents in terms of green chemistry principle for doing this, would reach the goal of a more sustainable process on a molecular level. Noteworthy, for making the circular economy model profitable and attractive to industrial stakeholders, sustainability on molecular level cannot disregard a *green* design of the whole process at industrial level, making multidisciplinary a key aspect of the research in this cutting-edge field.

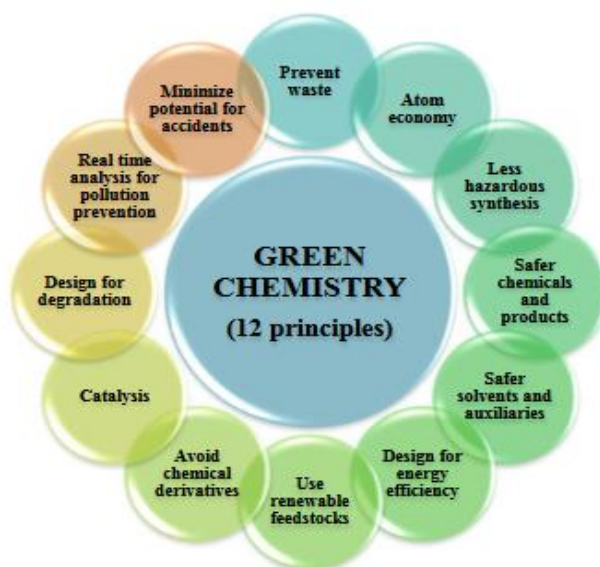


Figure 1.12: The 12 principles of “Green Chemistry” according to ref. [68] and Appendix A7.

1.8 Aims and scope of the work

In the described context and with the aim of implementing a circular economy model in HM manufacturing, based on the multidisciplinary expertise on *green* leaching systems for critical metals recovery from Hi-Tech wastes of the research group of the *Department of Civil Engineering, Environmental and Architecture (DICAAR), University of Cagliari (IT)*, where this PhD thesis work has been carried out in collaboration with *F.I.L.M.S. corp.*, an Italian leading company in the powder metallurgy of tungsten and HM, and *Green Chemistry Centre of Excellence, Department of Chemistry, University of York (UK)*,

the work presented here focuses on the design and application of new solvometallurgical methods for a sustainable, effective and selective metals recovery from the complex matrix of HM recovery powders, hazardous wastes of HM manufacturing.

IP, as anticipated in 1.2 section and summarized in Fig. 1.2, are cobalt-rich by-products generated by the shaping phase of the HM production process, which are problematic as their cobalt content and the WC-grain size features are not tunable. Co-content of these powders may also exceed both practical and legal thresholds (> 10 wt. %).[61] For this reason their re-employment in HM manufacturing is still at low rate.

With the view to turn this secondary material into a valuable and versatile resource of WC and Co completely reusable in the manufacturing process, new solvometallurgical routes for tuning the content of and/or recovering cobalt and WC from powders, have been studied through a twofold Co-leaching approach based on the use of sustainable acid and non-acid leaching

agents, then implemented in a full-cycle *green* and, potentially, wastewater-free circular economy model.

This approach is based on the different reactivity of the involved species. Specifically, W redox and coordination chemistry are poorer than those shown by Co, where both +2 and +3 oxidation numbers are easily achievable ($E^\circ \text{Co}^{2+}/\text{Co} = -0.277\text{V}$; $E^\circ \text{Co}^{3+}/\text{Co}^{2+} = +1.82\text{V}$) and common, characterized by a variety of different coordination numbers and geometries depending on the solvent and on the steric hindrance and strength of the ligands. Against, WC is a very poorly reactive species in mild conditions. Playing on the *borderline* nature of Co (in terms of Hard-Soft acid-base theory, Appendix A2),[69] a variety of leaching systems have been selected based on *hard* and *soft* donor ligands.

More specifically, the scope of this work lies in studying:

- 1) by **acid leaching**, a series of weak organic acids which can be obtained from biomasses, promising as selective leaching agents for cobalt in water and/or *green* organic solvents and highly appealing for designing cheap eco-sustainable processes,
- 2) by **non-acid leaching**, non-toxic *soft*- (thiourea, dithiooxamide, R₂-dithiomalonamide) and *hard*- (urea, N,N'-R₂-piperazine-2,3-dione, malonamide and lactate ion) donor complexing ligands able to impel cobalt leaching in the presence of an oxidant in *green* organic solvents, with the aim of finding new leaching systems able to couple effectiveness and environmental sustainability;
- 3) cobalt complexes isolation by solid-liquid extraction with Starbon® and precipitation from the leachate,
- 4) cobalt metal recovery from the complex, for pursuing the highest metals and reagents recovery rates;
- 5) the design of full-cycle WC and Co recovery processes from wasted internal recovered powders (IP) based on the found most promising acid and non-acid leaching systems and addressed to the highest materials economy rate, in order to assess the whole technical-economic-environmental sustainability of the proposed processes and to implement a circular economy model really applicable to the industrial scale.

Fig. 1.13 outlines the approach and scopes of this thesis.

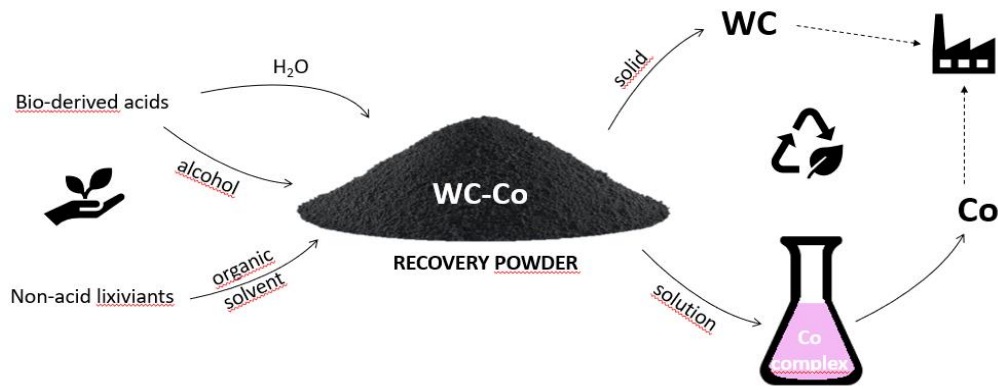


Figure 1.13: Thesis outline.

On these bases, following the present introductory chapter, this thesis will be divided into two parts:

Part I: Sustainable leaching systems

Part II: Designing sustainable processes for industrial application

1.9 References

- [1] H. M. Ortner, P. Ettmayer, H. Kolaska, and I. Smid, “The history of the technological progress of hardmetals?,” *Int. J. Refract. Met. Hard Mater.*, vol. 49, no. 1, pp. 3–8, 2015.
- [2] Y. Yoshisato and A. Takeoka, “International Conference on Recent Trends in Physics 2016 (ICRTP2016),” *J. Phys. Conf. Ser.*, vol. 755, p. 011001, 2016.
- [3] R. M. Genga, “Microstructure and Properties of Selected Wc-Cemented Carbides Manufactured By Sps Method,” no. September, 2014.
- [4] J. García, V. Collado Ciprés, A. Blomqvist, and B. Kaplan, “Cemented carbide microstructures: a review,” *Int. J. Refract. Met. Hard Mater.*, vol. 80, no. August 2018, pp. 40–68, 2019.
- [5] M. Tarraste *et al.*, “Ferritic chromium steel as binder metal for WC cemented carbides,” *Int. J. Refract. Met. Hard Mater.*, vol. 73, no. February, pp. 183–191, 2018.
- [6] C. M. Fernandes and A. M. R. Senos, “Cemented carbide phase diagrams: A review,” *Int. J. Refract. Met. Hard Mater.*, vol. 29, no. 4, pp. 405–418, 2011.
- [7] Z. Guo, J. Xiong, M. Yang, X. Song, and C. Jiang, “Effect of Mo₂C on the microstructure and properties of WC-TiC-Ni cemented carbide,” *Int. J. Refract. Met. Hard Mater.*, vol. 26, no. 6, pp. 601–605, 2008.

- [8] H. O. Andrén, “Microstructures of cemented carbides,” *Mater. Des.*, vol. 22, no. 6, pp. 491–498, 2001.
- [9] A. YOUSFI, *Microstructure Development of WC - Co Based Cemented Carbides During Creep Testing*. 2016.
- [10] C.-S. Kim, “Microstructural-mechanical property relationships in WC-Co composites,” *Ph.D. Thesis*, p. 214, 2004.
- [11] J. M. Tarragó, “Damage tolerance of cemented carbides under service-like conditions,” Ph/D thesis, September, 2016, Universitat Politècnica de Catalunya – Barcelona Tech, pp.124
- [12] Y. Kusaka, K. Yokoyama, Y. Sera, S. Yamamoto, S. Sone, H. Kyono, T. Shirakawa, S. Gotos. Goto, “Respiratory diseases in hard metal workers: an occupational hygiene study in a factory,” *British Journal of Industrial Medicine*, pp. 474–485, 1986.
- [13] National Toxicology Program, “Final report on carcinogens background document for cobalt-tungsten carbide: powders and hard metals.,” *Rep. Carcinog. Backgr. Doc.*, no. 9–5979, 2009.
- [14] K. Schädler, A. Etschmaier, and W. Lengauer, “Reactively sintered hardmetals from alloyed W-Co-C phases,” *Proc. Euro Powder Metall. Congr. Exhib. Euro PM 2007*, vol. 1, pp. 249–255, 2007.
- [15] B. Roebuck, M. Gee, E. G. Bennett, and R. Morrell, “A National Measurement Good Practice Guide No. 20 - Mechanical Tests for Hardmetals,” *Ceramics*, no. 20, pp. 1–74, 1999.
- [16] J. Weidow, *Effect of metal and cubic carbide additions on interface chemistry, phase composition and grain growth in WC-Co based cemented carbides*. 2010.
- [17] O. Sids and T. Carbide, “Introduction Tungsten Carbide Cas N ° : 12070-12-1.”
- [18] Cobalt Facts, “Cobalt in Metallurgical Uses,” *Cobalt Facts*, pp. 8–22, 2006.
- [19] M. Windows, M. Corporation, K. Hori, and A. Sakajiri, “Microstructure and corrosion.”
- [20] H. Aronsson, B. and Pastor, “Cobalt in Cemented Carbide,” *Congr. Cobalt Metall. Uses*, pp. 41–45, 1985.
- [21] L. P. Barbosa, H. Takiishi, and R. N. Faria, “The effect of cobalt content on the microstructure of Pr-Fe-Co-B-Nb alloys and magnetic properties of HDDR magnets,” *J. Magn. Mater.*, vol. 268, no. 1–2, pp. 132–139, 2004.
- [22] J. Gurland and P. Bardzil, “Relation of Strength, Composition, and Grain Size of Sintered WC-Co Alloys,” *JOM*, vol. 7, no. 2, pp. 311–315, 1955.
- [23] Z. Z. Fang, X. Wang, T. Ryu, K. S. Hwang, and H. Y. Sohn, “Synthesis, sintering, and

- mechanical properties of nanocrystalline cemented tungsten carbide - A review,” *Int. J. Refract. Met. Hard Mater.*, vol. 27, no. 2, pp. 288–299, 2009.
- [24] B. Roebuck, “Magnetic moment (saturation) measurements on hardmetals” *Int. J. Refract. Met. Hard Mater.*, vol. 14, no. 5–6, pp. 419–424, 1996.
- [25] S. Chandran, R. Jagan, R. Paulraj, and P. Ramasamy, “Spectral, mechanical, thermal, optical and solid state parameters, of metal-organic bis(hydrogenmaleate)-CO(II) tetrahydrate crystal,” *J. Solid State Chem.*, vol. 230, pp. 135–142, 2015.
- [26] E. Lassner and W.-D. Schubert, *Index. Tungsten Properties, Chemistry, Technology of the Element, Alloys, and Chemical Compounds Erik Lassner and Wolf-Dieter Schubert.* 1999.
- [27] D. R. Leal-Ayala, J. M. Allwood, E. Petavratzi, T. J. Brown, and G. Gunn, “Mapping the global flow of tungsten to identify key material efficiency and supply security opportunities,” *Resour. Conserv. Recycl.*, vol. 103, pp. 19–28, 2015.
- [28] J. Emsley, “The Elements (Oxford Chemistry Guides),” p. 300, 1998.
- [29] Refractory Materials, High Temperature Oxides, Oxides of Rare Earths, Titanium, Zirconium, Hafnium, Niobium and Tantalum, Academic Press, New York and London, 78-97487, 1970
- [30] H. Nakajima, T. Kudo, and N. Mizuno, “Reaction of metal, carbide, and nitride of tungsten with hydrogen peroxide characterized by ^{183}W nuclear magnetic resonance and raman spectroscopy,” *Chem. Mater.*, vol. 11, no. 3, pp. 691–697, 1999.
- [31] ITIA, “Recycling of Tungsten - Current share, economic limitations and future potential,” no. May, 2018.
- [32] Blengini, G.A.; Mathieux, F.; Mancini, L.; Nyberg, M. and Viegas, H.M., “*Recovery of critical and other raw materials from mining waste and landfills*”. Jrc Science For Policy Report, pp.130, 2019.
- [33] L. K. G. Ackerman, L. L. Anka-Lufford, M. Naodovic, and D. J. Weix, “Cobalt co-catalysis for cross-electrophile coupling: Diarylmethanes from benzyl mesylates and aryl halides,” *Chem. Sci.*, vol. 6, no. 2, pp. 1115–1119, 2015.
- [34] Cobalt Development Institute, “Cobalt in Chemicals,” *Cobalt Facts*, pp. 29–40, 2006.
- [35] X. Chen *et al.*, “Organic reductants based leaching: A sustainable process for the recovery of valuable metals from spent lithium ion batteries,” *Waste Manag.*, vol. 75, pp. 459–468, 2018.
- [36] L. Li, J. Ge, F. Wu, R. Chen, S. Chen, and B. Wu, “Recovery of cobalt and lithium from spent lithium ion batteries using organic citric acid as leachant,” *J. Hazard. Mater.*, vol.

- 176, no. 1–3, pp. 288–293, 2010.
- [37] L. Li *et al.*, “Recovery of metals from spent lithium-ion batteries with organic acids as leaching reagents and environmental assessment,” *J. Power Sources*, vol. 233, pp. 180–189, 2013.
- [38] L. Li *et al.*, “Succinic acid-based leaching system: A sustainable process for recovery of valuable metals from spent Li-ion batteries,” *J. Power Sources*, vol. 282, pp. 544–551, 2015.
- [39] T. Kojima, T. Shimizu, R. Sasai, and H. Itoh, “Recycling process of WC-Co cermets by hydrothermal treatment,” *J. Mater. Sci.*, vol. 40, no. 19, pp. 5167–5172, 2005.
- [40] P. Alves Dias, D. Blagoeva, C. Pavel, and N. Arvanitidis, *Cobalt: demand-supply balances in the transition to electric mobility*. 2018.
- [41] M. Nowakowska, “Defining Critical Raw Materials in the EU : Information Gaps and Available Solutions,” *US-EU Work. Miner. Raw Mater. Flows Data*, no. September, pp. 1–25, 2012.
- [42] V. Vadi and V. Vadi, “The world heritage and foreign direct investment,” *Cult. Herit. Int. Invest. Law Arbitr.*, no. May 2014, pp. 93–136, 2014.
- [43] Comisión Europea, *European Commission, Report on Critical Raw Materials and the Circular Economy, 2018*. 2018.
- [44] EC, “EU Critical raw materials in the circular economy and strategic value chains and EU R&D funding,” *Eur. Com.*, no. January, p. 19, 2019.
- [45] V. Correia, “Critical Raw Materials : the EU approach 1983 G7 summit.”
- [46] E. Commission, “Periodic Review of REACH,” 2013.
- [47] European Parliament and Council, “Directive (EU) 2018/851 of the European Parliament and of the Council of 30 May 2018 amending Directive 2008/98/EC on waste,” *Off. J. Eur. Union*, no. 1907, pp. 109–140, 2018.
- [48] A. Shemi, A. Magumise, S. Ndlovu, and N. Sacks, “Recycling of tungsten carbide scrap metal: A review of recycling methods and future prospects,” *Miner. Eng.*, vol. 122, no. January, pp. 195–205, 2018.
- [49] K. Shedd, “Tungsten Recycling in the United States in 2000,” *Usgs*, pp. 1–23, 2005.
- [50] S. Jewell, “Mineral commodity summaries 2014: U.S. Geological Survey,” p. 196, 2014.
- [51] R. R. Srivastava, J. chun Lee, M. Bae, and V. Kumar, “Reclamation of tungsten from carbide scraps and spent materials,” *J. Mater. Sci.*, vol. 54, no. 1, pp. 83–107, 2019.
- [52] B. Zeiler, “Recycling of Tungsten,” no. August, pp. 21–24, 2019.
- [53] A. A. Baba *et al.*, “Hydrometallurgical Processing of Manganese Ores: A Review,” *J.*

- Miner. Mater. Charact. Eng.*, vol. 02, no. 03, pp. 230–247, 2014.
- [54] E. Lassner and W.-D. Schubert, *Properties, chemistry, technology of the element, alloys, and chemical compounds*. 2005.
- [55] E. Altuncu, F. Ustel, A. Turk, S. Ozturk, and G. Erdogan, “Cutting-tool recycling process with the zinc-melt method for obtaining thermal-spray feedstock powder (WC-Co),” *Mater. Tehnol.*, vol. 47, no. 1, pp. 115–118, 2013.
- [56] C. S. Freemantle and N. Sacks, “Recycling of cemented tungsten carbide mining tool scrap,” no. May, pp. 1207–1213, 2015.
- [57] J. C. Lee, E. Y. Kim, J. H. Kim, W. Kim, B. S. Kim, and B. D. Pandey, “Recycling of WC-Co hardmetal sludge by a new hydrometallurgical route,” *Int. J. Refract. Met. Hard Mater.*, vol. 29, no. 3, pp. 365–371, 2011.
- [58] L. Ma, Z. Nie, X. Xi, and X. Han, “Cobalt recovery from cobalt-bearing waste in sulphuric and citric acid systems,” *Hydrometallurgy*, vol. 136, no. x, pp. 1–7, 2013.
- [59] J. Shibata, N. Murayama, and M. Niinae, “Recovery of tungsten and cobalt from tungsten carbide tool waste by hydrometallurgical method,” *Geosystem Eng.*, vol. 17, no. 2, pp. 120–124, 2014.
- [60] C. Edtmaier *et al.*, “Selective removal of the cobalt binder in WC/Co based hardmetal scraps by acetic acid leaching,” *Hydrometallurgy*, vol. 76, no. 1–2, pp. 63–71, 2005.
- [61] G. Kücher, S. Luidold, C. Czettel, and C. Storf, “First evaluation of semidirect recycling methods for the reclamation of cemented carbides based on a literature survey,” *Rev. Mater.*, vol. 23, no. 2, 2018.
- [62] B. Seo and S. Kim, “Cobalt extraction from tungsten carbide-cobalt (WC-Co) hard metal scraps using malic acid,” *Int. J. Miner. Process.*, vol. 151, pp. 1–7, 2016.
- [63] J. C. Lin, J. Y. Lin, and S. P. Jou, “Selective dissolution of the cobalt binder from scraps of cemented tungsten carbide in acids containing additives,” *Hydrometallurgy*, vol. 43, no. 1–3, pp. 47–61, 1996.
- [64] S. Wongsisa, P. Srichandr, and N. Poolthong, “Development of manufacturing technology for direct recycling cemented carbide (WC-Co) tool scraps,” *Mater. Trans.*, vol. 56, no. 1, pp. 70–77, 2014.
- [65] J. H. Clark, “Green chemistry: Challenges and opportunities,” *Green Chem.*, vol. 1, no. 1, pp. 1–8, 1999.
- [66] J. Attard, “Starbon® Materials for a Circular Economy,” Ph/D thesis, University of York, pp.249, December, 2018.
- [67] J. H. Clark, “Green chemistry: Today (and tomorrow),” *Green Chem.*, vol. 8, no. 1, pp.

17–21, 2006.

- [68] W. Filho, J. B. Andrade Guerra, M. Mifsud, and R. Pretorius, *Universities as Living Labs for sustainable development: A global perspective*, vol. 26. 2017.
- [69] P. Askalani, R. A. Bailey, R. P. Itlstitute, and U. Arab, “although only Stonestreet,” *Measurement*, vol. 47, no. Iii, pp. 2275–2282, 1969.

Part I

Sustainable leaching systems

**Bio-derived organic acids leaching agents
for selective cobalt dissolution in water**

2.1 Introduction

WC-Co based waste materials are refractory composites containing Co metal and W, as detailed in Chapter 1. Unlike cobalt, WC typically shows a negligible reactivity towards weak non-oxidizing acids. Moreover, W redox and coordination chemistry is poorer than that shown by Co, where both +2 and +3 oxidation numbers are common, characterized by a variety of different coordination numbers and geometries depending on the solvent and on the steric hindrance and the strength of the ligands. In this context, a selective Co-leaching seems to be possible if appropriate complexing/oxidizing species are selected. In the last decade, the use of bio-derived organic acids as leaching agents is gaining increasing attention being safe, renewable and, in some cases, cheap substances. Thanks to their capability to dissolve low reduction potential metals, some of them have been recently proposed as suitable leaching agents for transition and rare earth¹ elements recovery from several kind of waste. As an example, citric acid demonstrated to be a powerful and *green* agent for Cu-based slags enhancement, removing effectively and selectively Co, Ni and Fe metal impurities from the composite material.[1] Similarly, citric and acetic acids were satisfactorily employed as effective leaching agents for NbFeB magnets - where also Co, Ni and several other REE in low amount are present - in mild conditions, achieving material dissolution in short time.[2] In these processes the organic acid can work as complexing and/or oxidizing – by H⁺ – agent towards elemental state metals. More specifically, it will be able to couple complexing and oxidizing actions when its pK_a and/or the K_{diss} of the formed complex are very low. Differently, the role played by the acid is mainly related to the complexing properties of its deprotonated (anionic) form, thus an external oxidizing agent is necessary for the metal(0) leaching, as observed in the case of the use of acetic acid solutions (pK_a = 4.7) towards WC-Co wastes which requires O₂ addition to the leaching system for driving the Co-dissolution reaction.[3] Other examples are related to the use of organic acids for metal leaching from oxidized materials. Due to the amount of waste we will have to face on soon, the case is attracting wider attention recently is the application of organic acids like acetic, ascorbic, citric, lactic, maleic, malic and succinic, in the presence of H₂O₂, for lithium and cobalt recovery from spent Li-ion batteries (LIBs).[4][5] Besides, several examples for Co recovery from oxidized HM scraps were also proposed, as in the case of the use of malic acid/H₂O₂ for Co leaching from CoWO₄. [6] In these cases, the role of the organic acid is mainly related to its coordinative behavior towards the metal ion and the

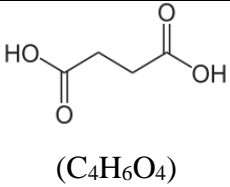
¹ Rare earth elements (REE), as defined by the International Union of Pure and Applied Chemistry, involve lanthanoides together with scandium and yttrium. Despite their name, their abundance in Earth's crust is relatively high.

formation of metal complexes soluble in the leaching solvent. In some cases, a lower effectiveness in leaching reactions carried out by weak organic acids vs. strong inorganic acids, is observed. Against, the use of weak coordinating acids increases selectivity, limits by-products formation and makes safer the process to operators and environment. Besides, a good exposure of metal values to the chemical etching results in good improvements in the leaching rate.

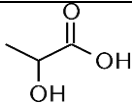
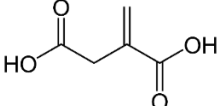
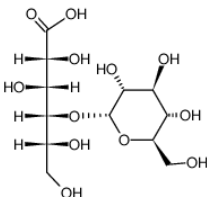
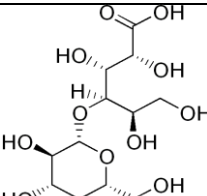
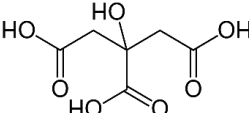
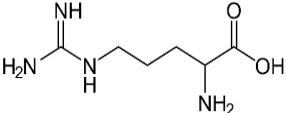
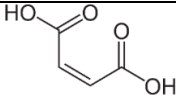
On these bases, this Chapter will describe the fundamental study of the reactions between several selected bio-derived organic acids (and amino acids) and cobalt metal in several solvents (primarily water and alcohols), investigating the role of the acid in the reaction, the most appropriate leaching conditions and solvent, and the obtained complexes, in order to assess the suitability of the different acids for applicative purposes in HM waste enhancement. Then, preliminary experiments on real recovery powders are described in order to highlight effectiveness and selectivity of the leaching. A selection of easily available, renewable, cheap and safe organic acids (and amino acids) was made in particular taking into account their acidity – in that sense they were selected having pK_{a1} values spanning in the 1.8-4.1 range - and solubility in water as well as the solubility in *green* solvents like ethanol.² Furthermore, all the selected species are carboxylic acids which can behave as complexing/chelating agents when in their deprotonated form, favoring metal oxidation and leaching.

Table 2.1 summarizes the selected acids for hydro- and solvo-metallurgy and their main features.

Table 2.1. Selection of organic acids (and amino acids) used throughout this work, listed by decreasing pK_{a1} values. MM = molar mass.

Name (acronym)	Formula	MM (g/mol)	pK_{a1} (25°)	Solubility (g on 100mL solvent)		Refs
				Water	Alcohol	
Succinic acid, 1,4- butanedioic acid (H₂Suc)	 (C ₄ H ₆ O ₄)	118.09	4.1	6.8 ^{20°} , 121 ^{100°}	EtOH, 5.4 MeOH, 15.8	[7]

² In collaboration with Green Chemistry Center of Excellence, Dept. of Chemistry – University of York (UK).

Lactic acid, 2-hydroxypropanoic acid (HLat)	 (C ₃ H ₆ O ₃)	90.10	3.9	100	EtOH, 192 ^{20°}	[8]
Itaconic acid, 1-Propene-2,3-dicarboxylic acid (H₂It)	 (C ₅ H ₆ O ₄)	130.09	3.8	8.33 ^{20°}	EtOH, 19.7 ^{15°}	[9]
Maltobionic acid, 4-O-beta-galactopyranosyl-D-gluconic acid (HMB)	 (C ₁₂ H ₂₂ O ₁₂)	358.30	3.8	20.7	-	[10]
Lactobionic acid, 4-O-beta-galactopyranosyl-D-gluconic acid (HLB)	 (C ₁₂ H ₂₂ O ₁₂)	358.30	3.6	10	-	[11]
Citric acid, 2-hydroxy-1,2,3-propane tricarboxylic acid (H₃Cit)	 (C ₆ H ₈ O ₇)	210.14	3.1	133	116 ^{25°}	[12]
L-arginine, 2-Amino-5-guanidinopentanoic acid (HArg)	 (C ₆ H ₁₄ N ₄ O ₂)	174.20	2.2	15 ^{21°}	-	[13]
Maleic acid, <i>cis</i> -Butenedioic acid (H₂Mal)	 (C ₄ H ₄ O ₄)	116.07	1.83	78.8 ^{25°}	70 ^{30°}	[14]

2.1.1 Selected leaching agents for cobalt

- Succinic acid (H₂Suc)

Succinic acid was purified for the first time from amber by Georgius Agricola in 1546.[22] It is a dicarboxylic acid with four carbon atoms, playing an important role as a precursor molecule for the synthesis of biodegradable polyester resins, dyestuffs and pharmaceuticals, and as an additive in food industry.[7] Song H. *et al.* reported also, various microorganisms have been used to produce succinic acid from different carbon sources namely *Anaerobiospirillum Succiniciproducers* and *Actinobacillus Succinogenes* growing on galactose, galactose/glucose, and galactose/lactose.[22][23] Nowadays, succinic acid is exclusively produced from crude oil by catalytic hydrogenation of maleic anhydride to succinic anhydride and subsequent hydration or by direct catalytic hydrogenation of maleic acid. The potential market for succinic acid itself and its derivatives is estimated to be more than 270.000t/year, while the market price of petrochemically produced succinic acid is about 5.9–8.8 USD kg⁻¹ depending on its purity whereas the raw material costs, based on production from maleic anhydride, are about 1 USD kg⁻¹ succinic acid.[7]

- Lactic acid (HLat)

Lactic acid was first discovered in 1780 by the Swedish chemist C. W. Scheele in sour milk. [8] It is a naturally occurring α -hydroxy acid. It is a chiral molecule, consisting of two enantiomers, the L-(+)-lactic acid (or (S)-lactic acid) and the D-(–)-lactic acid (or (R)-lactic acid).[15] The (S)-enantiomer is obtained from anaerobic glycidic catabolism. Päivi Mäki-Arvela *et al.* [16] reported that lactic acid can be converted into different useful chemicals such as acrylic acid, pyruvic acid, propylene glycol, 1,2-propanediol, 2,3-pentanone, becoming widely appealing for food, pharmaceutical, cosmetic, chemical and textile industries.[17] Its importance has recently grown up thanks to its use as a monomer in preparation of bio-polymers such as the polylactic acid (PLA).[18] Lactic acid can be produced in its racemic form by chemical synthesis from coal or oil through the reaction of acetaldehyde with hydrogen cyanide to give lactonitrile and subsequent hydrolysis of the intermediate acetonitrile catalyzed by strong acids.[19] However, up to 90% of commercial lactic acid is produced through fermentation of sugars, mainly glucose and sucrose, a biotechnological process also applied on renewable resources.[8] Abdel-Rahman *et al.* described numerous studies conducted on microorganisms that produce pure lactic acid through fermentation using *Lactobacillus* bacteria.[20]

Global lactic acid demand was around 714 kton in 2013 and expected to 1960 kton in 2020. [21]

- Itaconic acid (HIIt)

Itaconic acid was discovered in 1837 as a product of thermal decomposition of citric acid by S. Baup.[24] Later, it was produced from *Aspergillus itaconicus* in 1931 by Kinoshita.[9] Dan Cristian Vodnar and colleagues reported itaconic acid production can take place through biotechnology fermentation of bacteria with fungi like *Aspergillus terreus* and *Ustilago maydis* strains or with metabolically engineered bacteria like *Escherichia coli* and *Corynebacterium glutamicum*. [9] The initial industrial production of itaconic acid used a chemical approach, i.e., the pyrolysis of citric acid to itaconic anhydride, followed by the hydrolysis of the anhydride, and its production is about 41000t/year and its world market is predicted to surpass 216 million USD in 2020.[9]

-Lactobionic (HLB) and maltobionic (HMB) acids

Lactobionic and maltobionic acids are patented α -hydroxy acid belonging to the “bionic” family. Bionics are polyhydroxy acids (PHAs) with an additional sugar molecule attached to the PHA structure. Lactobionic acid was synthesized for the first time by Fisher and Meyer in 1889 as the oxidation product of the lactose-free aldehyde group after a chemical oxidation with bromine i.e produced by chemical synthesis from refined lactose.[11] It can be also produced from whey by *Pseudomonas taetrolens* [25] or through biological oxidation of lactose.[11] Maltobionic acid is a maltose-derived stereoisomer of lactobionic acid. Both these acids, displays antioxidant, biodegradable, biocompatible and chelating properties that make them useful in different chemical fields, first of all in cosmetics and skin care fields.[26] The demonstrated capability of these highly functionalized acids to work as divalent and/or trivalent metals chelating agent,[26] makes them promising lixivants for Co by HM waste.

- Citric acid (H₃Cit)

Citric acid was first isolated by Karls Scheels in 1874, in England, from the lemon juice imported from Italy. Later, in 1923, Wehmer observed the presence of citric acid as a by-product of calcium oxalate produced by a culture of *Penicillium glaucum*. [27] Citric acid is a commodity chemical produced and consumed throughout the world. It is used mainly in the food and beverage industry, primarily as an acidulant and its global production in 2007 was over 1.6 million tones.[28] P. Luciana *et al.* reported that some micro-organisms including

bacteria, fungi and yeasts have been employed to produce citric acid such as yeasts *Saccharomycopsis* sp, fungus *Aspergillus niger* by fermentation of glucose or sucrose.[12][27] The main advantages of this acid are that it is a biodegradable, eco-friendly, low-cost, safe and versatile chemical for sequestering, buffering, wetting, cleaning and dispersing.

- L-arginine (HArg)

L-arginine is an important amino acid for industrial applications. It was discovered in 1986 from a lupine seedling extraction and was recognized as a casein component in 1895.[32] Arginine is primarily produced by fermentation from natural carbon sources and the main raw materials used are constituted of starches from cassava and corn, sugar and sugar syrup.[32] It has been almost six decades since amino arginine production has been explored and studied using microorganisms such as *Corynebacterium glutamicum* and *Escherichia coli* in order to improve its industrial level production.[33]

- Maleic acid (H₂Mal)

Maleic acid is an important intermediate in the chemical industry with a production of about 1,800,000t/year, constantly increasing.[29] Besides the main industrial route of production from benzene,[30] maleic acid can be also easily synthesized from renewable resources based on catalytic oxidation of furfural in liquid media with oxygen,[14] by fungi such as *Aspergillus niger* from renewable substrates [30] or synthesized through sustainable biomass-based feedstocks catalytic conversion.[31] Maleic acid was chosen as a selective leaching agent for cobalt due to its low pK_{a1} (1.83), its relatively low cost and its good solubility in ethanol.

2.1.2 Test specimen definition

WC-Co IP (RC-627C and RC-631L) studied throughout this work are by-products of HM production, generated by FILMS during machining operations. The Co content of the binder phase in the test specimens was 19.55 and 20.4 wt. %, respectively (full composition is provided in Appendix A1). The morphology and WC particle size of these samples were determined from Scanning Electronic Microscopy (SEM) images of the powders as well as by optical microscopy (OM) of the corresponding sintered samples (**Fig. 2.1**).

Test specimens differ mainly for the WC grain size and the mean free path value. Specifically, RC-631L shows a wider grain size distribution than RC-627C that is more conveniently appreciated by studying the grain size distribution they impart to the corresponding sintered materials (evaluated according to ISO 4499-2:2008). Indeed, RC-627C determines a grain size

in the $2\div 6\ \mu\text{m}$ range, while RC-631L a grain size in the $0.8\div 6\ \mu\text{m}$ range, in the corresponding sintered HM products which result in different properties and classification of these materials.[34][35] Moreover, with a similar metallic binder volume fraction, the microstructure of the RC-627C powder mixture will show a higher mean free path value (thickness of cobalt layer on WC grains) than RC-631L. Mean free path value may affect the reactivity of the binder phase, expecting the higher the mean free path, the higher the Co-reactivity. The choice of the two test specimens aimed to highlight the effect of the mean free-path value on the leaching process.

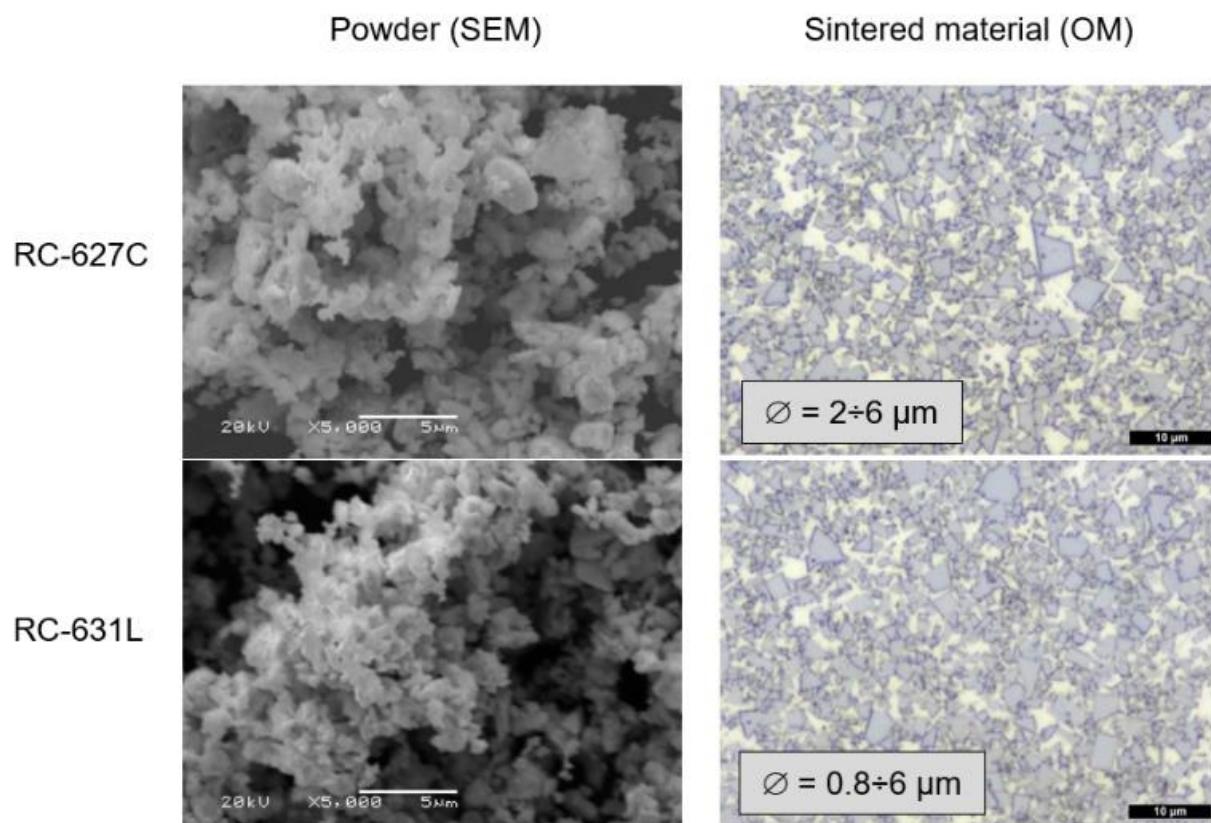


Figure2.1: Scanning Electron Microscopy (SEM) and Optical Microscopy (OM) micrographs of RC-627 C and RC-631L test specimens and related sintered materials, respectively.

2.2 Results and Discussion

2.2.1 Leaching experiments on Co powder

With the view to study the chemical reaction occurring between the selected lixiviants and cobalt in water, Co metal powders were reacted with diluted aqueous leaching solutions of the acids in an open flask under room conditions (approximately 20°C and 1 atm) and magnetic bar stirring (300 rpm). In those conditions, the expected leaching reactions, beside Co complexation, may involve the oxidizing action of the organic acid (through the H^+ ion

reduction), which would result in H₂ gas evolution, and/or the oxidizing action of dissolved O₂, which would be instead accompanied by O₂ consumption and H₂O formation.

Table 2.2 summarizes the Co-leaching reactions occurring with the different acids in water.

Table 2.2: Leaching reactions occurred with the different acids in water. *Not isolated yet.

Organic acids	Main leaching pathway found in water media	Leach. time (h)	Eq.
HLat	$2\text{Co} + \text{O}_2 + 4\text{HLat} \rightarrow 2[\text{Co}(\text{Lat})_2(\text{H}_2\text{O})_2]$	5	2.1
H ₂ Suc	$\text{Co} + \text{H}_2\text{Suc} + n\text{H}_2\text{O} \rightarrow [\text{Co}(\text{Suc})(\text{H}_2\text{O})_n] + \text{H}_2$ $2\text{Co} + \text{O}_2 + 2\text{H}_2\text{Suc} + (n-2)\text{H}_2\text{O} \rightarrow 2[\text{Co}(\text{Suc})(\text{H}_2\text{O})_n]$	4	2.2
H ₂ It	$3\text{Co} + \text{H}_2\text{It} + 3n\text{H}_2\text{O} \rightarrow [\text{Co}(\text{It})(\text{H}_2\text{O})_n]_3 + \text{H}_2$ $6\text{Co} + 3\text{O}_2 + 6\text{H}_2\text{It} \rightarrow 2[\text{Co}(\text{It})(\text{H}_2\text{O})_n]_3 + (6-3n)\text{H}_2\text{O}$	4	2.3 2.4
HLB	$2\text{Co} + \text{O}_2 + 4\text{HLB} \rightarrow 2[\text{Co}(\text{LB})_2(\text{H}_2\text{O})_2]$	4	2.5
HMB	$2\text{Co} + \text{O}_2 + 4\text{MLB} \rightarrow 2[\text{Co}(\text{MB})_2(\text{H}_2\text{O})_2]$	4	2.6
H ₃ Cit	$3\text{Co} + 2\text{H}_3\text{Cit} + n\text{H}_2\text{O} \rightarrow [\text{Co}_3(\text{Cit})_2(\text{H}_2\text{O})_n] + 3\text{H}_2$	12	2.7
H ₂ Mal	$\text{Co} + 2\text{H}_2\text{Mal} + 4\text{H}_2\text{O} \rightarrow [\text{Co}(\text{HMal})_2(\text{H}_2\text{O})_4] + \text{H}_2$	3	2.8
L-Arg	$\text{Co} + n\text{HArg} + m\text{H}_2\text{O} \rightarrow [\text{Co}(\text{Arg})_n(\text{H}_2\text{O})_m]^* + n/2\text{H}_2$	5	2.9

Preliminary experiments were performed on 20 mg of Co with an excess of reactant (50 mL of 0.5M leaching solution) in order to identify the leaching products and clarify the leaching reaction pathway. Under these conditions, the solutions turned readily from colorless to different shades of bright pink depending on the used acid and the disappearance of Co powder occurred in short times (3-12h), as shown in Table 2.2. In the case of H₃Cit and H₂Mal leaching, an abundant precipitation of a slightly pink product, supposed to be the cobalt complex, was also observed when the reactions went on. The leaching reactions occur by oxidation and simultaneous complexation of the metal forming, in a single-stage, the corresponding Co-complex which was isolated, in most cases, at the solid state by concentration and selective precipitation and fully characterized (see Experimental, section 2.4). The most part of the compounds obtained here by leaching are well-known, even if almost found in the literature as products of complexing reactions. More specifically, [Co(Lat)₂(H₂O)₂], [Co(LB)₂(H₂O)₂] and [Co(HMal)₂(H₂O)₄] complexes were identified by the agreement between the Fourier transform-infrared (FT-IR) spectra of the obtained compounds with those available in the literature, supported by an accordant CH-elemental analysis. Thermogravimetric analysis (TG) was also recorded for the obtained solid samples. Being an unknown compound, [Co(MB)₂(H₂O)₂] was supposed on the basis of the full agreement of the cited solid state characterization and the similarities in the coordination behavior expected for LB⁻ and MB⁻ ions. Several attempts for growing up well-shaped crystals of the compound suitable for single crystal X-ray characterization, were unfruitful. Nevertheless, the comparison of the FT-IR spectra recorded for [Co(LB)₂(H₂O)₂] and for the supposed [Co(MB)₂(H₂O)₂], shown in **Fig.**

2.1, pointed out just slight shifts for the main peaks and differences between the spectra, supporting the hypothesis of very similar structures.

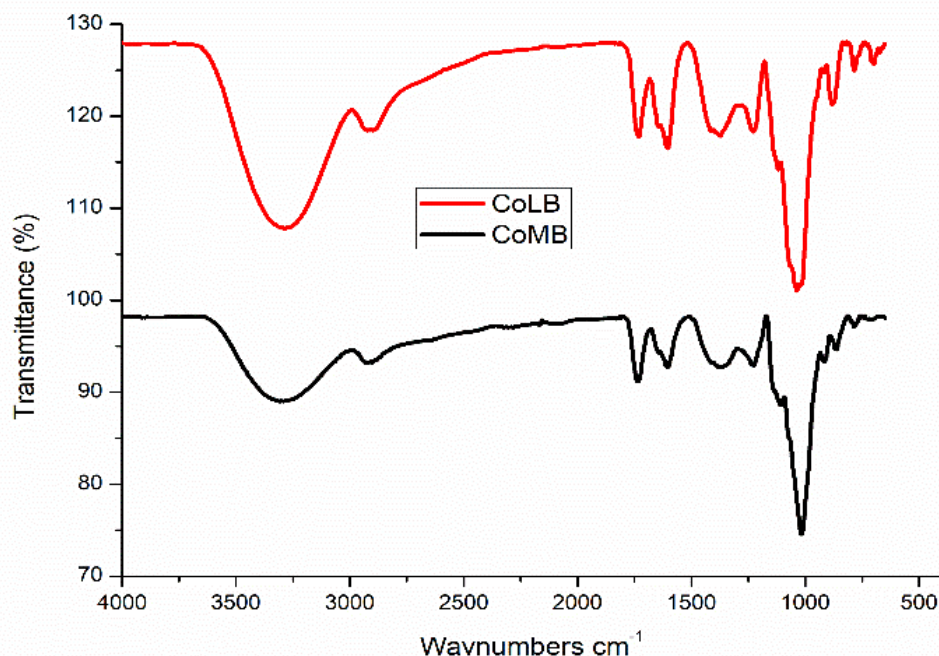


Figure 2.1: FT-IR spectra (500-4000cm⁻¹) of the Co-leaching products with HLB and HMB identified as [Co(LB)₂(H₂O)₂] (red spectrum) and supposed to be [Co(MB)₂(H₂O)₂] (black spectrum), respectively.

The known [Co₃(Cit)₂(H₂O)_n] and [Co(HMal)₂(H₂O)₄] were isolate and fully characterized from ethanol solutions and their characterization is described in Chapter 3. [Co(HMal)₂(H₂O)₄] crystals suitable for X-ray characterization, were also grown from this solvent.

Besides the FT-IR and CH-elemental analysis characterization for the bulk material, well-shaped crystals for [Co(Suc)(H₂O)_n] and [Co(It)(H₂O)_n]₃ were obtained by slow diffusion of acetone into an aqueous solution of the product mediated by agar gel. Single crystal X-ray measurements on the two samples identified the former as the known [Co(Suc)(H₂O)₄], while the latter as the novel [Co(It)(H₂O)₂]₃ complex.

Fig. 2.2 summarizes crystal structure and parameters (details in Appendix A5).

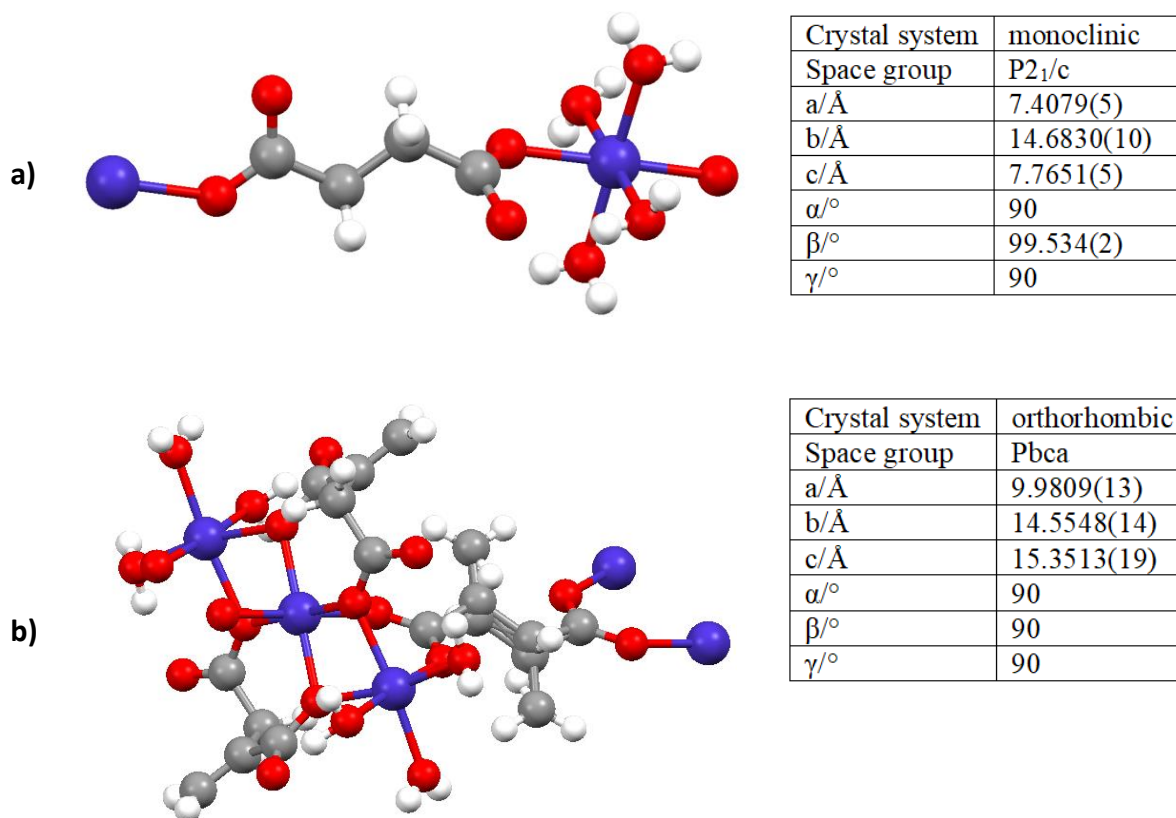


Figure 2.2: Molecular structure and crystal parameters for: a) [Co(Suc)(H₂O)₄][36] and b) [Co(It)(H₂O)₂]₃ complex.³ Color legend: blue, Co; red, O; grey, C; white, H.

Even if an extensive description of the crystal structure of the products overcomes the scope of this work, it is worthy to note that all the compounds reported here are characterized bearing Co(II) in an octahedral environment, where the anionic form of the acid coordinates the metal center as monodentate or bidentate, chelating and/or bridging ligand and the coordination sphere is completed by water molecules according with the literature.[36][37][38][39][40] Specifically, the new [Co(It)(H₂O)₂]₃ compound shows a peculiar trimeric structure where two It²⁻ anions behave as bidentate chelating ligands on the central Co atom and bridged with the two peripheral Co atoms. Further two It²⁻ anions act as monodentate on the central Co atom and behave as bridging ligands between two adjacent trimeric structures. The coordination sphere of the two peripheral Co atoms is completed by water molecules.

Finally, due to the pink color of the leachate, we can speculate an octahedral Co(II) compound was also formed in the reaction between Co and HArg despite the identification is still in

³ Single crystal X-ray diffractometric studies were performed by Prof. Luciano Marchiò, Department of Chemical Science, Life and Environmental Sustainability, University of Parma (IT). See Appendix A5 for details.

progress. Examples of crystal structures for Co-argininate compounds are also not reported in the literature for suggesting a possible stoichiometry.

Among the reactions, in the case of maleic, citric, succinic, itaconic and L-arginine acids, the leaching was accompanied by a noticeable H₂ gas evolution. These results were supported by running the reactions into capped plastic bottles in rotation mixing mode: where noticeable H₂ evolution in an open flask under magnetic bar stirring was observed, a visible bottle expansion in the rotating closed system occurred; where there was no evidence of gas formation in the open flask, an evident gas consumption in the closed vessel (visible bottle shrink) occurred. Differently, in the case of succinic and itaconic acid leaching, despite a noticeable gas evolution was present in the open flask reaction, no significant effects on the volume of the bottle when performed in the closed environment, were observed. This evidence suggested that, besides H₂ production, O₂ consumption may occur with similar rates, stimulating further investigations. On the bases of the demonstrated complexing and oxidizing capabilities towards Co, an attempted classification of the different acids is here proposed and summarized in **Table 2.3**.

Table 2.3 Classification of the selected bio-derived organic acids.

Class	Main oxidizing agent	pK _{a1}	Complexing behaviour of the anion	Examples
1	H ⁺	≤3.1	coordinating	H ₂ Mal (pK _{a1} : 1.83; monodentate HMal) HArg (pK _{a1} : 2.2; unknown coordination) H ₃ Cit (pK _{a1} : 3.1; polydentate chelating & bridging Cit ³⁻)
2	O ₂	>3.5	coordinating	HLB (pK _{a1} : 3.6; bidentate chelating LB ⁻) HMB (pK _{a1} : 3.8; bidentate chelating MB ⁻) HLat (pK _{a1} : 3.9; bidentate chelating Lat ⁻)
3	H ⁺ , O ₂	>3.5	highly coordinating	H ₂ It (pK _{a1} : 3.8; polydentate chelating & bridging It ²⁻) H ₂ Suc (pK _{a1} : 3.8; bidentate bridging Suc ²⁻)

This classification is based on the assumption that the relative occurrence of the two observed oxidation reactions is related to the relative concentration of the oxidizing species in solution. Indeed, despite the higher reduction potential of O₂, the low solubility and diffusion rate of gaseous O₂ in solution make it a low competitive oxidizing agent. For this reason, H⁺ oxidation is the main reaction towards low potential elements in the case of strong acids (low pK_{a1}) able to provide highly acidic solutions and/or when highly coordinative polydentate anionic species

are formed by metal ion complexation, liberating low acidic H⁺ ions in solution. The stability of the formed complex can also lower the reduction potential of the metal making it easier to be oxidized and affecting the effectiveness of the reaction.

2.2.2 Leaching experiments on recovery powders in water

According to the leaching efficiency and product solubility in aqueous solutions, HLat, H₂Suc, H₂It, HLB, HMB and HArg were selected as the most promising agents to be investigated on real samples in water. H₃Cit and H₂Mal, thanks to their higher acidity which allow them to work as both complexing and oxidizing agents, and good solubility in ethanol, seemed to be more promising for solvometallurgy and their leaching action will be described in Chapter 3. A comparison of leaching systems of succinic acid in methanol and water will be also performed.

Leaching experiments on real WC-Co recovery powders were carried out in the same conditions applied to Co metal powder. Specifically, 250mL of 0.5M aqueous solutions of HLat, HSuc and HArg, as representative of the three different classes of organic acids, were reacted in an open flask with 0.500g aliquots of RC-627C and RC-631L test specimens, at room temperature under magnetic bar stirring. Fig. 3.3 shows the Co-leaching profiles, in terms of yield of leached cobalt (wt. %, by the starting Co amount in the sample) vs time (h), obtained by monitoring the amount of cobalt in the leachates of the test specimens in time (1h steps). The Co amount in the leachate was determined by ICP-OES measurements on digested measured aliquots of the solution, as detailed in Appendix A6

As shown, the three acids demonstrated to be effective in cobalt dissolution achieving an almost complete Co-dissolution in very mild conditions and short times, specifically 3 and 4h for HLat and H₂Suc, respectively from RC-627C. Co-leaching on RC-631L demonstrated to be slightly less efficient than observed on RC-627C but still satisfactory, obtaining around the 90% Co-dissolution in 5, 5 and 10h by HLat, H₂Suc and HArg, respectively. This difference can be reasonably attributed to the lower values of the WC particles mean grain size and of the metallic binder mean free-path of the RC-631L test specimen.

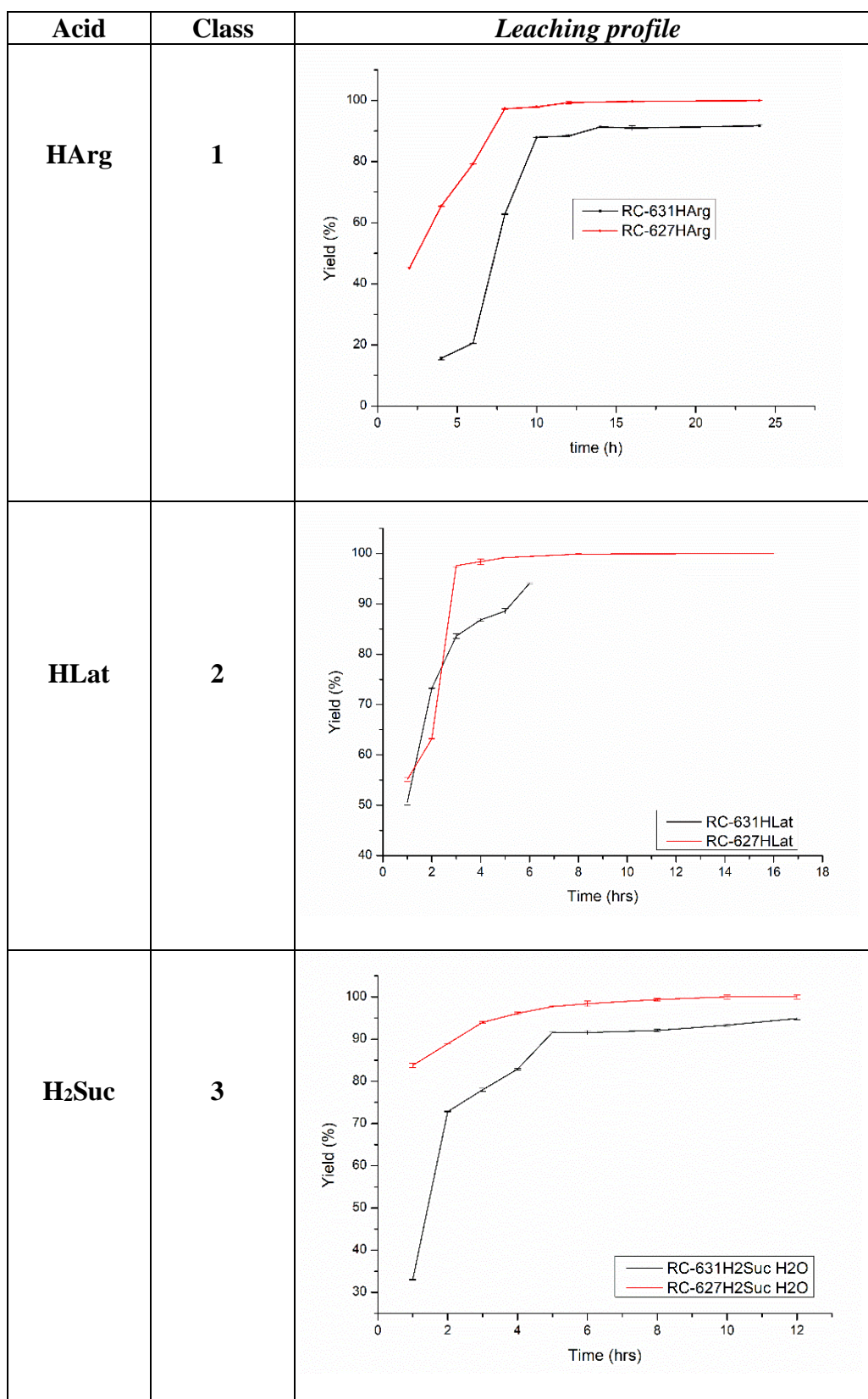


Figure 2.3: Co-leaching profiles from RC-627C and RC-631L recovery powders (0.5g) on varying the leaching agent and times. Experimental conditions: [Acid] = 0.5M; r.T. and pressure; stirring. Results are reported as the average values of two different experiments. Bars represent the standard deviation.

Additional characterization was performed on the solid residues after leaching to point out the complete Co-dissolution and the presence of W-based phases. In particular, powder X-ray diffraction (p-XRD)⁴ and SEM/EDS analysis were made on the RC-631L sample before and after leaching with several of the systems under study. Specifically, treatments lasting 4h on 0.5g test specimen and 6h on 0.1g test specimen were carried out with HLat and H₂Suc 0.5M solutions, respectively, at room conditions under magnetic bar stirring. Fig. 2.4 summarizes p-XRD patterns for RC-631L before and after treatment with HLat and H₂Suc.

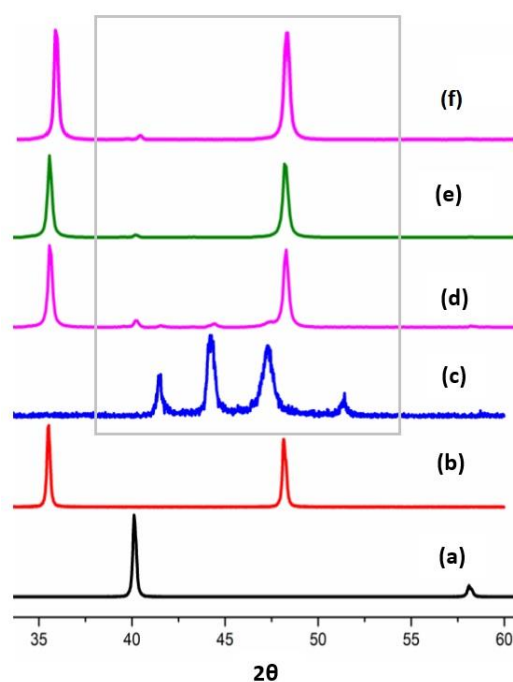


Figure 2.4: P-XRD patterns⁴ of: a) W powder; b) WC powder; c) Co powder; d) RC-631C before Co-leaching; e) RC-631L after 6h leaching with H₂Suc; f) RC-631L after 4h leaching with HLat. Patterns collected for the RC-627C samples, before and after leaching, were superimposable to those of RC-631L samples and are omitted.

The XRD pattern of the sample before (**Fig. 2.4d**) and after leaching (**Figs. 2.4 e and f**) clearly showed the disappearance of Co metal peaks after treatment, highlighting the dissolution of cobalt in HLat and H₂Suc solutions after 4 and 6h leaching, respectively. Furthermore, the patterns collected after treatment showed no changes in the other parts of the diffractogram in terms of the disappearance of existing species or the appearance of new peaks related to newly formed species. This evidence demonstrates the capability of the solutions of these acids to

⁴ Powder X-Ray diffractometric studies (p-XRD) were performed by Dr. Stefano Cara, IGAG-CNR institute, Cagliari, Italy. See Appendix A3 for details.

dissolve Co selectively leaving W and WC unreacted. A deeper investigation was done on the two treated samples by SEM/EDS measurements. Figs. 2.5 and 2.6 illustrated the SEM/EDS images of RC-631L before and after 4 and 6h of cobalt leaching with HLat and H₂Suc respectively.

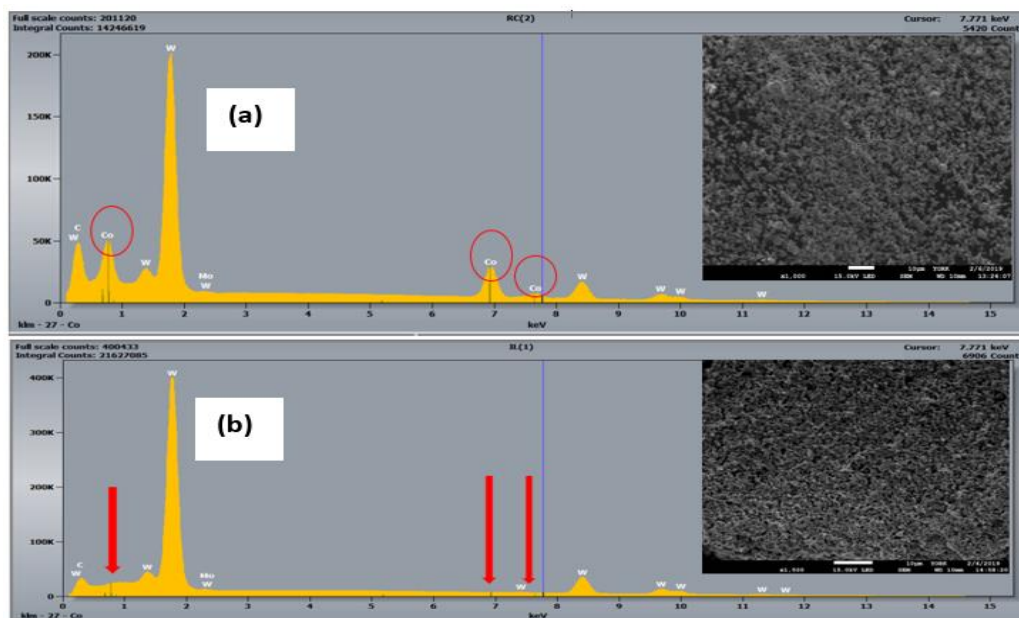


Figure 2.5: SEM micrographs and EDS spectra (wt. %) of RC-631L; (a) before Co-leaching (W = 73.44; Co = 25.87; Ni = 0.14); and b) after 4 hours Co-leaching in 0.5M HLat solution at r.T. in water (W= 100).

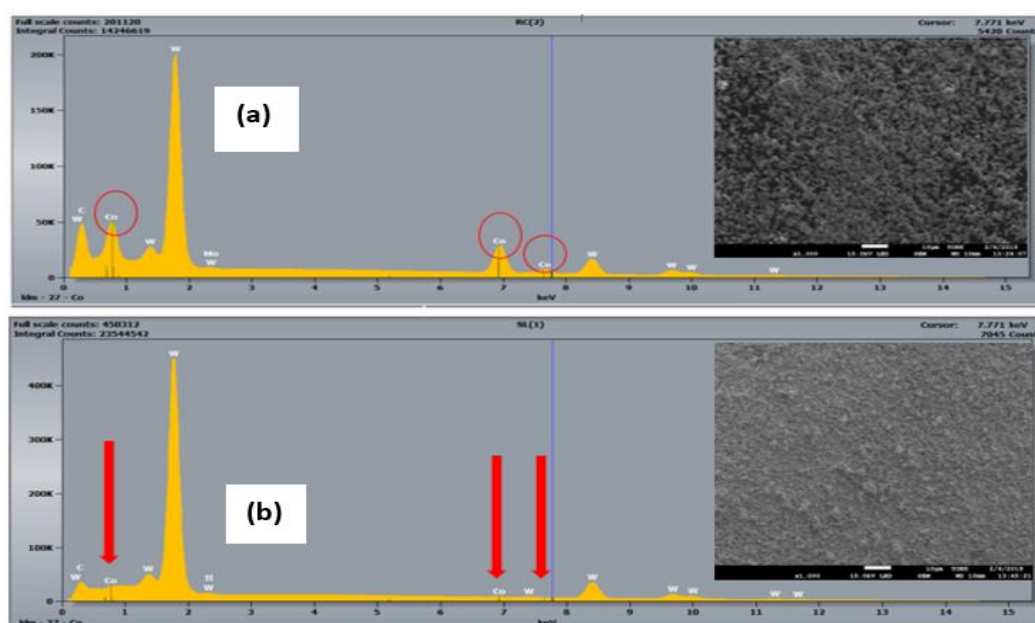


Figure 2.6: SEM micrographs and EDS spectra (wt. %) of RC-631L; (a) before Co-leaching (W = 73.44; Co = 25.87; Ni = 0.14); and b) after 6h of Co-leaching with 0.5M H₂Suc water solution (W= 99.18; Co = 0.49).

P-XRD and SEM/EDS demonstrated to be very diagnostic and fast tools for monitoring the reactions being able of pointing out the progress of the Co-leaching through the lowering of Co peaks without requiring any additional sample treatment for analysis.

In order to check the activity on real samples treated by lactobionic, maltobionic and itaconic acids, 0.5M leaching solutions were prepared and applied for treatment on 0.1g of the RC-631L test specimen for 4h at room conditions. P-XRD and SEM/EDS measurements were hence performed for solid residues characterization and the graphics are reported in **Figs. 2.7** and **2.8**, respectively.

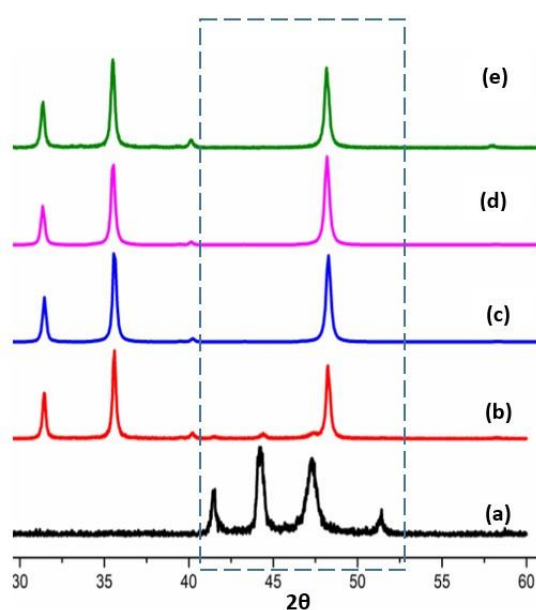


Figure 2.7: P-XRD patterns⁴ of: a) Co powder; b) RC-631L before Co-leaching; and after 4h laching with (c) HLB; (d) HMB and (e) H₂It. [Acid] = 0.5M; room conditions.

As shown, solid state characterization highlights the complete Co removal in just 4h with these three leaching solutions.

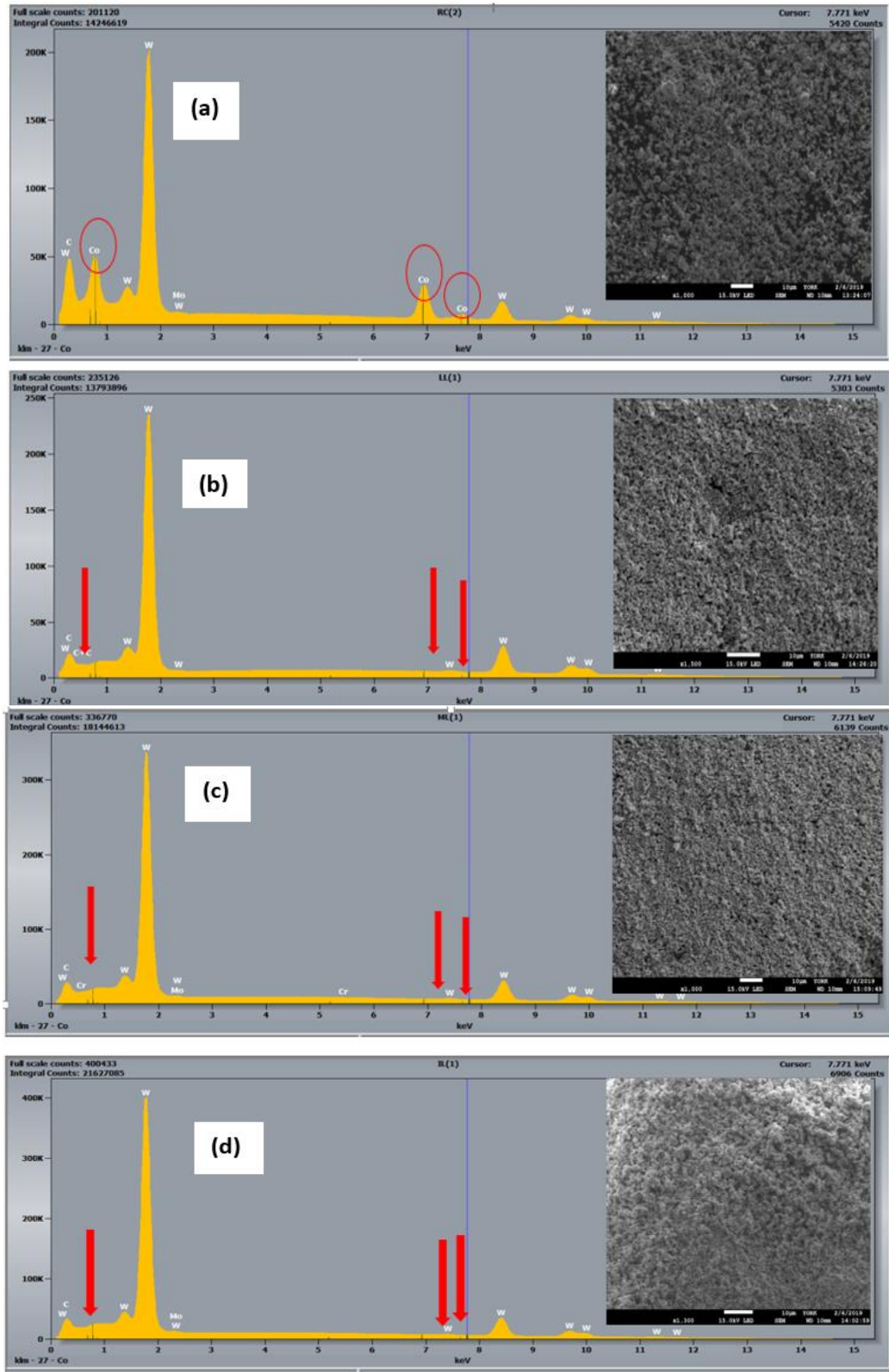


Figure 2.8: SEM micrographs and EDS spectra (wt. %) of RC-631L; (a) before Co-leaching (W = 73.44; Co = 25.87; Ni = 0.14); and after 4h leaching at room conditions and [Acid] = 0.5M; of (b) HLB (W = 100); (c) HMB (W = 99.37; Co = 0.67) and (d) H₂It (W = 99.76).

2.3 Conclusion

A simple and environmentally friendly hydrometallurgical route for Co selective dissolution from HM wastes was developed by using weak, bio-derived and easily biodegradable organic acids. In this study organic acids namely HLat, H₂Suc, HLB, HMB, H₂It and HArg were tested for finding the best conditions for leaching cobalt from WC-Co wastes in water. Thereby, all of them seemed to be very efficient due to their capacity to dissolve quantitatively Co in aqueous solutions from HM by-products at low concentration level and room conditions in a very short time and leaving the residual WC unreacted and ready to be re-employed for industrial purposes. Among them, particular attention will be devoted to the use of HLat in hydrometallurgy because its effectiveness, low cost, sustainability and large availability through biotechnological fermentative processes. H₃Cit and H₂Mal were also preliminarily checked in water, showing good efficiencies but they were not more deeply investigated due to the undesired abundant precipitations occurring during the reactions and for their good solubility in EtOH which makes them very appealing for solvometallurgy. Finally, two new unknown compounds were found and characterized in this work, namely [Co(It)(H₂O)₂]₃ and [Co(MB)₂(H₂O)₂], the former isolated in crystals suitable for X-Ray analysis.

2.4 Experimental⁵

2.4.1 Synthesis of Co-complexes by acid leaching in aqueous solution

Co metal powder (0.020g, 0.34mmol) was reacted for around 4h with 0.050L of a 0.5M aqueous leaching solution of the selected acid in an open flask under room conditions (approximately 20°C and 1 atm) and magnetic bar stirring (300 rpm). The solutions turned readily from colorless to bright pink and the disappearance of Co powder occurred in short time. The obtained cobalt complex was easily precipitated from the leaching solution through solvent evaporation and acetone washing. The dried solid was subsequently characterized as follows.

2.4.2 Characterization of cobalt complexes

[Co(Lat)₂(H₂O)₂]

Leaching time: 4h; Yield: 71%

CH-elemental analysis. Found: C% 26.39, H% 5.17 (calculated for CoC₆H₁₄O₈, FW=273.10 g

⁵ See Appendix A3 for the materials and methods.

mol⁻¹: C% 26.39, H% 5.16).

FT-IR (ATR-mode, cm⁻¹). 3050br; 2974mw; 2943w; 2735vw; 2680br; 1628vs; 1465w; 1350s; 1272w; 1110vs; 1040s; 940vw; 860vs; 760s; 668s.

Thermogravimetric analysis (TGA): see Appendix A4.

[Co(Suc)(H₂O)_n]_m

Leaching time: 4h. Yield: 73%

CH-elemental analysis. Found: C% 24.50, H% 3.41 (calculated for CoC₄H₁₂O₈, FW=193.01 g mol⁻¹: C% 24.89, H% 3.13)

FT-IR (ATR-mode, cm⁻¹). 3200vbr; 2929vw; 2533vw; 1837vw; 1685w; 1550vs; 1400s 1395s; 1310w; 893s; 799w; 660vw.

Thermogravimetric analysis (TGA): see Appendix A4.

Well-shaped crystals suitable for single crystal X-ray diffraction measurements were growing up by slow diffusion of acetone in the aqueous solution of the purified product with the addition of 0.5% w/w of agar gel and washed with ethyl ether. As reported in Fig. 2.2a, the found molecular structure for the sample corresponds to the already known [Co(Suc)(H₂O)₄]_m compound.

[Co(LB)₂(H₂O)₂]

Leaching time: 4h.

CH-elemental analysis. Found: C% 35.15, H% 6.10 (calculated for CoC₂₄H₄₆O₂₆, FW=809.53 g mol⁻¹: C% 35.61, H% 5.73).

FT-IR (ATR-mode, cm⁻¹). 3276s; 2897br; 1728m; 1604s; 1372br; 1233w; 1039vs; 877mw; 784w; 691vw.

Thermogravimetric analysis (TGA): see Appendix A4.

[Co(MB)₂(H₂O)₂]

Leaching time: 4h.

CH-elemental analysis. Found: C% 35.35, H% 5.26 (calculated for $\text{CoC}_{24}\text{H}_{46}\text{O}_{26}$, FW=809.53g mol⁻¹: C% 35.61, H% 5.73).

FT-IR (ATR-mode, cm⁻¹). 3300vbr; 2928br; 1736m; 159m); 1364br; 1225mw; 1016vs; 916vw; 861vw; 784vw; 714vw.

Thermogravimetric analysis (TGA): see Appendix A4.

[Co(It)(H₂O)_n]₃

Leaching time: 4h.

CH-elemental analysis. Found: C% 30.43, H% 2.86 (calculated for $\text{Co}_3\text{C}_{15}\text{H}_{18}\text{O}_{15}$, FW=615.08g mol⁻¹: C% 29.30, H% 2.94).

FT-IR (ATR-mode, cm⁻¹). 3362vbr; 2974vw; 1543vs; 1387vs; 1241s; 1147w; 947m; 877w; 830m; 768vw; 691w.

Thermogravimetric analysis (TGA): see Appendix A4.

Well-shaped crystals suitable for single crystal x-ray diffraction measurements were growing up by slow diffusion of acetone in the aqueous solution of the purified product with the addition of 0.5% w/w of agar gel and washed with ethyl ether. See Appendix A5 for tables, data and .cif file of the refined molecular structure of $[\text{Co}(\text{It})(\text{H}_2\text{O})_2]_3$.

2.4.3 Leaching experiments in attrition mode

Cobalt powder (0.16g) was reacted with the leaching solution (400mL) inside a closed plastic container housed on a Heidolph REAX 20 rotating system at a speed of 5 rpm.

2.5 References

- [1] P. Meshram, L. Bhagat, U. Prakash, and B. D. Pandey, "Organic acid leaching of base metals from copper granulated slag and evaluation of mechanism," *Can. Metall. Q.*, 2017, vol. 56(2), pp. 168–178.
- [2] M. Gergoric, C. Ravaux, B. Steenari, and F. Espegren, "Leaching and Recovery of Rare-Earth Elements from Neodymium Magnet Waste Using Organic Acids," pp. 1–17, 2018.
- [3] C. Edtmaier *et al.*, "Selective removal of the cobalt binder in WC/Co based hardmetal scraps by acetic acid leaching," *Hydrometallurgy*, vol. 76, no. 1–2, pp. 63–71, 2005.

- [4] R. Golmohammadzadeh, F. Faraji, and F. Rashchi, "Recovery of lithium and cobalt from spent lithium ion batteries (LIBs) using organic acids as leaching reagents: A review," *Resour. Conserv. Recycl.*, vol. 136, no. February 2018, pp. 418–435, 2018.
- [5] L. Li *et al.*, "Recovery of metals from spent lithium-ion batteries with organic acids as leaching reagents and environmental assessment," *J. Power Sources*, vol. 233, pp. 180–189, 2013.
- [6] B. Seo and S. Kim, "Cobalt extraction from tungsten carbide-cobalt (WC-Co) hard metal scraps using malic acid," *Int. J. Miner. Process.*, vol. 151, pp. 1–7, 2016.
- [7] T. Kurzrock and D. Weuster-Botz, "Recovery of succinic acid from fermentation broth," *Biotechnol. Lett.*, vol. 32, no. 3, pp. 331–339, 2010.
- [8] M. Dusselier, P. Van Wouwe, A. Dewaele, E. Makshina, and B. F. Sels, "Lactic acid as a platform chemical in the biobased economy: The role of chemocatalysis," *Energy Environ. Sci.*, vol. 6, no. 5, pp. 1415–1442, 2013.
- [9] B. E. Teleky and D. C. Vodnar, "Biomass-derived production of itaconic acid as a building block in specialty polymers," *Polymers (Basel)*, vol. 11, no. 6, 2019.
- [10] V. Abilities, "a N D Visuospatial a N D," vol. 1, no. 2, pp. 439–452, 1978.
- [11] S. Alonso, M. Rendueles, and M. Díaz, "Bio-production of lactobionic acid: Current status, applications and future prospects," *Biotechnol. Adv.*, vol. 31, no. 8, pp. 1275–1291, 2013.
- [12] N. Vassilev, "Organic acid production by immobilized filamentous fungi," *Top. Catal.*, vol. 5, no. 4, pp. 188–190, 1991.
- [13] V. L. Albaugh, M. K. Stewart, and A. Barbul, *Cellular and Physiological Effects of Arginine in Seniors*. Elsevier Inc., 2017.
- [14] S. Shi, H. Guo, and G. Yin, "Synthesis of maleic acid from renewable resources: Catalytic oxidation of furfural in liquid media with dioxygen," *Catal. Commun.*, vol. 12, no. 8, pp. 731–733, 2011.
- [15] A. Komesu, J. A. R. de Oliveira, L. H. da S. Martins, M. R. W. Maciel, and R. M. Filho, "Lactic acid production to purification: A review," *BioResources*, vol. 12, no. 2, pp. 4364–4383, 2017.
- [16] P. Mäki-Arvela, I. L. Simakova, T. Salmi, and D. Y. Murzin, "Production of lactic acid/lactates from biomass and their catalytic transformations to commodities," *Chem. Rev.*, vol. 114, no. 3, pp. 1909–1971, 2014.
- [17] S. Trakarnpaiboon, N. Srisuk, K. Piyachomkwan, S. T. Yang, and V. Kitpreechavanich, "L-Lactic acid production from liquefied cassava starch by thermotolerant *Rhizopus*

- microsporus: Characterization and optimization,” *Process Biochem.*, vol. 63, pp. 26–34, 2017.
- [18] M. A. Abdel-rahman, Y. Tashiro, and K. Sonomoto, “Recent advances in lactic acid production by microbial fermentation processes,” *Biotechnol. Adv.*, vol. 31, no. 6, pp. 877–902, 2013.
- [19] L. A. Anderson, M. A. Islam, and K. L. J. Prather, “Synthetic biology strategies for improving microbial synthesis of ‘green’ biopolymers,” *J. Biol. Chem.*, vol. 293, no. 14, pp. 5053–5061, 2018.
- [20] M. A. Abdel-Rahman, Y. Tashiro, and K. Sonomoto, “Lactic acid production from lignocellulose-derived sugars using lactic acid bacteria: Overview and limits,” *J. Biotechnol.*, vol. 156, no. 4, pp. 286–301, 2011.
- [21] M. A. Abdel-rahman and K. Sonomoto, “Authors : Affiliations :,” *J. Biotechnol.*, 2016.
- [22] H. Song and S. Y. Lee, “Production of succinic acid by bacterial fermentation,” *Enzyme Microb. Technol.*, vol. 39, no. 3, pp. 352–361, 2006.
- [23] P. C. Lee, S. Y. Lee, and H. N. Chang, “Succinic acid production by *Anaerobiospirillum succiniciproducens* ATCC 29305 growing on galactose, galactose/glucose, and galactose/lactose,” *J. Microbiol. Biotechnol.*, vol. 18, no. 11, pp. 1792–1796, 2008.
- [24] J. C. da Cruz, E. F. Camporese Sérvulo, and A. M. de Castro, *Microbial Production of Itaconic Acid*, no. November. Elsevier Inc., 2017.
- [25] S. Alonso, M. Rendueles, and M. Díaz, “Efficient lactobionic acid production from whey by *Pseudomonas taetrolens* under pH-shift conditions,” *Bioresour. Technol.*, vol. 102, no. 20, pp. 9730–9736, 2011.
- [26] N. Minal, Bharwade, S. Balakrishnan, N. N. Chaudhary, and A. K. Jain, “Lactobionic Acid: Significance and Application in Food and Pharmaceutical,” *Int. J. Fermented Foods*, vol. 6, no. 1, p. 25, 2017.
- [27] F. Smeets, “Microbial production of citric acid,” *Antonie Van Leeuwenhoek*, vol. 49, no. 1, pp. 86–87, 1983.
- [28] M. Berovic and M. Legisa, “Citric acid production,” *Biotechnol. Annu. Rev.*, vol. 13, no. 07, pp. 303–343, 2007.
- [29] N. Araji, D. D. Madjinza, G. Chatel, A. Moores, F. Jérôme, and K. De Oliveira Vigier, “Synthesis of maleic and fumaric acids from furfural in the presence of betaine hydrochloride and hydrogen peroxide,” *Green Chem.*, vol. 19, no. 1, pp. 98–101, 2017.
- [30] M. Sethurajan, E. D. Van Hullebusch, and Y. V. Nancharaiyah, “Biotechnology in the management and resource recovery from metal bearing solid wastes : Recent advances,”

- J. Environ. Manage.*, vol. 211, pp. 138–153, 2018.
- [31] R. Wojcieszak, F. Santarelli, S. Paul, F. Dumeignil, F. Cavani, and R. V Gonçalves, “Recent developments in maleic acid synthesis from bio-based chemicals,” *Sustain. Chem. Process.*, vol. 3, no. 1, pp. 1–11, 2015.
- [32] T. Utagawa, “and Clinical Significance Production of Arginine by Fermentation 1,” *J. Nutr.*, vol. 134, no. February, pp. 2854–2857, 2004.
- [33] J. H. Shin and S. Y. Lee, “Metabolic engineering of microorganisms for the production of L-arginine and its derivatives,” *Microb. Cell Fact.*, vol. 13, no. 1, pp. 1–11, 2014.
- [34] F. J. J. Kellner, H. Hildebrand, and S. Virtanen, “Effect of WC grain size on the corrosion behavior of WC-Co based hardmetals in alkaline solutions,” *Int. J. Refract. Met. Hard Mater.*, vol. 27, no. 4, pp. 806–812, 2009.
- [35] J. Gurland and P. Bardzil, “Relation of Strength, Composition, and Grain Size of Sintered WC-Co Alloys,” *Jom*, vol. 7, no. 2, pp. 311–315, 1955.
- [36] “Studies on cobalt succinate tetrahydrate crystals Chapter 6 Studies on cobalt succinate tetrahydrate crystals,” 2014.
- [37] A. A. Frutos, G. M. Escandar, J. M. Salas Peregrin, M. Gonzalez Sierra, and L. F. Sala, “Complex formation between D-lactobionate and bivalent metal ions. Studies in solution and in the solid state,” *Can. J. Chem.*, vol. 75, no. 4, pp. 405–413, 1997.
- [38] L. Wang, N. Xu, X. Pan, Y. He, X. Wang, and W. Su, “Cobalt lactate complex as a hole cocatalyst for significantly enhanced photocatalytic H₂ production activity over CdS nanorods,” *Catal. Sci. Technol.*, vol. 8, no. 6, pp. 1599–1605, 2018.
- [39] Cobalt Development Institute, “Cobalt in Chemicals,” *Cobalt Facts*, pp. 29–40, 2006.
- [40] S. Chandran, R. Jagan, R. Paulraj, and P. Ramasamy, “Spectral, mechanical, thermal, optical and solid state parameters, of metal-organic bis(hydrogenmaleate)-CO(II) tetrahydrate crystal,” *J. Solid State Chem.*, vol. 230, no. June 2015, pp. 135–142, 2015.

Non-water selective bio-derived organic acid lixiviants for cobalt

3.1 Introduction

As described in Chapter 1, HM life-cycle involves the production of WC-Co waste materials that need a fine tuning of the Co content for making them reusable for practical purposes. Hydrometallurgy may represent an attractive alternative to energy-intensive thermal treatments, providing, if well designed, a direct and selective dissolution of the binder phase leaving WC-matrix unreacted. A promising attempt of hydrometallurgical leaching of Co from WC-Co HM scraps was proposed using acetic acid (concentration: 3.6 M; pressure: 1–5 kPa; T: 40-80°C; t: 2.6-6.5 days) in the presence of oxygen, achieving a quite satisfactory 85% Co-leaching yield.[1] This fundamental finding demonstrated the possibility of using eco-friendly weak organic acids as a valued alternative to the hazardous strong inorganic acids more widely used in this field. Nevertheless, the effectiveness of this approach is in some way limited by the relatively high pKa of the acetic acid which, indeed, require the addition of an external oxidant, i.e. O₂ under pressure, to promote leaching. Beside its ready availability, the low solubility of gaseous O₂ in water heavily affects the reaction rate. In order to overcome this limitation, organic acids, such as acetic or formic acids, were proposed acting in the presence of a stronger and water soluble oxidant, H₂O₂, with promising results.[2] However, undesirable oxidation/hydration phenomena were observed on the recovered WC particles' surfaces, due mainly to the use of water as solvent [3] and the presence of a strong oxidizing agent such as H₂O₂ able to interact both with W and WC.[4][5][6][7][8] Recovered powders with O% > 0.40 would result in poor quality HM tools. Thus, further thermal treatments under reducing conditions are required to achieve the desired powder composition for HM manufacturing, adding costly steps to the recovery process. The use of non-water solvents for leaching sounds as an intriguing alternative to water systems. To the best of our knowledge, to date no solvometallurgy processes have been still proposed. The working hypothesis is that the use of sustainable organic solvents like alcohols instead of water on treating HM powders would be particularly desirable, because it promises to prevent undesired oxidation and hydration phenomena on the WC surface. Moreover, besides some critical aspects such as cost and flammability, they can be easily recycled at the end of the process avoiding wastewater production. Among, alcohols, ethanol seems particularly appealing being a good solvent for several organic acids and considered a *green* solvent being renewable, increasingly available, easy to transport, safe to handle, biodegradable, low in toxicity and largely produced from biomasses, plants and wasted materials.[9]

In this context, Chapter 3 will describe the use of several organic acids in diluted alcoholic solutions as leaching agents for cobalt, also contained in the complex matrix of WC-Co recovery powders.

3.1.1 Selected leaching agents for cobalt in alcohol

Maleic and citric acids were chosen as optimal candidates for Co-solvometallurgy due to their good solubility in ethanol, relatively low cost, and the demonstrated capability in water to couple oxidizing, by H^+ , with complexing properties (lower pK_{a1} with respect to the other tested organic acids, see Chapter 2).

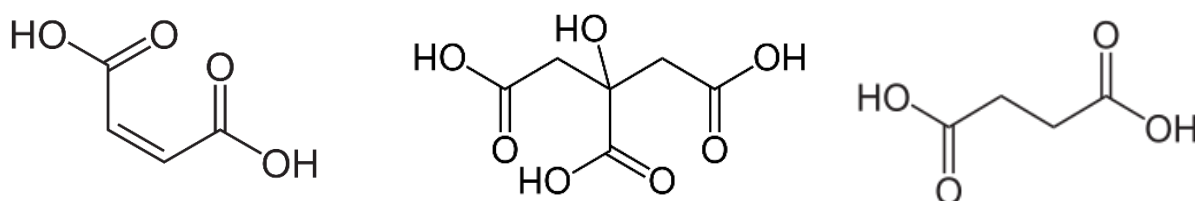


Figure 3.1. Maleic (H₂Mal), citric (H₃Cit) and succinic (H₂Suc) acids.

Besides its conventional low sustainable industrial production from benzene, maleic acid is a non-toxic compound which can be produced, through a greener process, by fungi such as *Aspergillus niger*, from renewable substrates[10] or synthesized through sustainable biomass-based feedstocks catalytic conversion.[11] Citric acid is well-known to be biodegradable, eco-friendly, economical and safe and is produced chemically from glycerol after being isolated previously from the lemon juice as calcium citrate.[12] Several micro-organisms, including bacteria, fungi and yeasts, were reported to be employed to produce citric acid such as yeasts *Saccharomycopsis sp.*, fungus *Aspergillus niger* by fermentation of glucose or sucrose.[14][13] On the bases of similar considerations, good solubility in methanol and demonstrated oxidizing behavior in water, succinic acid was also selected to be studied as Co-leaching agent in methanol.

Finally, lactic acid was checked for reactivity in ethanol, as an example of acid with negligible oxidizing properties, expecting low reaction rates towards cobalt due to the low solubility of O₂ in alcohol.

3.1.2. Test specimen definition

As introduced in Chapter 2, the real samples studied in this work are WC-Co recovery powders (RC-627C and RC-631L) generated during machining operations of HM manufacturing. The Co content of the binder phases in the recovery powders was 19.55 and 20.4 wt. % respectively (see details in Appendix A1 and 2.1.2 section).

3.2 Results and Discussion

3.2.1 Leaching experiments on Co powder in ethanol

With the view to study the chemical reactivity of the selected lixivants towards metallic cobalt in ethanol, Co powders were reacted with a calculated excess of H₂Mal, H₃Cit and HLat ethanol solutions at concentrations ranging from 0.1 to 1M both at room and refluxing temperature under magnetic bar stirring. Table 3.1 summarizes the found leaching times, in terms of times of complete disappearance of Co powder, for the different agents and conditions.

Table 3.1. Indicative Co powder (20 mg) leaching times by 50mL of H₂Mal, H₃Cit and HLat ethanolic solutions, at room temperature (r.T., 20-25°C) as well as at reflux (Δ , 78.4°C), on varying the lixiviant concentration. *Results obtained as the average value of two independent repetitions.

Acid	Temp.	Leaching time (h) at		
		0.1M	0.5M	1M
Hlat	r. T.	48	40	38
	Δ	n.a.	40	48
H ₃ Cit	r. T.	n.a.	12	12
	Δ	9	7	4
H ₂ Mal	r. T.	3	3	2

As shown, H₂Mal solutions demonstrated remarkable high efficiency still at low concentration level and room temperature dissolving almost quantitatively Co-powder in very short times. Although the reaction in water still provided satisfactory rates (3h at 0.5M), H₂Mal ethanol leaching adds the significant benefit of not being accompanied by undesired Co-complex precipitation during the process, thanks to the good solubility of the complex in ethanol. Besides, citric acid demonstrated to achieve satisfactory rates working at the refluxing temperature of the solvent still at low concentration level. It is worthy to note that further

experiments were performed at higher H₃Cit concentrations (up to 3M). Despite the Co dissolution rate improved (3M solution: 1h30', Δ; 5h, r.T), a dense gel phase was formed at the bottom of the flask making the separation phase of the cobalt complex by the leachate very difficult. Finally, as expected, HLat demonstrated to be significantly less effective in ethanol than in water both at room temperature and at reflux (5h vs 40h, for both r.T and Δ in water and ethanol, respectively), reasonably due to the low acidity of the compound still in ethanol and the negligible presence of dissolved O₂ in the leaching solution.

On these bases, in order to pursue the best ethanol solvometallurgy leaching agents and conditions for real WC-Co samples treatments, H₂Mal 0.1-1M solutions were selected as the most performing leaching systems at r.T., and H₃Cit as most eco-friendly appealing reagent working in refluxing ethanol at concentrations not higher than 1M.

The studied leaching reactions in ethanol confirmed pathway and main obtained Co-complexes found for the corresponding reactions in water. While citrate complex precipitated from the leachate in form of powder and hence it was identified by the agreement of the fundamental characterization (CH-elemental analysis, FT-IR and TGA) of the reaction product with literature data, well-shaped crystals of the maleic acid leaching product, suitable for single crystal X-ray diffraction measurements, were growing up by slow diffusion of acetone in the ethanol solution and identified as the known [Co(HMal)₂(H₂O)₄] complex (see crystal structure and parameters in Fig. 3.2)³ in agreement with the bulk characterization (see Experimental).[15]

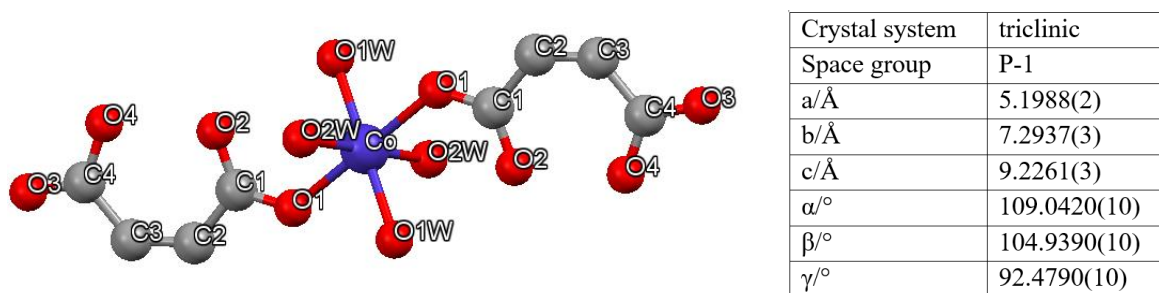
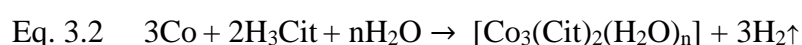


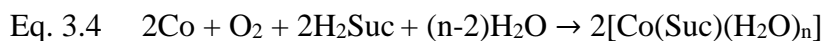
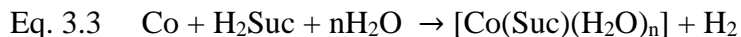
Figure 3.2: Molecular structure and crystal parameters for [Co(HMal)₂(H₂O)₄].[15][16]

Thus, the reactions occur by oxidation and simultaneous complexation of the metal forming, in a single-stage, the known complexes [Co(HMal)₂(H₂O)₄] and [Co₃(Cit)₂(H₂O)_n] by H₂Mal and H₃Cit, respectively, according to the following equations:



3.2.2 Leaching experiments on Co powder with H₂Suc in methanol

As anticipated in Chapter 2, H₂Suc leaching action in water seemed to be based on the twofold pathways involving H⁺ and O₂ as oxidizing agents according to the following reactions:



On these bases, the reaction was run in methanol, where O₂ contribution to the reaction is expected to be negligible. Even in this case, 20mg of Co powder were treated with a 0.5M H₂Suc solution at room temperature in an open flask under magnetic bar stirring. The solution quickly turned to pink and a noticeable gas evolution was observed when the reaction went on and the recorded leaching time, in terms of complete Co-powder dissolution, was about 5h (vs 4h recorded in water). The slightly longer time found in methanol by water furtherly support our hypothesis of a twofold process: 1) H₂Suc works well as complexing/oxidizing specie; 2) the negligible concentration of O₂ in methanol solution limits the occurrence of the reaction of eq. 3.4, lowering the reaction rate.

3.2.3 Leaching experiments on recovery powders

Figure 3.3 shows the Co-leaching profiles, in terms of yield of leached cobalt (wt. %) vs. time (h), obtained by monitoring the amount of cobalt in the leachate of the RC-627C and RC-631L recovery powders in time by treatment of 500mg of test specimen with (a) H₂Mal; (b) H₃Cit; (d) H₂Suc alcoholic solutions. The experimental conditions on recovery powders mimic the most balanced, and comparable among the different acids, conditions applied to Co-powders, in terms of acid solution concentration and volume (0.5M, 250mL), Co:acid molar ratio, temperature and stirring. The Co amount in the leachate was determined by ICP-OES measurements on measured aliquots of the solution, following drying and acid digestion (see Appendix A6).

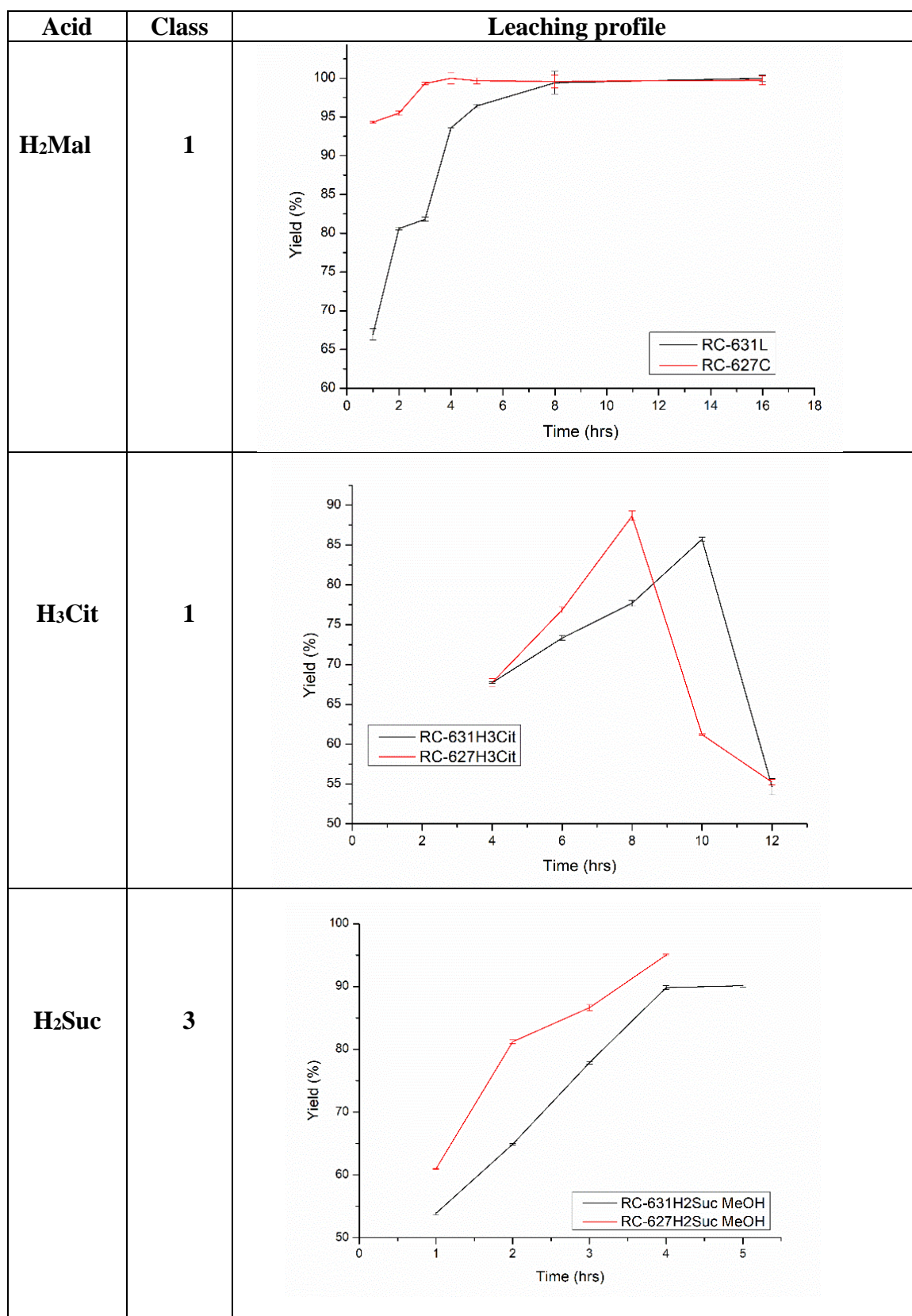


Figure 3.3 Co-leaching profiles from RC-627C and RC-631L recovery powders on varying the leaching times. Leaching system (0.5M): (a) H₂Mal, EtOH, r.T.; (b) H₃Cit, EtOH, r.T and Δ;

(c) H₂Suc, MeOH, r.T. Results obtained as the average value of two independent repetitions. Error bars reported as standard deviation.

Figure 3.3a shows that both test specimens reacted promptly to the leaching with H₂Mal ethanolic solutions, obtaining a 96% yield after just 1h and complete Co removal within 3h for RC-627C, and a 95% yield after 4h and a complete Co removal in 6h for RC-631L. Interesting results were also obtained by H₂Suc methanolic solutions (Figure 3.3c) which showed a good effectiveness, reaching 95% and 90% yields after 5h treatment for RC-627C and RC-631L, respectively. Even if a possible application of H₂Suc in MeOH seemed appealing and can be pursued, the comparative study of H₂Suc water and MeOH Co-leaching profiles, reported respectively in Figure 2.3c and 3.3c, suggested to select hydrometallurgy as the most performing approach for practical purposes. Unexpected trends were instead found for H₃Cit leaching. As shown in Figure 3.3b, experiments both at r.T. and Δ were performed in order, on the one hand, to compare the different leaching systems in the same experimental conditions (i.e. r.T.), and, on the other hand, to investigate on real samples the best conditions previously selected on Co metal (see section 3.2.1) for the specific H₃Cit/EtOH leaching system (i.e. Δ). Focusing on room temperature profiles, Co-dissolution efficiency increases in the first section of the curve, up to 88% in 8h for RC-627C and up to 85% in 10h for RC-631L. Following, the yield of Co dissolution seems to significantly decrease, showing a trend over time contrary to what was expected. A similar, even more dramatic, trend over time was observed under heating the system, where an almost quantitative Co-dissolution yield was recorded after 4h, followed by a ready and continue decrease of the Co amount in solution. In order to correctly interpret the data, it is worthy to note the leaching profiles report the relative amount of cobalt in the leachate with respect to the total amount of Co presents in the treated aliquot of test specimen. These odd results sounded compatible with the precipitation of a low solubility Co-containing compound and led us to investigate deeply the course of the reaction. In agreement, a light pink insoluble compound was found mixed to the residue WC powder, characterized by FT-IR spectroscopy as the known [Co(ox)] (ox = C₂O₄²⁻; oxalate ion). Moreover, High-Performance Liquid Chromatography (HPLC) on the leachate pointed out the presence of oxalic acid in solution. Thus, we speculated during the reaction oxalic acid formation takes place and lead to the low solubility compound. This degradation phenomenon, that is not uncommon with H₃Cit, [12] leads to the decrease of Co-concentration in solution. Despite this hitch that discouraged us from continuing in this direction, due to the found high leaching rates of H₃Cit, its low cost and sustainability, as well as the very low solubility of the

oxalate complex, experiments are in progress with the view to assess the possibility to discriminate the phase of Co efficient leaching by the quantitative precipitation and recovery of the [Co(ox)] product.

Noteworthy, profiles in Figure 3.2 highlighted also the higher leaching efficiency found working on RC-627C powder with respect to RC-631L. This slightly different behavior can be reasonably attributed to the lower values of the WC particles mean grain size and of the metallic binder mean free path.[17]

3.2.4 Solid state characterization of the recovered WC powders after leaching

Among the several acid systems investigated for solvometallurgy, the one based on the use of H₂Mal seemed to be the most promising and worthy to be furtherly investigated for applicative purposes. As anticipated in Chapter 2, p-XRD⁴ and SEM-EDS measurements demonstrated to be diagnostic and fast tools for monitoring the leaching process. Figure 3.3 compares the p-XRD patterns for the RC-627C sample before and after a 4h leaching with 0.5M H₂Mal ethanolic solutions, with the patterns for Co metal e WC as references.

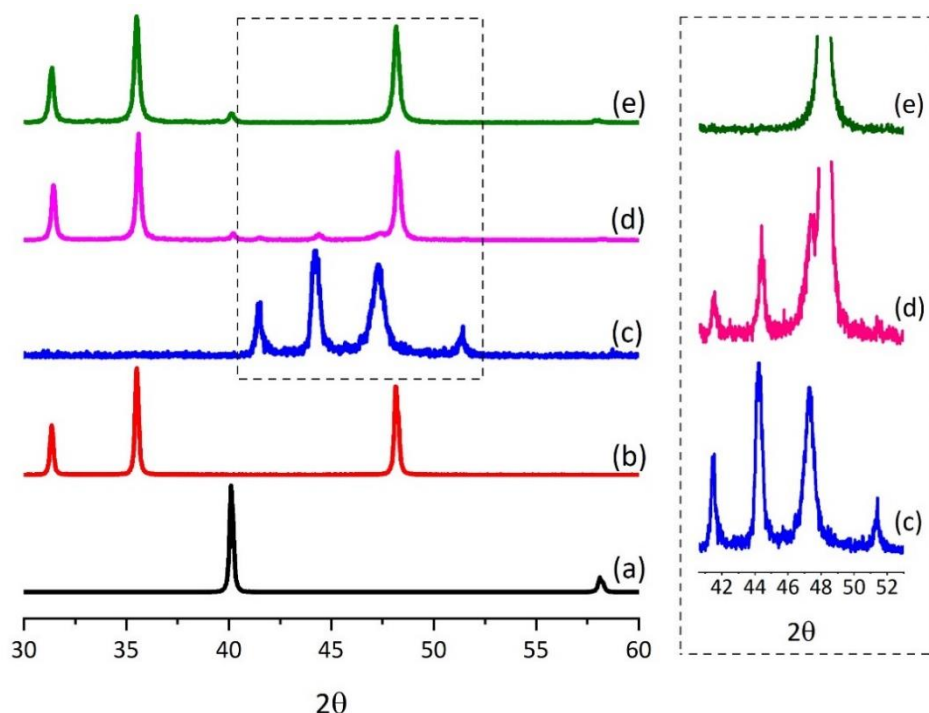


Figure 3.3 P-XRD patterns of: a) W powder; b) WC powder; c) Co powder; d) RC-627C before Co-leaching; e) RC-627C after 4h leaching with 0.5M H₂Mal ethanolic solutions. In the zoom, magnification of c), d and e). Patterns collected for the RC-631L samples, before and after leaching, were superimposable to those of RC-627C samples and are omitted.

The XRD patterns plotted for RC-627C and RC-631L samples before and after leaching, clearly showed the disappearing of Co metal peaks after treatment, highlighting the dissolution of cobalt in the H₂Mal solution after 4h leaching. Furthermore, the patterns collected after treatment showed no changes in the other parts of the spectrum in terms of the disappearance of existing species or the appearance of new peaks related to newly formed species. This evidence demonstrates the capability of ethanolic maleic acid solutions to dissolve Co selectively leaving W and WC unreacted. The evidence related to the complete disappearing of Co peaks in the RC-631L pattern after 4 h leaching, seemed not completely in agreement with the ICP-OES characterization of the leachate which suggested a residual 5% Co in the powder after treatment. A deeper investigation was hence done by SEM/EDS measurements. Figure 3.4 summarizes the SEM/EDS spectra collected on RC-631L sample powder before and after 4h leaching.

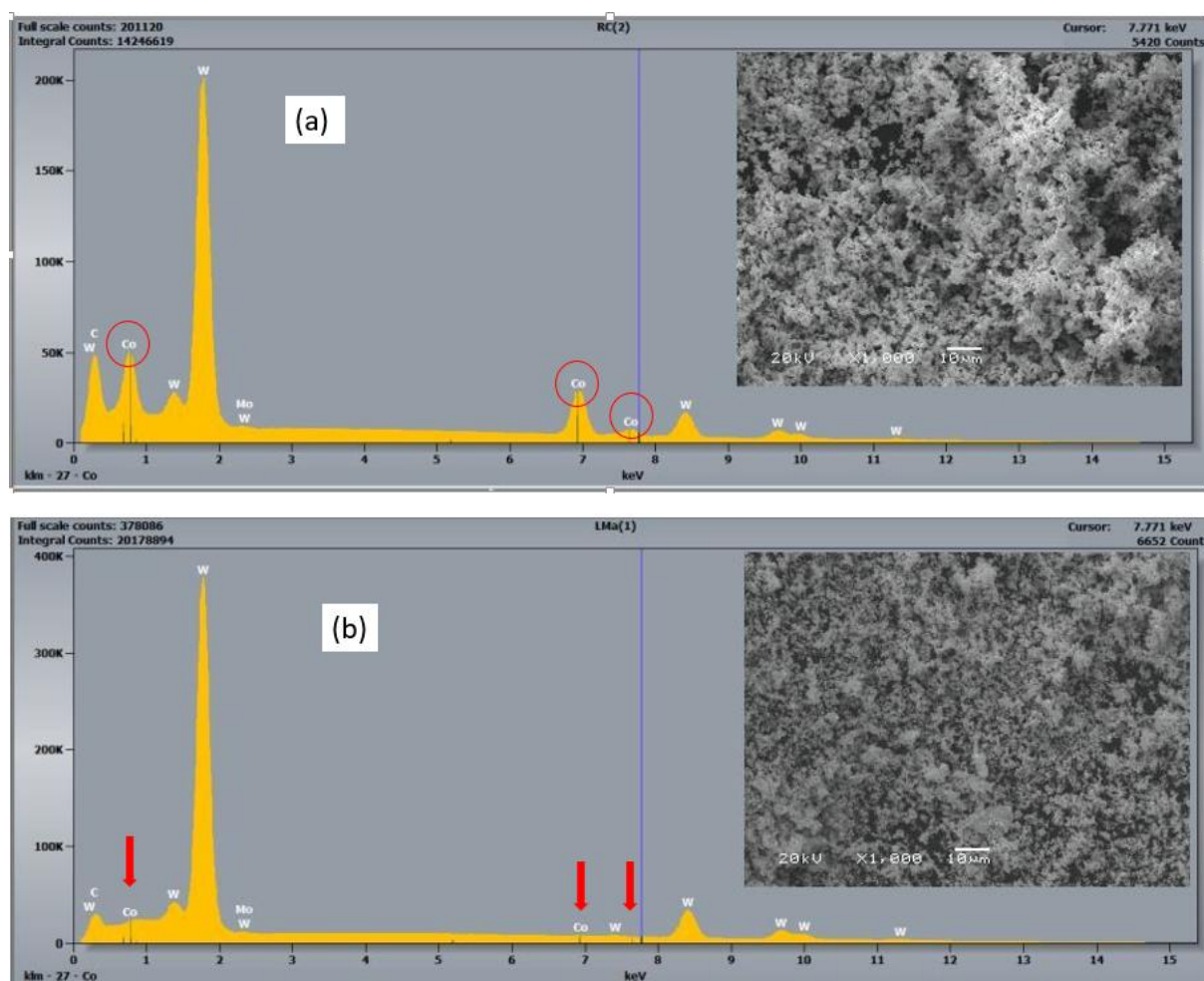


Figure 3.4 SEM micrographs and EDS spectra (wt. %) of RC-631L; (a) before Co-leaching (W = 73.44; Co = 25.87; Ni = 0.14); and b) after 4h Co-leaching with 0.5M H₂Mal ethanolic solutions (W = 99.37; Co = 0.67).

As shown, SEM/EDS demonstrated slight higher sensitivity with respect to the p-XRD measurements, being able to point out, on the one hand, and the progress of the Co-leaching process (through the lowering of Co peaks) and, on the other hand, the small residual amount of Co in this sample after 4h leaching.

It is worthy to note that, as shown, the WC matrix seems to remain unaffected by leaching treatment, first requirement for a ready re-employment of the recovered material in HM manufacturing. Furthermore, with the same aim, leaching times can be tuned in order to achieve recovered powders with the desired Co amounts for production.

3.3 Conclusions

A selection of organic acids – H₂Mal, H₃Cit, H₂Suc – were selected as potential leaching agents for cobalt in alcohol, in order to provide new solvometallurgy systems able to overcome hydrometallurgy disadvantages. Among them, H₂Mal ethanol solutions demonstrated to be the most promising for practical application achieving high efficiency still at low concentration level and room conditions without the addition of external oxidizing agents, dissolving almost quantitatively and selectively Co from HM waste in a short time and leaving the residual WC unreacted. The experiments highlighted also the potential of the proposed method to tune the percentage of Co in the treated powders, meeting the compositional requirements of the industrial HM manufacturing process. Despite slightly less effective, H₂Suc/MeOH demonstrated to be a promising alternative to H₂Mal/EtOH solutions, when solvometallurgy would be preferred to hydrometallurgy. Nevertheless, the higher leaching efficiency as well as the lower concerns related to the industrial use of water with respect to MeOH, prompted us to focus on its use in aqueous solution. Finally, in the case of H₃Cit, despite the effectiveness found in short-time refluxing ethanol leaching reactions, degradation phenomena enhanced by heating promote [Co(Ox)] precipitation and make the reaction less predictable. Further experiments are in progress in order to point out a set of experimental conditions able to discriminate the phase of leaching by the phase of precipitation avoiding undesired separation processes between the residual WC-powder and the insoluble Co-compound.

Based on the promising results obtained by H₂Mal solvometallurgy in EtOH, further investigations addressed to the scale-up of the process, the metallurgical quality assessment of HM artifacts obtained by recovered powders and the recyclability of Co metal, were performed and the results of these studies are described in Chapter 5.

3.4 Experimental⁵

3.4.1 Synthesis of Co-complexes by acid leaching in alcohol

Co metal powder (0.020g, 0.34mmol) was reacted with 0.050L of a 0.5M alcoholic leaching solution of the selected acid (EtOH for H₂Mal and H₃Cit; MeOH for H₂Suc) in an open flask, magnetic bar stirring (300 rpm) at room conditions (approximately 20°C and 1 atm) for H₂Mal and H₂Suc or at the refluxing temperature of the solvent (78.4°C) for H₃Cit. The solutions turned readily from colorless to bright pink and the disappearance of Co powder occurred in short time. The obtained cobalt complexes were easily precipitated from the leaching solution through solvent evaporation and acetone washing. The dried solids were subsequently characterized as follows.

3.4.2 Characterization of cobalt complexes

[Co(Mal)₂(H₂O)₄]

Leaching time: 4h; Yield: 81%.

CH-elemental analysis. Found: C% 26.71; H% 3.71 (calculated for CoC₈H₁₄O₁₂, FW=359.16g/mol: C% 26.75, H% 3.93).

FT-IR (ATR-mode, cm⁻¹). 3406br; 3362s, 3053w, 1678m, 1609vw; 1539br, 1465s, 1392w, 1360s, 1223m, 1125br; 993vw; 894vw; 862s, 663s.

Thermogravimetric analysis (TGA): see Appendix A4.

Well-shaped crystals suitable for single crystal X-ray diffraction measurements were growing up by slow diffusion of acetone in the aqueous solution of the purified product with the addition of 0.5% w/w of agar gel and washed with ethyl ether. As reported in Fig. 3.2, the found molecular structure for the sample corresponds to the already known [Co(HMal)₂(H₂O)₄] compound.

[Co(Suc)(H₂O)_n]_m

Leaching time: 4h; Yield: 77%

See Chapter 2 for characterization.

[Co₃(Cit)₂(H₂O)₂]·H₃Cit

CH-elemental analysis. Found: C% 27.67; H% 2.94 (calculated for $\text{Co}_3\text{C}_{16}\text{H}_{22}\text{O}_{23}$, FW=782.8g/mol: C% 27.60; H% 2.81

3.5 References

- [1] C. Edtmaier *et al.*, “Selective removal of the cobalt binder in WC/Co based hardmetal scraps by acetic acid leaching,” *Hydrometallurgy*, vol. 76, no. 1–2, pp. 63–71, 2005.
- [2] G. Kücher, S. Luidold, C. Czettel, and C. Storf, “First evaluation of semidirect recycling methods for the reclamation of cemented carbides based on a literature survey,” *Rev. Mater.*, vol. 23, no. 2, 2018.
- [3] K. M. Andersson and L. Bergstr, “m,” vol. 18, pp. 121–129, 2000.
- [4] L. Zhang, Y. Chen, Q. L. Wan, T. Liu, J. F. Zhu, and W. Tian, “Electrochemical corrosion behaviors of straight WC-Co alloys: Exclusive variation in grain sizes and aggressive media,” *Int. J. Refract. Met. Hard Mater.*, vol. 57, pp. 70–77, 2016.
- [5] L. Ma, Z. Nie, X. Xi, and X. Han, “Cobalt recovery from cobalt-bearing waste in sulphuric and citric acid systems,” *Hydrometallurgy*, vol. 136, no. x, pp. 1–7, 2013.
- [6] B. Seo and S. Kim, “Cobalt extraction from tungsten carbide-cobalt (WC-Co) hard metal scraps using malic acid,” *Int. J. Miner. Process.*, vol. 151, pp. 1–7, 2016.
- [7] T. Kojima, T. Shimizu, R. Sasai, and H. Itoh, “Recycling process of WC-Co cermets by hydrothermal treatment,” *J. Mater. Sci.*, vol. 40, no. 19, pp. 5167–5172, 2005.
- [8] W. G. Jung, “Recovery of tungsten carbide from hard material sludge by oxidation and carbothermal reduction process,” *J. Ind. Eng. Chem.*, vol. 20, no. 4, pp. 2384–2388, 2014.
- [9] S. Cetinkaya and S. Eroglu, “Reduction of tungsten trioxide with ethanol,” *Int. J. Refract. Met. Hard Mater.*, vol. 64, pp. 184–189, 2017.
- [10] M. Sethurajan, E. D. van Hullebusch, and Y. V. Nancharaiah, “Biotechnology in the management and resource recovery from metal bearing solid wastes: Recent advances,” *J. Environ. Manage.*, vol. 211, pp. 138–153, 2018.
- [11] R. Wojcieszak, F. Santarelli, S. Paul, F. Dumeignil, F. Cavani, and R. V Gonçalves, “Recent developments in maleic acid synthesis from bio-based chemicals,” *Sustain. Chem. Process.*, vol. 3, no. 1, pp. 1–11, 2015.
- [12] M. Berovic and M. Legisa, “Citric acid production,” *Biotechnol. Annu. Rev.*, vol. 13, no. 07, pp. 303–343, 2007.

- [13] F. Smeets, "Microbial production of citric acid," *Antonie Van Leeuwenhoek*, vol. 49, no. 1, pp. 86–87, 1983.
- [14] N. Vassilev, "Organic acid production by immobilized filamentous fungi," *Top. Catal.*, vol. 5, no. 4, pp. 188–190, 1991.
- [15] A. S. Rosenberg *et al.*, "Reactivity of metal-containing monomers 48. Thermal transformations of cobalt(II) maleate," *Russ. Chem. Bull.*, vol. 47, no. 2, pp. 259–264, 1998.
- [16] S. Chandran, R. Jagan, R. Paulraj, and P. Ramasamy, "Spectral, mechanical, thermal, optical and solid state parameters, of metal-organic bis(hydrogenmaleate)-CO(II) tetrahydrate crystal," *J. Solid State Chem.*, vol. 230, no. June 2015, pp. 135–142, 2015.
- [17] G. Zhang, H. Chen, L. Dong, Y. Yin, and K. Li, "Microstructure and mechanical properties of ultrafine WC/Co cemented carbides with cubic boron nitride and Cr₃C₂ additions," *Ceram. - Silikaty*, vol. 60, no. 1, pp. 85–90, 2016.

Chapter 4

Ligand-based leaching systems for solvometallurgy

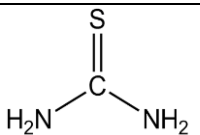
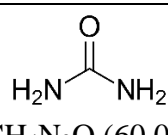
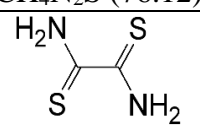
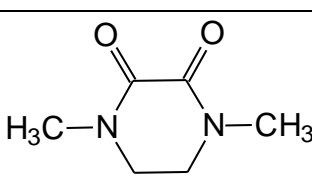
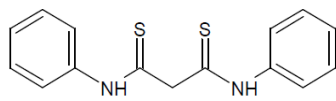
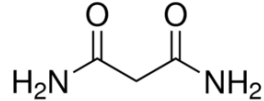
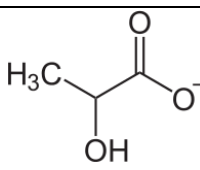
4.1 Introduction

Complexing organic ligands containing various donor atoms (like N, O, S...) have significant importance in the fields of coordination chemistry because they are capable to form stable complexes with different metal ions. As mentioned in Chapter 1, the coordination properties of the ligands play a key role in favoring the leaching reaction and determining its pathway and products.[1] With the view to promote Co leaching in non-acidic environment, a careful selection of organic ligands able to effectively coordinate the metal and of appropriate oxidizing species, both safe and potentially recyclable, should be made. Among the ligands, *soft* sulfur donor organic molecules widely demonstrated their capability to effectively coordinate Co(II) ($3d^7$ configuration) and Co(III) ($3d^6$ configuration) species. Among them, Co(II) compounds with thiourea (tu) and its various substituted derivatives are known since long time.[2] Despite several different coordination numbers and geometries are found, the most common in the presence of anionic species like halides (X^-) are the neutral tetracoordinated $[Co(Tu)_2X_2]$ with tetrahedral geometry[1][3] and the hexacoordinate $[Co(R-Tu)_2X_2]$ with octahedral geometry through a S,N-coordination of the organic ligand.[2] Similarly, Co(II) and Co(III) complexes with the dithiooxamide (DTO, also known as rubeanic acid) and functionalized dithiooxamides are well-known.[4] While tetrasubstituted dithiooxamides invariably give S, S-chelation, several examples of N,S-coordination were found with unsubstituted DTO. The hexacoordination with octahedral geometry is the most common with both Co(II) and (III).[5] Due to the high stability of its complexes with metals, DTO have been used for a long time in analytical chemistry as selective precipitating agent [6] or, attached on high surface area materials, as extractant and pre-concentrating materials for Co^{2+} . [7] Because it is stable, odorless, and commercially available, DTO is an excellent alternative to thiol reagents or to toxic phosphines and arsines often used as *soft* ligands as well, which are foul-smelling and often require strictly controlled and harsh reaction conditions. Besides the wide coordination chemistry with *soft*-donors, cobalt forms highly stable complexes also with *hard*-donors, as well-known and observed also in Chapters 2 and 3. Co is indeed classified by the HSAB theory⁶ as a *borderline* acid that mean it can effectively interact with both *hard* and *soft* bases. Indeed, as observed for thiourea, Co(II)- and Co(III)-urea complexes are well-known.[1] In these cases, O works as primary donor atom and the octahedral geometry is preferred. In this context, this chapter will describe the use of

⁶ Hard-Soft acid-base theory, Appendix A2.

selected S- and O-donor ligands belonging to the thiourea, dithiooxamide, dithiomalonamide *soft*-donors families and the corresponding urea, oxamide, malonamide *hard*-donors families, as complexing agents of new solvometallurgical leaching systems for Co from WC-Co HM recovery powders, where iodine plays the role of *green* oxidizing agent. Iodine is a very versatile reagent because it shows appreciable oxidizing properties ($E^\circ \text{I}_2/\text{I}^- = +0.54\text{V}$) forming I^- which can, on the one hand, work as coordinating ligand and, on the other hand, be quite easily oxidized back to I_2 favoring safe “closed-loop” leaching and recovery processes. Moreover, iodine/S-donor ligands mixtures demonstrated to work as powerful leaching systems in organic solvents, widely tested for the innovative and sustainable noble-metals recovery from Hi-Tech scraps.[8][9][10] Besides the cited ligands, this chapter will present preliminary results on Co-leaching obtained by the HLat/ I_2 mixture in ethanol, as a case study of a solvometallurgy system based on bio-derived complexing agents. The selected complexing agents used throughout this study are summarized in **table 4.1**.

Table 4.1: Selection of complexing used throughout this work. *FW=formula weight g/mol.

Soft ligands		Hard ligands	
Name (acronym)	Formula (FW)*	Formula (FW)*	Name (acronym)
Thiourea (Tu), thiocarbamide [11][12]	 $\text{CH}_4\text{N}_2\text{S}$ (76.12)	 $\text{CH}_4\text{N}_2\text{O}$ (60.06)	Urea (U), Carbamide
Dithiooxamide (DTO), rubeanic acid [13]	 $\text{C}_2\text{H}_4\text{N}_2\text{S}_2$ (120.20)	 $\text{C}_6\text{H}_{10}\text{N}_2\text{O}_2$ (142.16)	N,N'- dimethyl- piperazine- 2,3-dione (Mezpipdo)
Diphenyl- dithiomalon- amide (PhDTMA)	 $\text{C}_{15}\text{H}_{14}\text{N}_2\text{S}_2$ (286.42)	 $\text{C}_3\text{H}_6\text{N}_2\text{O}_2$ (102.09)	Malonamide (MA), Propane- diamide
		 $\text{C}_3\text{H}_5\text{O}_3$ (89.07)	Lactate ion (Lat)

4.1.1 Test specimen definition

Real samples studied in this chapter are the recovery powders of the HM manufacturing namely RC-627C and RC-631L already described in Chapter 2, 2.1.2 section. The Co content of the binder phases in the recovery powders was 19.55 and 20.4 wt. %, respectively (see details in Appendix 1 and 2.1.2 section).

4.2 Results and discussion

4.2.1 Leaching experiments on cobalt powder by neutral ligands/I₂ mixtures in organic solvents

With the view to select the most promising leaching systems for non-acid solvometallurgy, an extensive set of experiments were performed with the leaching systems obtained by coupling a neutral *soft*- or *hard*-donor ligand with I₂ in several solvents. 10mg of Co metal powder were treated at room conditions (~20°C, 1atm) with 50mL of organic solution containing iodine and the ligand to get a Co:I₂:L molar ratio equal to 1:2:3. The reaction occurred under magnetic bar stirring and monitored until all cobalt powder disappeared. Table 4.2 summarizes leaching times and experimental evidences recorded for all the performed reactions.

Table 4.2: Leaching times (h) and experimental observations for Co-powder (10mg) dissolution in 50mL of organic solutions containing I₂ (86mg) and the ligand (Co:L molar ratio 1:3) at room conditions. The reported results are the average values of two different experiments.

Ligand	Leaching time (h)					Exp. Evidences Solution (s) and precipitate (ppt) colors at the end of the reaction
	EtOH	ⁱ PrOH	EtOAc	Acetone	MEK	
Tu	2	n.a.	n.a.	4	n.a.	s: dark green. No precipitates.
DTO	- ⁱ	- ⁱ	12	2	12	s: red-brown. No precipitates.
PhDTMA	1	- ⁱ	3	3	>24	s: yellow (EtOH, EtOAc); dark green (Acetone). No precipitates.
U	6	14	14	6	12	s: red (EtOH), brown (Acetone); green (ⁱ PrOH, MEK); yellow (EtOAc). No precipitates.
MA	13	10	10	13	10	s: red (EtOH, ⁱ PrOH, Acetone, EtOAc); yellow (MEK). Ppt: black (EtOH, EtOAc, MEK); yellow (Acetone, ⁱ PrOH).
Me ₂ pipdo	>24	>24	>24	>24	n.a.	No noticeable reaction.

n.a. not available; ⁱ ligand insoluble in that solvent.

Despite the reaction pathway and products are not clarified yet because to date just the cobalt product with DTO has been isolated and the characterization is still in progress, a variety of different Co-complexes were obtained depending on the ligand and the solvent, as pointed out by the colors of the leaching solutions. Apart from thiourea-based leaching, where the green solution found suggested the known $[\text{Co}(\text{Tu})_2\text{I}_2]$ tetrahedral compound can be formed, this behavior is quite typical for Co(III) octahedral complexes where the color of the solutions, given the solvent, allow an assessment of the ligand field strength. Further investigations are required for clarifying the obtained products, but some important considerations on the relative efficiency of the different leaching systems can be made. Firstly, *soft*-donor ligands in the presence of iodine demonstrated to work more effectively than the corresponding *hard*-donor ligands, achieving complete Co dissolution within 4h in EtOH and Acetone. Apart from the affinity between the ligand and the metal ion, a further effect on the leaching efficiency may be related to the well-known interaction between S-ligands (σ -donor) and I_2 (σ -acceptor) still in solution, which can promote the leaching reaction and worthy to be deeper investigated. These preliminary results suggested to select Tu, DTO and PhDTMA as the most promising ligands for practical application as well as the easily available and eco-friendly EtOH and acetone as solvents, making really effective the leaching reaction also if compared with the acidic systems described in Chapter 2 and 3. As a comparison, Co metal was reacted with I_2 (1:2 molar ratio) in absence of ligands and in the same experimental conditions described previously, both in EtOH and acetone for 4h, no noticeable Co-powder dissolution was achieved.

4.2.2 Leaching experiments on IP

On the bases of the results on Co metal powders, Tu/ I_2 (EtOH), DTO/ I_2 (acetone) and PhDTMA/ I_2 (EtOH) mixtures were hence tested on the RC-627C and RC-631L test specimens. Leaching experiments on real WC-Co recovery powders were carried out in the same conditions applied to Co metal powder. Specifically, 50mL of 0.01M organic solutions of the ligands were reacted in an open flask with 0.050g aliquots of RC-627C and RC-631L test specimens in the presence of 86mg I_2 , at room temperature under magnetic bar stirring. Fig. 4.2 shows the Co-leaching profiles, in terms of yield of leached cobalt (wt. %) vs time (h), obtained by monitoring the amount of cobalt in the leachates of the test specimens in time. The Co amount in the leachate was determined by ICP-OES on measured aliquots of the solution, as detailed in Appendix A6.

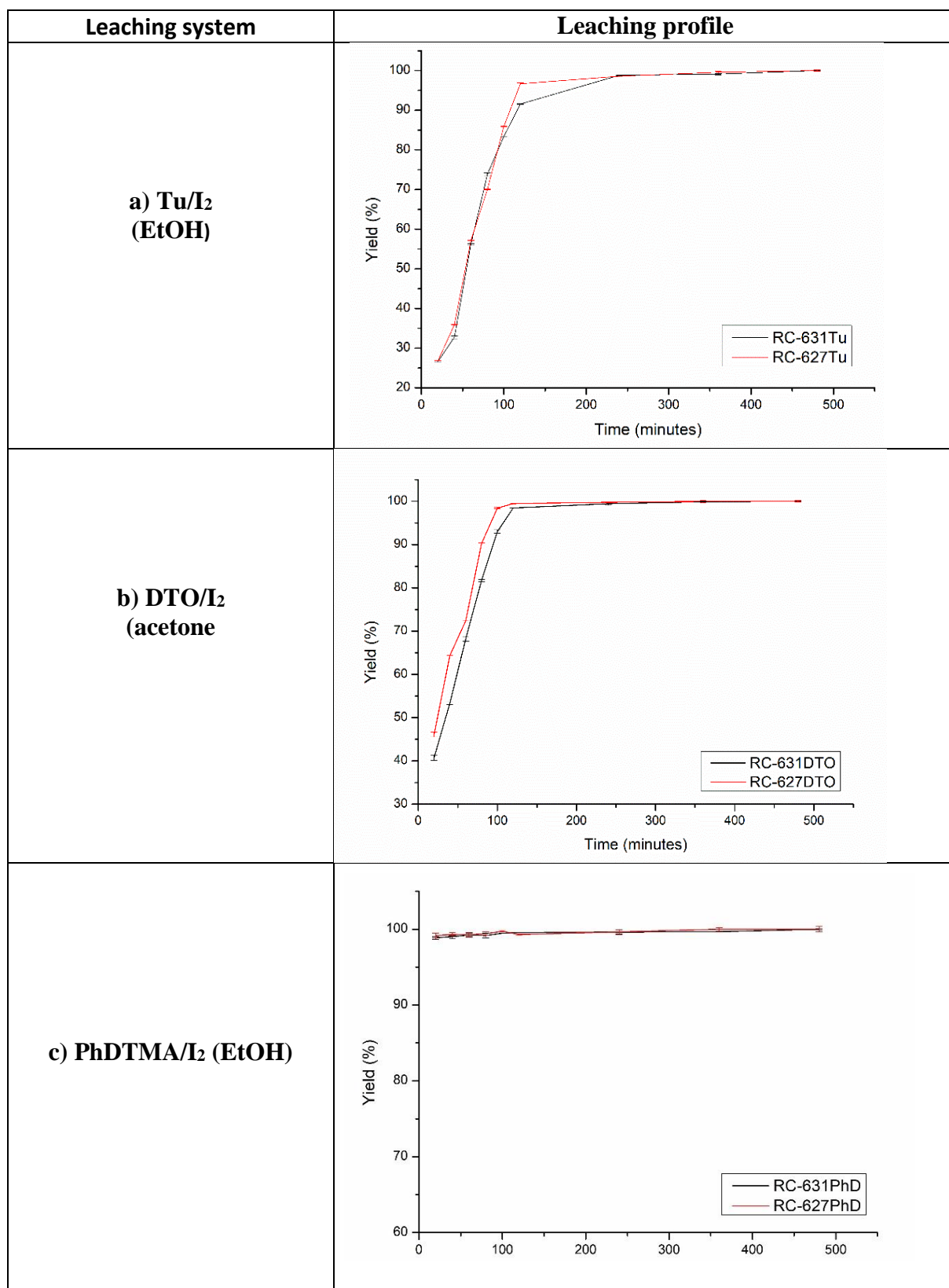


Figure 4.1: Co-leaching profiles from RC-627C and RC-631L recovery powders (50mg) on varying the leaching agent and times. Experimental conditions: $[L] = 0.01M$; $[I_2] = 6.8 \cdot 10^{-3}M$;

solvent: EtOH (Tu, PhDTMA), acetone (DTO); r.T. and pressure; stirring. The reported results are the average values of two different experiments. Error bars reported as standard deviation.

As shown, the three leaching systems demonstrated to be very effective in cobalt dissolution confirming and, in some cases, lowering leaching times on real samples. Specifically, Tu/I₂ (EtOH) leaching system achieved complete Co-dissolution in 2h on RC-627C and within 4h on RC-631L. Similarly, the DTO/I₂ (acetone) leaching system achieved complete Co-dissolution in 1h40' on RC-627C and within 2h on RC-631L. Finally, an unexpected increasing in efficiency was found with PhDTMA/I₂ (EtOH) leaching system that, in the face of 1h leaching time found on Co-powder, demonstrated to remove completely Co from both the test specimens within just 20'. Also in this case, slightly longer leaching times were recorded for RC-631L than RC-627C, which can be reasonably attributed to the lower values of the WC particles mean grain size and of the metallic binder mean free path of the RC-631L test specimen. Besides, no reaction was observed by treating WC and W raw powders with I₂-EtOH and acetone solutions.

4.2.3 Preliminary leaching experiments with HLat/I₂ mixture in ethanol

The very promising results obtained by non-acid solvometallurgy in the selective Co-dissolution from WC-Co powders, stimulated the selection of a bio-derived ligand to be used, as a case study, in a non-water solvent coupled with I₂ for pursuing sustainability as much as possible. Due to the widely applied production of HLat by agroindustrial waste fermentation, Lat⁻ was selected as a bio-derived complexing agent. The experiments on Co-powder were carried out at room temperature on 0.358g of Co-powder with 25mL of HLat 1M and 1.6g I₂ in a 1:4:1 Co:Lat⁻:I₂ molar ratio. The cited molar ratio was defined in order to provide Co with the stoichiometric amount of oxidant and a slight excess of complexing agent. The reactions have proven extremely effective, achieving complete Co-dissolution in 45'. In the absence of iodine, the reaction does not take place. Indeed, lowering the amount of iodine the leaching reaction did not reach completeness, proving to be a limiting factor if a molar ratio Co:I₂ equal to 1:1 is not provided. Furthermore, the known complex [Co(Lat)₂(H₂O)₂] was isolated at the solid state as the reaction product from the leachate, suggesting the reaction reported in Eq. 4.1:



On these bases, the first experiment on 32.46g RC-627C test specimen was run by using the same experimental conditions reported above. Even if the complete characterization of the

leaching solution and the residue solid sample are still in progress, preliminary results showed an almost quantitative Co dissolution within 24 hours.

In order to prevent undesired by-reactions, e.g. EtI formation which may be promoted in EtOH by acids as in the reaction $\text{Co} + 2\text{HLat} + 2\text{EtOH} + \text{I}_2 \rightarrow [\text{Co}(\text{Lat})_2(\text{H}_2\text{O})_2] + 2\text{EtI}$, the use of lactate salts instead of HLat would be preferable for industrial purposes.

4.3 Conclusion

In this chapter, new powerful non-acid leaching systems based on the use of an organic ligand and iodine in organic solvents, were discussed. Among the several tested mixtures, the leaching system based on complexing *soft* S-donor ligands, namely Tu, DTO and PhDTMA, with iodine in EtOH and acetone were found to be optimal for a selective and effective Co-dissolution. The most powerful leaching system was found to be PhDTMA/I₂ in EtOH being able to dissolve almost quantitatively Co from both the available test specimens in just 20 minutes at room temperature. DTO and Tu-based leaching systems were able to achieve this result in more than satisfactory 2 and 3h, adding the advantage to be commercially available with respect to the PhDTMA ligand which, to date, is still not available on the market.

These organic ligands and iodine were selected to obtain high leaching efficiencies, as confirmed by the obtained results. Leaching rates were found comparable and even more performing than those obtained in the case of the leaching with bio-derived organic acids which show the lowest environmental impact. Preliminary results obtained with the HLat/I₂ mixture in EtOH seems to put together the power of this latter approach with the eco-friendliness and low cost related to the use of bio-derived substances. Finally, the use of safe complexing ligands in organic solvents which does not produce toxic fumes when reacting as leaching agents and the potential recyclability of the solvent and reactants after metal recovery, make these systems a very versatile, easy-to-handle and *green* tool for non-water metal dissolution and recovery. The absence of large amounts of water, combined with the selectivity, efficiency, and eco-friendliness of the proposed solvometallurgy process, stimulates further investigations on the obtained Co-complexes and optimizations for larger scale application.

4.4 Experimental⁵

4.4.1 Leaching experiments on the Cobalt-powder with Tu/DTO/PhDTMA

50mL of ligand solutions (0.01M; Tu and PhDTMA in EtOH; DTO in acetone) and 86mg of

I₂, were reacted in an open flask with 10mg of cobalt powder at room temperature and pressure under magnetic bar stirring (300 rpm) until Co powder disappeared. When the reaction went on, the solution turned from dark brown to the final color (see Table 4.2). Co complexes of DTO and PhDTMA were precipitated from the leachate by concentration under vacuum and diethylether washing. The characterization of the obtained products is still in progress.

- **Co-DTO complex**

FT-IR (ATR-mode, cm⁻¹). 3390vw; 3164br; 2968vw; 2120m; 1996vw; 1905br; 1685br; 1483vs; 1330s; 1251w; 1159m; 1093m; 983w; 903vw; 860s; 750w; 701vw; 634vw; 567m; 512vw.

4.5 References

- [1] P. Askalani, R. A. Bailey, R. P. Itlstitute, and U. Arab, “although only Stonestreet,” *Measurement*, vol. 47, no. Iii, pp. 2275–2282, 1969.
- [2] S. K. Nandi, B. Banerjea, and B. Sur “Ligational Behaviour of Pyridyl-2-thiourea with Cobalt(II), Nickel(II), Copper(II), Zinc(II), Cadmium(II) & Mercury(II),” vol. 22, no. December, pp. 1073–1075, 1983.
- [3] D. V Ramana AND K. C. DASH "Thiourea Complexes of Cobalt(II)" vol. 1209, no. 1957, pp. 3–7, 1964.
- [4] E. S. S. A, G. C. Pellacani, and G. Peyronel, Cobalt(III) Complexes with Dithiooxamide, N,N'-dimethyl- and N,N'-dicyclohexyl-dithiooxamide: CoL,X, (X = Cl, Br, I),” vol. 9, pp. 189–192, 1974.
- [5] L. Pilia *et al.*, “Tuning the oxidation state and magnetic and coordination behaviour of iron and cobalt complexes by O/S variation in mono-thio and dithio-oxamide chelating ligands,” *New J. Chem.*, vol. 39, no. 6, pp. 4716–4725, 2015.
- [6] O. W. Kolling, Dithiooxamide as an analytical reagent, Mster of sciences, 1958.
- [7] A. Mirabi, A. S. Rad, and M. Abdollahi, “Preparation of Modified MWCNT with Dithiooxamide for Preconcentration and Determination of Trace Amounts of Cobalt Ions in Food and Natural Water Samples,” *ChemistrySelect*, vol. 2, no. 16, pp. 4439–4444, 2017.
- [8] A. Serpe *et al.*, “Pd-dissolution through a mild and effective one-step reaction and its application for Pd-recovery from spent catalytic converters,” *Chem. Commun.*, no. 8, pp. 1040–1042, 2005.
- [9] A. Serpe, F. Artizzu, M. L. Mercuri, L. Pilia, and P. Deplano, “Charge transfer

- complexes of dithioamides with dihalogens as powerful reagents in the dissolution of noble metals,” *Coord. Chem. Rev.*, vol. 252, no. 10–11, pp. 1200–1212, 2008.
- [10] A. Serpe, A. Rigoldi, C. Marras, F. Artizzu, M. L. Mercuri, and P. Deplano, “Chameleon behaviour of iodine in recovering noble-metals from WEEE: Towards sustainability and ‘zero’ waste,” *Green Chem.*, vol. 17, no. 4, pp. 2208–2216, 2015.
- [11] C. Dai, H. Zhang, R. Li, and H. Zou, “Synthesis and characterization of thiourea,” *Polish J. Chem. Technol.*, vol. 21, no. 3, pp. 35–39, 2019.
- [12] G. Vettorazzi and I. Macdonald, “Chemical and Physical Data,” vol. 1974, no. 3962, pp. 9–17, 1988.
- [13] A. Roger and M. Jacqueline, “United States Patent (19),” vol. 1059, no. 19, 1991.

Part II

Designing sustainable processes **for industrial application**

Chapter 5

Scale-up of acid-based leaching processes and materials recovery for HM production

5.1 Introduction

Chapters 2-4 introduced and discussed the selective Co-leaching systems investigated in this work with the view to select the most promising solvometallurgical processes for both environmental and industrial purposes. Acid and non-acid leaching agents bearing complexing properties were checked accordingly, and compared each other in terms of chemical behavior, efficiency and eco-friendliness, also taking into account the solvents where the reactions occurred. On the basis of our screening, thanks to its low cost, high efficiency towards both Co powder and Co contained as a binder in the real WC-Co powders and large availability through agroindustrial waste fermentation, HLat was selected as the most interesting case study for industrial application among the bio-derived organic acids working in water due to its ready availability from dairy waste dark fermentation. HLat action is strictly related to the presence of an oxidizing specie (Class 2 acid), i.e. oxygen in water and I₂ in ethanol, which makes the reaction working and whose availability during the reaction affects leaching times. Its diluted aqueous solutions (0.5M) demonstrated high efficiency and selectivity being able to almost completely remove Co from 0.5g of recovery powders in around 4h at room conditions. Against, HMal demonstrated to be largely the most promising acidic leaching agent with oxidizing behavior working in non-water solvent and its action is accompanied by H₂ gas evolution (Class 1 acid). In the studied conditions, its ethanolic solutions were able to dissolve almost completely Co in 4h. Finally, H₂Suc was selected among the most interesting bio-derived species due to its twofold reactivity (Class 3 acid) with H⁺-oxidizing action supported by O₂, in open flask conditions, that increase the efficiency, as demonstrated by comparing water (2.2.2 section) and methanol (3.2.3 section) experiments. Despite these highly encouraging preliminary results, industrial requirements for application furtherly involve optimal conditions in terms of reagents and solvents consumption, definition and management of critical process parameters, minimum L/S ratio for plant design, efficiency tested on scale-up experiments. Moreover, the achievement by leaching of WC-Co powders with the desired composition - Co% < 10, O%: <0.4%; C: W ratio = 1:1 - for direct re-employment in HM production, would be really desirable. Thus, for these acids further studies addressed to the process set-up and products recovery and quality assessment, were performed supported by the environmental and sanitary group of the DICAAR (UniCA)⁷ and F.I.L.M.S. corp. for increasing the technology readiness level (TRL) from the experimental proof of concept (TRL 3) to the full validation of the technology in lab (TRL 4) and following technology validation in relevant

⁷ This part of the work was conducted with the help of MSci students, Stefano Trudu and Martina Cera.[1][2]

environment (TRL 5), as here described. Differently, although solvometallurgy based on the use of non-acid ligands/I₂ demonstrated to be the most powerful tool for carrying the Co-leaching out, the too early stage of the experimentation still requires further insights before being able to move on to the next validation phase and will be the starting point of following studies.

5.1.1 Definition of the test specimen

Real samples studied in this chapter are the recovery powders of the HM manufacturing namely RC-627C and RC-631L already described in Chapter 2, 2.1.2 section. The Co content of the binder phases in the recovery powders was 19.55 and 20.4 wt. %, respectively (see details in Appendix A1 and 2.1.2 section).

5.2 Results and discussion

5.2.1 Set-up of operative conditions: Liquid/Solid (L/S) ratio

With the view of meeting industrial requirements for technological transfer and improving the sustainability of the process, experiments addressed to limit the amount of leaching agents and solvents were performed. Specifically, attempts to fix the Co/Acid molar ratio to lower values than the previous 1:74 (0.5g of test specimen approximately 20 wt. % Co; [Acid] = 0.5M; Volume = 0.250L), but providing the cobalt a calculated excess of lixiviant and the acid concentration to a still low 1M, were performed. The experiments were firstly carried out on 0.375g of Co-powder with 1M solutions at room temperature under magnetic bar stirring, monitoring the time of complete disappearance of Co powder from the reaction vessel. Table 5.1 summarizes Co-leaching yields and experimental conditions applied on Co-powder.

Table 5.1: Co-leaching from 0.375g Co powder by varying the Co:Acid molar ratio by using magnetic bar stirring. [Acid]=1M. *Calculated values referring to the corresponding amounts of recovery powders 20 wt. % Co.

L/S*	Volume (mL)	Co:Acid Molar ratio	Leaching time (h)		
			HLat (H ₂ O)	H ₂ Su (H ₂ O)	H ₂ Mal (EtOH)
14	25	1:4	7-8	9	6
28	50	1:8	6	6	5
42	75	1:12	6	6	5

As shown, keeping all other conditions fixed, as the excess of reagent increases, the leaching times decrease. In all cases, Co:Acid 1:8 molar ratio seemed guarantee the minimum excess of

that allow the leaching to be almost quantitative in a short time. A further increase to 1:12 does not show a significant time reduction.

On these bases, 18.8g of RC-631L sample were treated in an open vessel with 0.250 and 0.500mL of HLat 1M at room conditions under mechanical stirring. In this case, Co-leaching yields were determined by ICP-OES on digested aliquots of the leachate as detailed in Appendix A6. Table 5.2 and Fig. 5.1 summarize the Co-leaching yields recorded in the reported conditions and leaching profiles, respectively.

Table 5.2: Co-leaching from 18.8g RC-631L by varying the L/S and Co:HLat molar ratio by using mechanical stirring. [HLat]=1M.

L/S ratio (L/kg) (Co:HLat molar ratio)	Mechanical stirring	
	Leaching Time (h)	Yield (%)
14 (1:4)	4	34
	6	43
	8	54
	24	78
	48	96
28 (1:8)	4	33
	6	36
	8	49
	24	100
	48	100

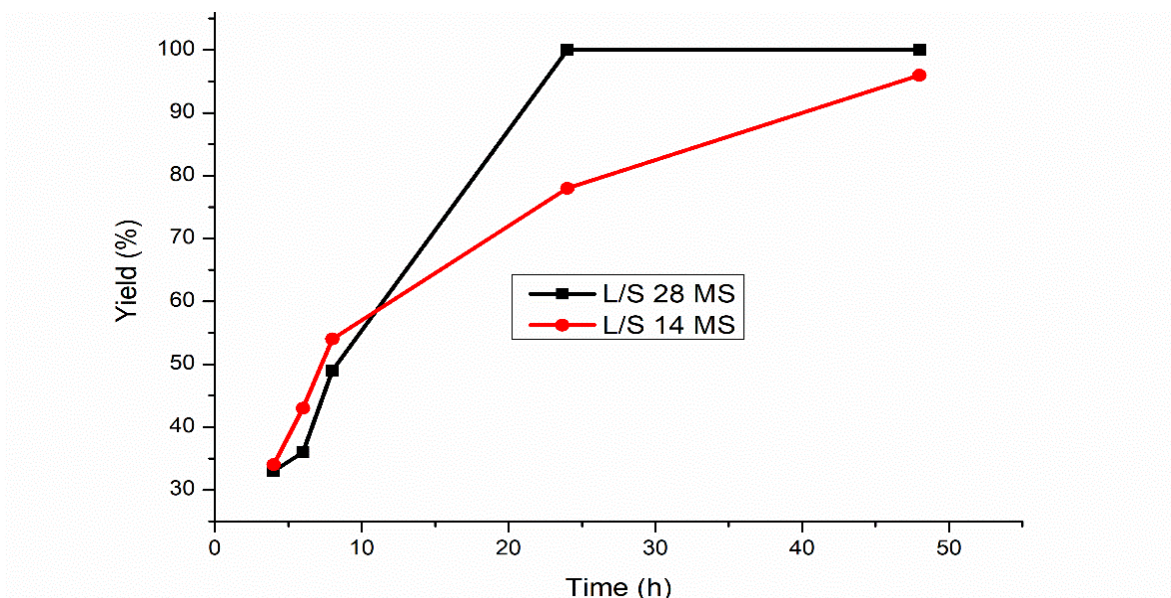


Figure 5.1: Co-leaching profiles on RC-631L sample shown as Co-dissolution yield (%) vs time (h) by varying L/S ratio (14 and 28) by mechanical stirring.

Table 5.2 and Fig. 5.1 pointed out again that L/S = 14L/kg (1:4 molar ratio) seems does not meet efficiency requirements, needing at least 48 hours for a complete cobalt dissolution. Nevertheless, it can be considered more acceptable if thinking that a recovered powder with a tuned WC-(5%)Co composition can be achieved in 24h. Increasing the L/S ratio up to 28L/kg and, hence, to 1:8 Co:HLat molar ratio, increased Co dissolution efficiency from 78 to 100% at 24 hours was found. Despite the leaching times were longer than those found on Co-powder, results obtained by this L/S set-up seemed satisfactory obtaining almost quantitative Co dissolution within 24h. Furthermore, such an increase of leaching time with the amount of starting material (0.375g Co powder vs 3.75g of Co in 18.8g RC-631L) supported the hypothesis of a key role of dissolved oxygen in the reaction rate which was worthy to be deeper investigated.

In the case of H₂Mal and H₂Suc, experiments on both RC-627C and RC-631L samples were performed on 0.500g aliquots providing the powder 7 mL of H₂Mal ethanol solution and H₂Suc water solution ([Acid] = 1M; Co/Acid molar ratio = 1:4; L/S ratio = 14L/kg). The experiments tried to highlight the Co-leaching yields in conditions more suitable for industrial plants, able, at the same time, of providing recovered powders with the desired WC-Co composition. In these conditions, in the face of a substantially lowered amount of employed reagents, the leaching reactions in H₂Mal led to a more than satisfactory 89% and 82% cobalt removal in 4h for RC-627C and RC-631L respectively, corresponding to recovered powders with about WC-(3%)Co and WC-(4%)Co composition. Similarly, H₂Suc leaching provided 84% and 79% cobalt dissolution in 9h for RC-627C and RC-631L respectively, corresponding to recovered powders with about WC-(4%)Co and WC-(5%)Co composition. Co-dissolution yields were determined by ICP-OES measurements on 3 digested leachate aliquots after 4 and 9h leaching, respectively. These results demonstrated the suitability of the improved, more sustainable, operating conditions for providing WC-Co powders with a properly tuned composition and, hence, ready to be re-employed in the HM manufacturing process.

5.2.2 Studying the oxygenation effect on Co leaching by aqueous HLat solutions

The influence of the oxygen available for the reaction was deeply investigated comparing Co-metal leaching times with and without forced aeration conditions, as summarized in **Table 5.3**. As shown, significantly shorter times were found for Co-leaching experiments performed through forced aeration, confirming the relevant effect of O₂ on the reaction. However, to

confirm the key role of oxygen in this leaching reaction, an additional experiment was carried out using a Sapromat respirometer.

Table 5.3: Effect of the oxygenation (forced aeration by blowing air through a thin glass tube) on the metallic cobalt leaching time.

V (mL)	[HLat] (M)	Co (mg)	pH	Leaching time (h)	
				Natural O ₂	Forced O ₂
50	1	357	1.7	13	3-4

The respirometer is a system typically used for the measurement of the biochemical oxygen demand (BOD) in water, or the amount of oxygen that is consumed during the decomposition of organic matter in soils or composts. The system consists of a flask containing the sample, connected to a sensor and a generator. At the time when there is a net oxygen consumption (i.e. in absence of any other gas production due to the specific reaction involved), an electrode system detects the depression in the flask and supplies a parceled amount of oxygen. Flasks are placed in a thermostated bath at 20°C under magnetic bar stirring. Fig. 5.2 shows the profile of oxygen consumption *vs* leaching time determined by the “unusual” application of respirometry to the O₂-dependant HLat leaching reaction.

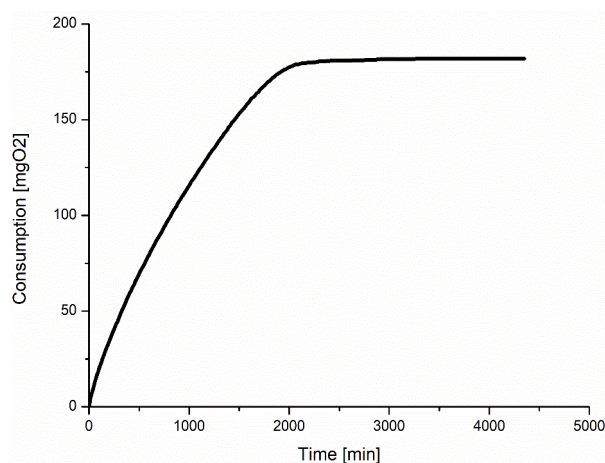


Figure 5.2: Metallic Co-leaching reaction with 0.1L of HLat 1M under Sapromat respirometer conditions: oxygen consumption curve. Amount of Co powder: 0.714g.

The monitoring of oxygen consumption allows to estimate the end of the reaction, represented by the achievement of the plateau of the curve, being the only element within the system that consumes oxygen (HLat solution does not consume oxygen). Despite longer leaching times

(approximately 30h) were found using this method,⁸ it points out some relevant aspects of the leaching reaction. Specifically, the amount of oxygen consumption (mgO_2) during the reaction almost reflected the stoichiometric need: in the face of 193 mgO_2 theoretically required by the reaction ($0.27 \text{ gO}_2/\text{gCo}$), 180 mgO_2 were consumed during the experiment, confirming the primary role of O_2 in the leaching reaction. Experiments carried out at various pH values, obtained by adding a controlled amount of NaOH(aq) to the leaching solution, pointed out that at pH above 4.5, formation of abundant precipitations (oxides and hydroxides of Co(II) and (III)), occurred in agreement with the literature.[3] Against, $\text{pH} < 4.5$ prevented oxides and hydroxides formation allowing the reaction to occur efficiently towards $[\text{Co(Lat)}_2(\text{H}_2\text{O})_2]$ complex formation. This is a key point, because the formation of insoluble by-products is undesired in selective leaching processes. Furthermore, despite the pH of 1 M HLat solutions is 1.7, more complex systems where HLat and Lat^- may co-exist in concentration depending on the chemical equilibrium (such in the case of solutions obtained by dark fermentation of carbohydrates; see Chapter 6) may be also used without forcing the system at pH values lower than 3.9, pH of the HLat/Lat^- buffer solution at 25°C , with a not negligible saving of chemicals (e.g. HCl). These results were confirmed by applying the same methods to the recovery powders. Before testing the powders, experiments were run in the same experimental conditions of raw WC and W powders in order to highlight possible oxidation phenomena on these materials which can be detrimental for the final WC-Co recovered powders as anticipated in Chapter 1 (section 1.3). Fig. 5.3 shows the O_2 consumption profiles, obtained by using Sapromat respirometer, for WC and W powders in the presence of a 1 M HLat solution.

As shown, tungsten does not consume oxygen. Tungsten carbide, on the other hand, consumes a small and linearly increasing amount of O_2 reaching 12.5 mgO_2 value ($0.145 \text{ mgO}_2/\text{gWC h}$) after 30 hours (average leaching time found for cobalt powder). This finding that should be taken into account assessing global O_2 consumption during the process confirms the knowledge of slow but occurring oxidative phenomena involving WC.

⁸ Sapromat respirometer works in a "static" mode, supplying parceled amounts of oxygen in the head space of the closed reactor. This delivering mode does not favor, from a kinetical point of view, the oxygen availability for the leaching reaction, resulting in longer leaching times with respect to those recorded even just in an open flask. This delivering mode could limit the availability of oxygen in the liquid phase and thus the rate of the leaching reaction.

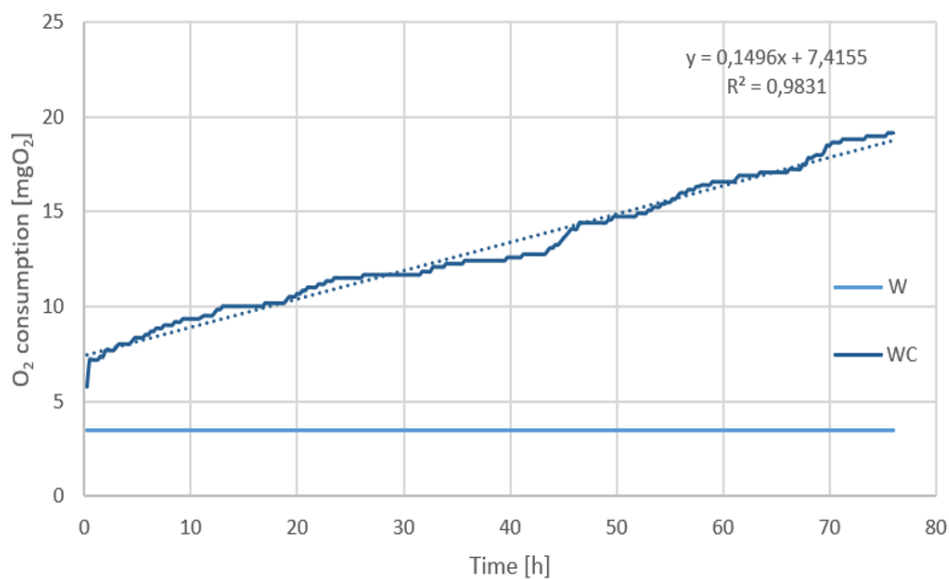


Figure 5.3: O₂ consumption profiles for WC and W powders (2.86g) in the presence of 0.1L of 1M HLat solution.

Finally, further leaching tests were performed for defining the best oxygenation system. The reactions were carried out in open beakers, using 0.2L of a 1M HLat solutions and 1.47 g of metallic cobalt powder. As shown in Fig. 5.4, the solutions were mechanically stirred in a jar test equipment and air was blown through the solutions by a thin glass tube providing large bubbles and, for comparison, a porous stone providing fine bubbles, both powered by a small air compressor. Each experiment was performed twice.

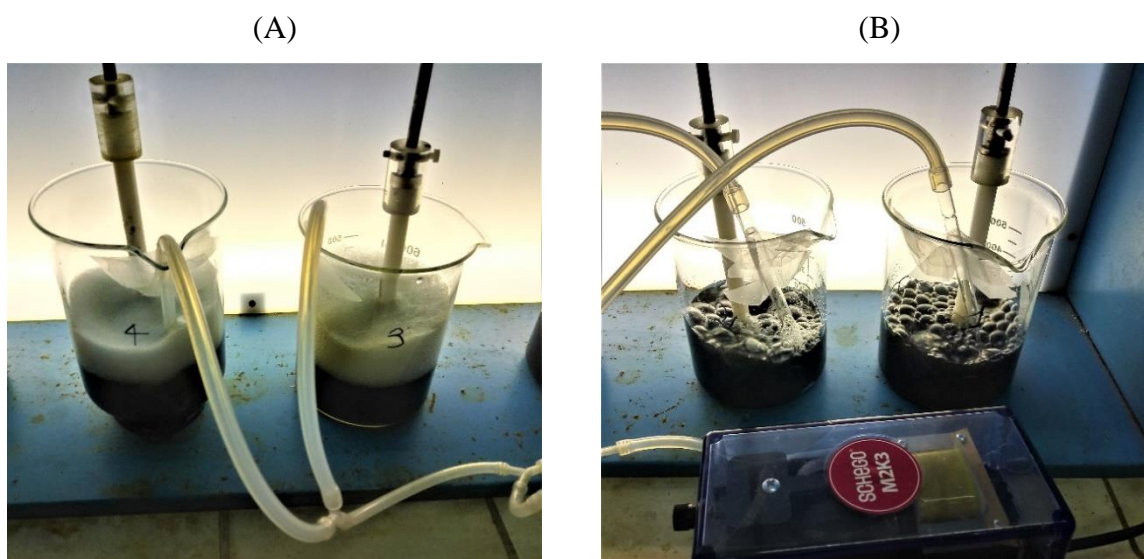




Figure 5.4: Fine bubble (A) and large bubble (B) oxygenation systems at the start of the leaching reaction.

Table 5.4 summarizes conditions and results obtained by 4h leaching. As shown, the fine bubble system is significantly more efficient and manages to almost completely leach the Co in 4 hours. These results were also confirmed by increasing the scale of the experiment, obtaining an almost quantitative Co dissolution in 4-5h by treating 2.94g and 5.89g of Co powder with respectively 0.4 and 0.8L of HLat 1M. This result suggests presumably the fine bubble diffuser provides available oxygen with a rate compatible with its consumption by the reaction.

Table 5.4: Cobalt (1.47g) leaching efficiency with HLat (1M, 0.2L) under large and fine bubble aeration. *Determined by ICP-OES on the leachate and obtained as average values of two independent experiments.

Aeration system	Leaching yield [%]*	Leaching systems after 4h treatment
Large bubbles	61.5	
Fine bubbles	92.5	

5.2.3 Scale-up of the solvometallurgy process

Herein, a larger scale experiment was performed on 300 g of RC-631L with a H₂Mal ethanol solution (1M, 4.2L) in order to obtain a treated sample in amount compatible with assessing scalability and testing the recovered materials. The leaching reaction was performed at room conditions for 6h into a 5L mixing reactor equipped with a mechanical stirring (400 rpm) in the L/S=14L/kg. After 6 h, the reaction was stopped and the resulting mixture separated by gravity filtration and collected for characterization. ICP-OES determinations of cobalt on the leachate and the solid residue after digestion demonstrated that, under the reported conditions, around the 70% Co was removed leaving a 6% Co into the solid residue, and agreed with the SEM/EDS solid state characterization on the WC-Co recovered powder, as shown in **Fig. 5.5**. Thus, the final compositional results of this experiment are in line with the need for tuning the amount of Co, providing good quality WC-based recovered powders with a Co content lower than 10%.

Further experiments are in progress in order to provide a robust relationship between the starting test specimen composition and the required leaching time for obtaining the desired final Co percentage.

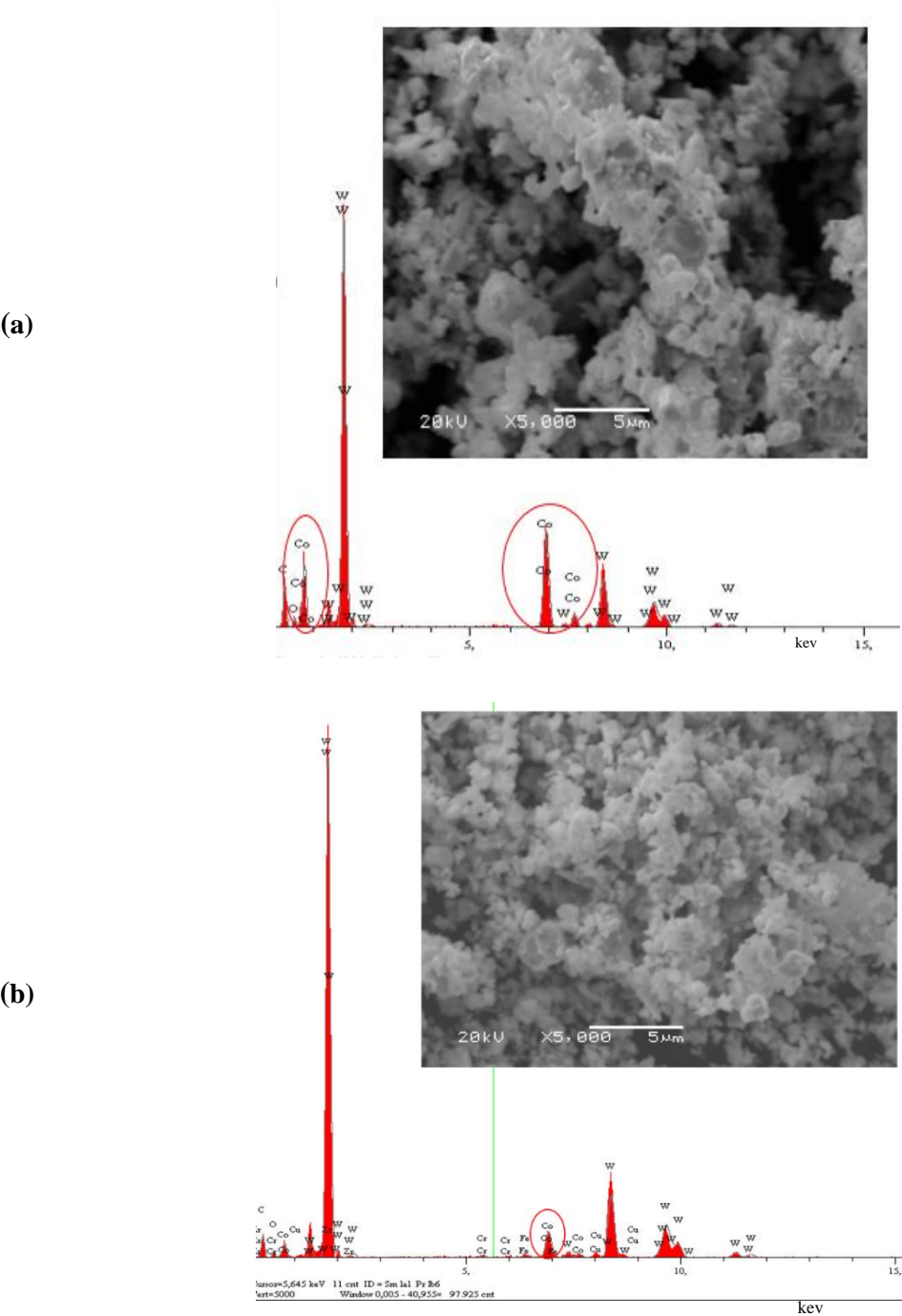


Figure 5.5: SEM micrographs and EDS spectra of RC-631L: (a) before and (b) after 6h H₂Mal (1M, EtOH) Co-leaching at room conditions.

5.2.4 Scale-up of hydrometallurgy leaching processes

Larger scale experiments were performed also for HLat and H₂Suc hydrometallurgical treatments. A HLat solution (1M, 7L, L/S=14 for limiting the amount of solution) was reacted with 650g of RC-631L powder in the presence of forced aeration in a 30L mixing vessel. Stirring was provided by bubbling air from the bottom of the vessel through spherical porous stones connected to an air compressor (see Fig. 5.6). Leaching reaction was monitored from 1 to 24h by sampling the leachate and analyzing for Co the digested aliquots by ICP-OES (see Appendix A6 for details). Fig. 5.7 shows the leaching profile for the process.

Under the above conditions, ICP-OES measurements on the leachate showed a 79% of Co dissolution occurred in 24h. This data fully agreed with the corresponding ICP-OES characterization of the digested solid sample where a WC-(5,7%)Co composition was found. Furthermore, these results were supported by XRD and SEM/EDS solid state characterization on the recovered powder which highlighted the lowering of cobalt peaks and a residual amount of cobalt in the final mixture. Fig. 5.8 and 5.9 show respectively the XRD patterns and SEM/EDS plots and powder micrographs, before and after 24h HLat/O₂ leaching.

(a)



(b)

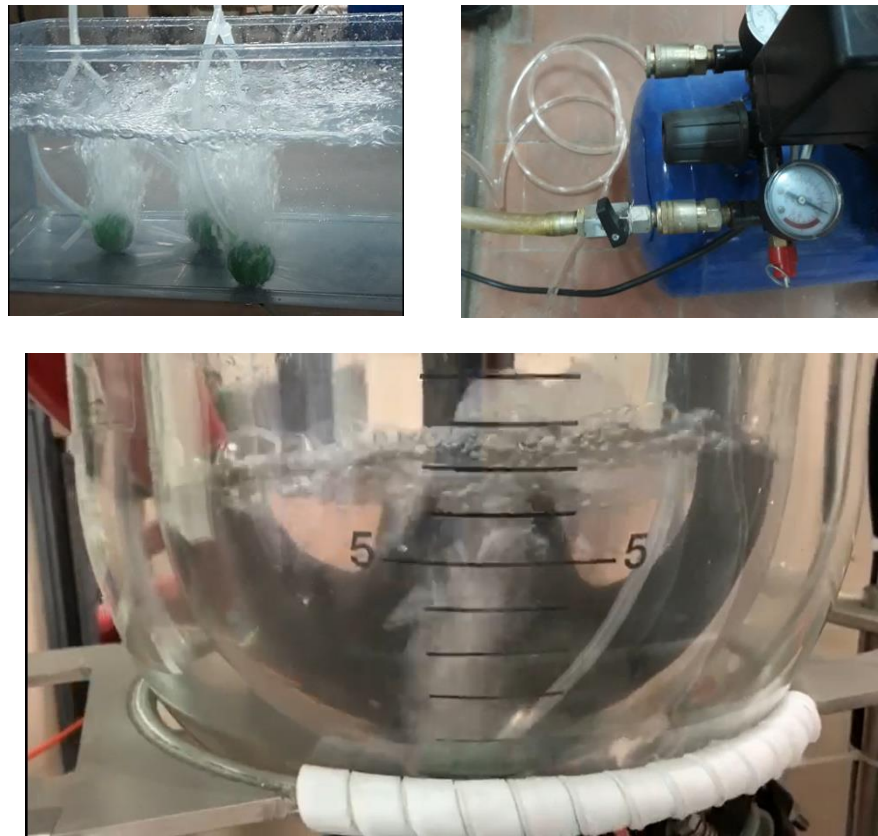


Figure 5.6: (a) Thermostated double-wall 30L mixing vessel equipped with motovariator for mechanical stirring, pH control and distillation line; (b) Forced aeration set-up experiments.

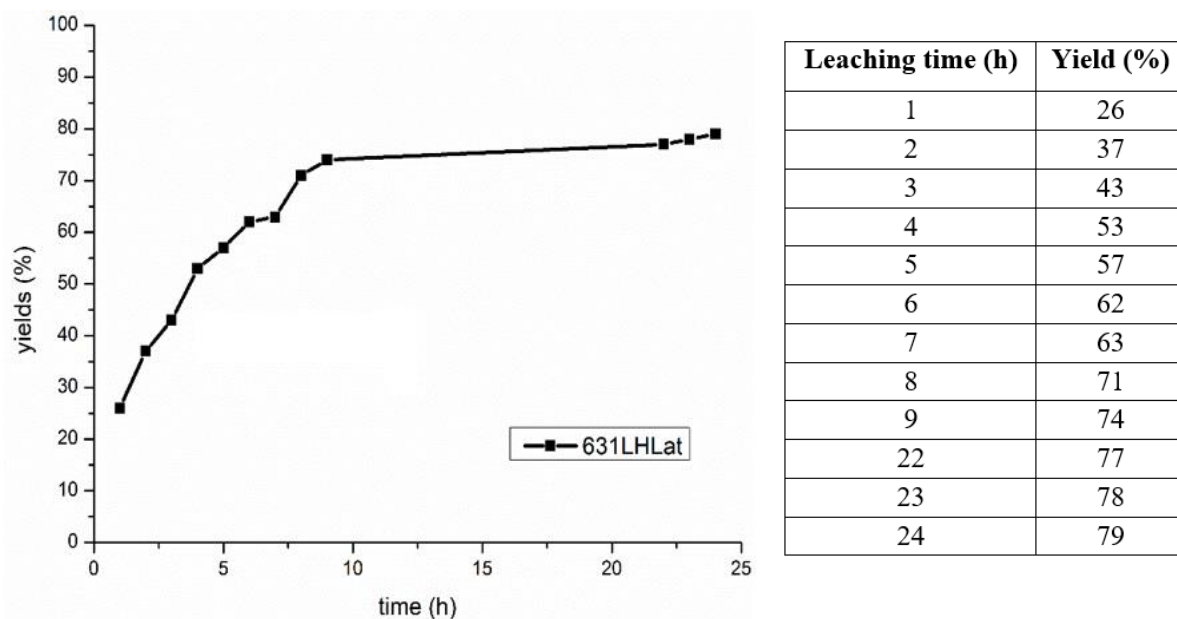


Figure 5.7: Co-leaching profile for the scale-up experiment on RC-631L powder (650g) with HLat (H₂O, 1M) under aerated conditions.

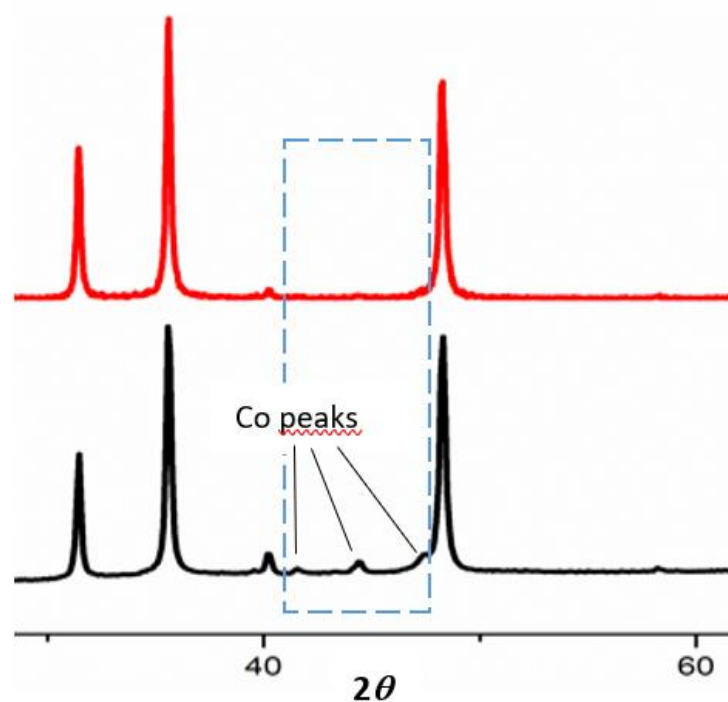


Figure 5.8: P-XRD patterns of RC-631L: a) before and b) after 24h leaching with HLat (H₂O, 1M)/O₂ at room conditions.

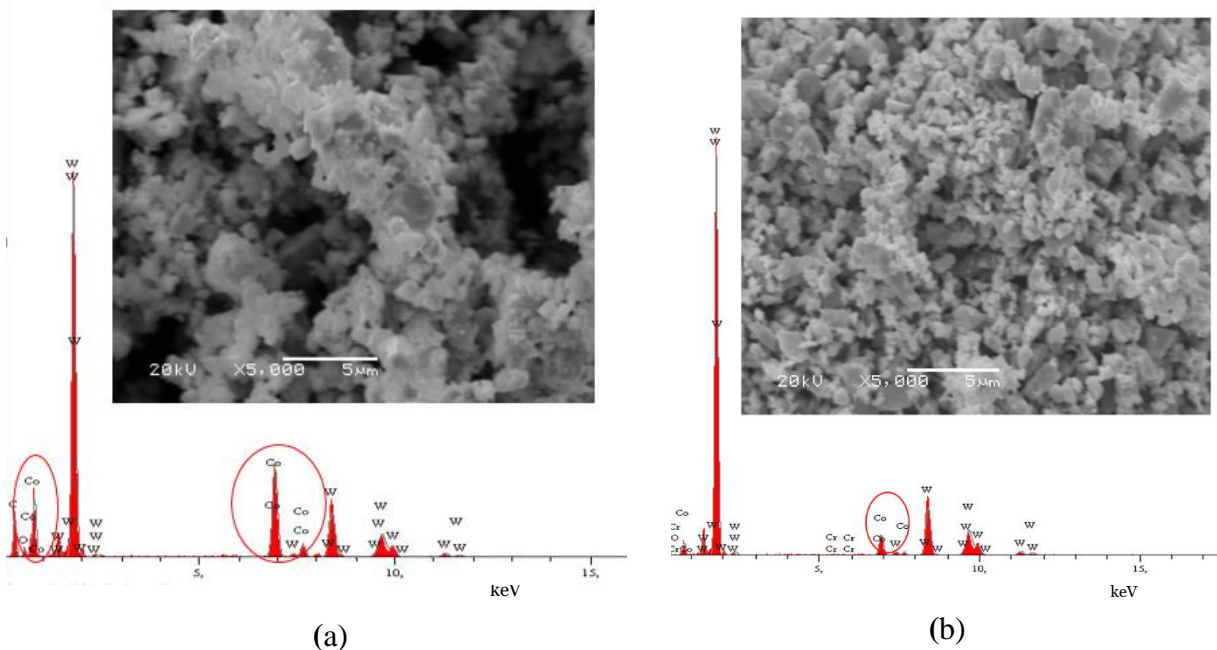


Figure 5.9: SEM micrographs and EDS spectra of RC-631L: a) before and b) after 24h leaching with HLat (H_2O , 1M)/ O_2 at room conditions.

Also in the case of H_2Suc a larger scale experiment on 650g of RC-631L, applying the same conditions reported above for HLat, was carried out in absence of forced aeration. The solution was stirred mechanically and left to react with the powder for 24h at room conditions. H_2 gas evolution was observed. After this treatment, around the 48% of Co was found in the leachate (by ICP-OES measurements). This result was confirmed by the p-XRD characterization (see **Fig. 5.10**) that highlighted a relevant residual amount of Co compatible with a supposed WC-(12%)Co composition.

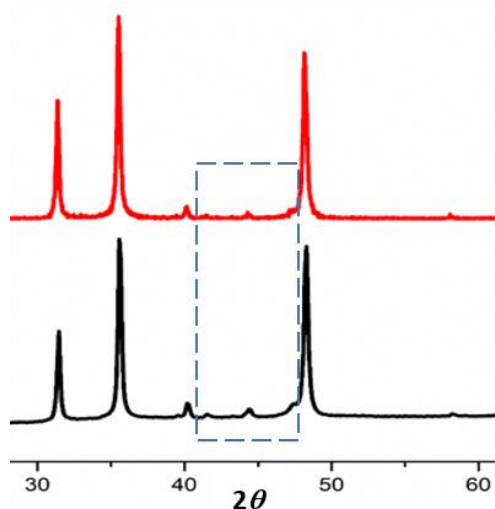


Figure 5.10: P-XRD patterns of RC-631L (650g): a) before and b) after 24h leaching with H_2Suc (H_2O , 1M) at room conditions.

On the bases of this not completely satisfactory result, a further experiment, addressed to improve effectiveness pointing out a relationship with the presence of available O₂ for the reaction, was attempted. In this case, 1500g of RC-631L test specimen were treated under mixed oxygenation conditions for 50h. Specifically, the mixture was stirred mechanically for 24h without forced aeration (PART 1), as done in the previous experiment, then a repeated sequence of mechanical stirring without forced aeration (45') and particle suspension by forced aeration from the bottom of the vessel (15'), was applied up to the end of the experiment (PART 2), monitoring the Co-leaching yields in the time throughout the experiment. **Fig. 5.11** shows the Co-leaching profile for this two-stage process, highlighting by colors the data related to the two parts of the experiment. PART 1 of the experiment fully reproduced the yields obtained by the first scale-up attempt, providing a 48% Co-dissolution in 24h, as expected by applying the same unoxygenated experimental conditions. PART 2, showed instead a significant increase of effectiveness, reaching an 85% Co-dissolution yield after 50h. This two-steps approach is based on the cited class 3 behavior of H₂Suc and was addressed to improve efficiency limiting material oxidation phenomena as much as possible. Unfortunately, the frequency of data collection during this phase and the unavoidable long temporal gaps in the monitoring, did not allow to highlight a possible “sawtooth” trend related to the O₂ supply, but the increase of effectiveness can be reasonably related to the forced aeration conditions due to the found increased slope of the trend.

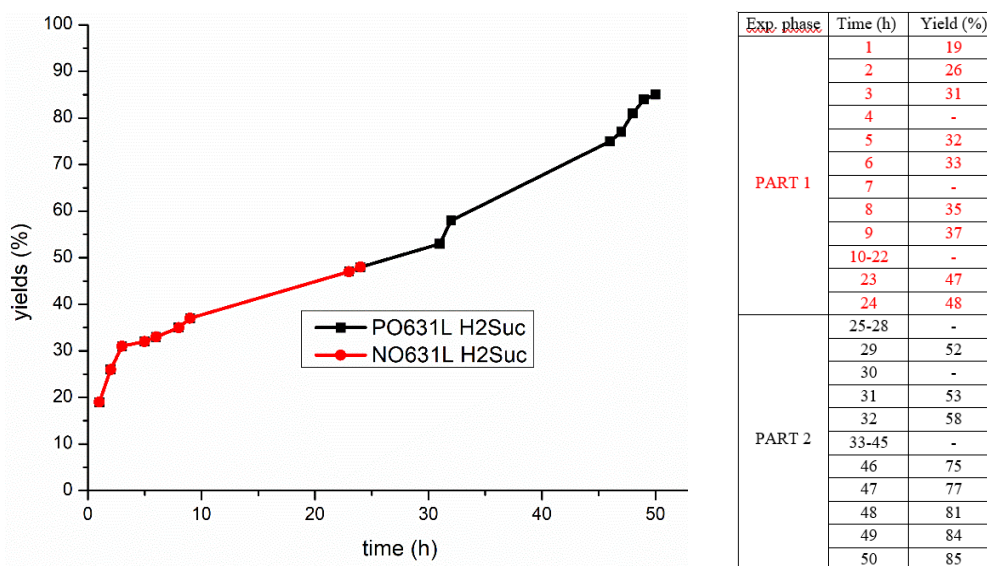


Figure 5.11: Co-leaching profile for the scale-up experiment on RC-631L powder (1500g) with H₂Suc (H₂O, 1M) without aeration for 24h (red color, PART 1) and under mixed aeration conditions (no aeration, stirring for 45' and fine bubbling forced aeration for 15') up to 50h (black color, PART II).

The leaching yield calculated by ICP-OES measurement on the leachate after 50h treatment, fully agreed with the corresponding ICP-OES characterization of the digested solid residue where a WC-(3.1%)Co composition was found, as well as with the SEM/EDS characterization (see Fig. 5.12).

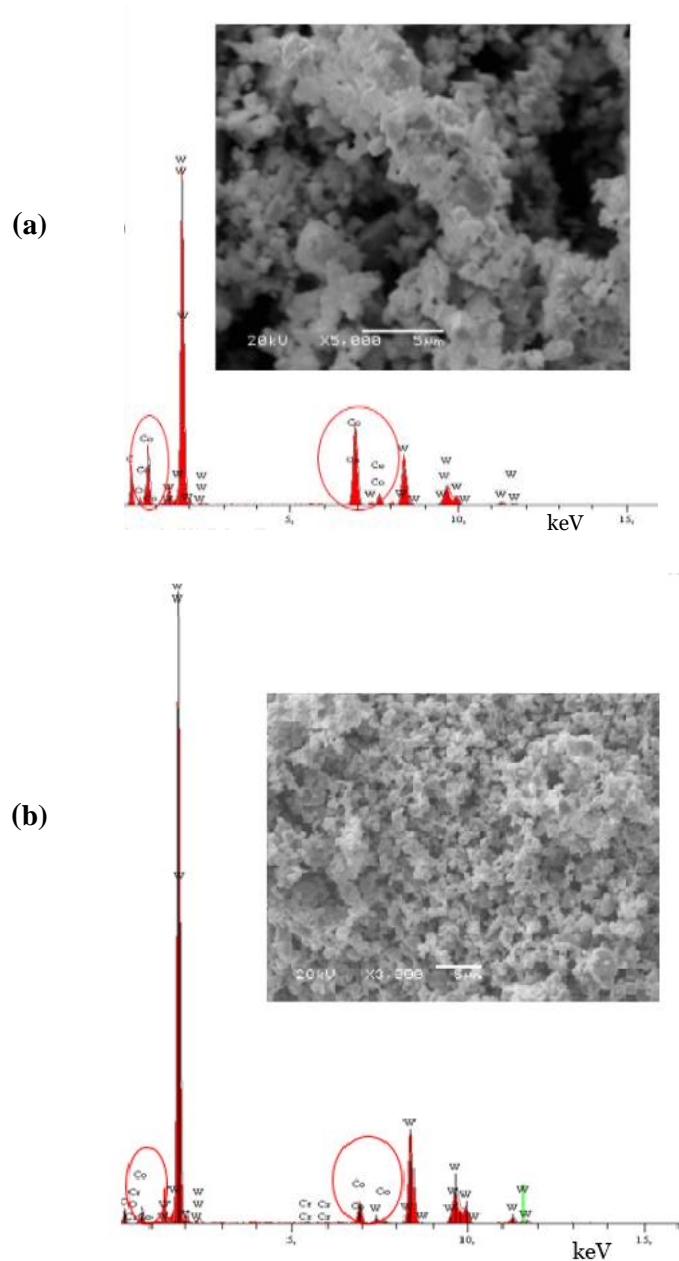


Figure 5.12: SEM micrographs and EDS spectra of RC-631L: a) before and b) after 50h leaching with H₂Suc (H₂O, 1M) under mixed aeration conditions.

Final compositional results in the residual mixtures were found, for all the samples treated by affordable conditions, in perfect line with the aim of this study which needs to tune the cobalt

content of HM waste powders to values $\leq 10\%$ Co as required for direct and profitable re-employment in HM manufacturing.

5.2.5 Metallurgical quality control (MQC) and assessment of the WC-recovered powders

C and O content in the WC-Co powders suitable to be directly employed in HM manufacturing is a critical parameter for obtaining HM tools with performing properties. Indeed, as anticipated in Chapter 1 (section 1.3) the co-presence of C and O into a WC-based powders lower the C content of the mixture during the sintering phase, affecting the final properties of the HM material due to the occurrence of the so-called η -phase in the final material.

Table 5.5 reports the optimal C and O elemental composition values for WC-Co powders suitable for HM manufacturing, as well as C and O contents found in the recovered powders from hydro- and solvo-metallurgy scale-up processes.

Table 5.5: Desired and found* C and O percentage composition for WC-Co recovered powders. *Obtained as the average value of three measurements. Appendix A1 for method.

	C (%)	O (%)
Optimal WC-Co powder	5.70	≤ 0.40
HMal _(EtOH) -recovered powder	5.99	0.65
HLat _(aq) /O ₂ -recovered powder	6.24	1.60
H ₂ Suc _(aq) -recovered powder	11.8	11.60
H ₂ Suc _(aq) /O ₂ -recovered powder	6.93	3.88

The very little excess of C and O into the recovered material from HMal treatment, demonstrates that massive hydration/oxidation phenomena on the sample, as well as the retention of the most part of organic substances from the surface, are prevented by using the proposed solvometallurgy process in ethanol, making this material suitable for application in HM manufacturing. Against, WC-Co powders recovered after hydrometallurgical treatments showed to be the most critical in terms of C and O content. Very high O% values were found for all the treated samples in water, with the highest value recorded for the non-aerated leaching system. This odd evidence may suggest that hydration phenomena of the WC-surface may occur beside the oxidative phenomena pointed out through respirometry experiments. Also the retention of unwashed organic leaching agents/complexes may occur, affecting C-O elemental analysis. WC-Co powders with this kind of composition are unsuitable for direct application in HM manufacturing. For this reason, thermal treatments under inert environment (1000°C, 2h, N₂; Appendix A3 for details) were attempted for improving the quality of the powders. Table 5.6 summarizes the C-O elemental analysis recorded for the treated samples.

Table 5.6: C and O percentage composition for WC-Co recovered powders after thermal treatment.

	C (%)	O (%)
Optimal WC-Co powder	5.70	≤0.40
HLat _(aq) /O ₂ -recovered powder	5.65	0.19
H ₂ Suc _(aq) -recovered powder	6.02	0.40
H ₂ Suc _(aq) /O ₂ -recovered powder	5.93	0.14

As shown, thermal treatments demonstrated to be able of driving powders composition within the desired ranges, making these samples suitable for HM production.

In order to process the recovered powders and test their quality in HM manufacturing, the treated RC-631L powder with H₂Mal ethanol solution was selected as a case study, was homogenized by lab-scale ball milling as detailed in Experimental (5.4.1 section), then shaped and sintered in forms of small bars to undergo Metallurgical Quality Control (MQC). WC-Co powders obtained by HLat and H₂Suc leaching are still under study. MQC procedures are detailed in Appendix A1. The results of the MQC procedure are collected in **Table 5.7**, where the values of density, hardness (HV10 and HRA), coercitive force (H_c) and magnetic moment saturation (σ) related to the pristine WC-Co powder (RC-631 L), are also reported for comparison.

Table 5.7: Results of the MQC on bars obtained by sintering the recovered RC-631L powder after leaching with a 0.5M HMal/EtOH solution, compared with the same values related to the use of the pristine powder.

	Density g/cm ³	Hardness		H _c ⁽¹⁾ Oe	σ ⁽²⁾ G cm ³ /g	Optical Microscopy	
		HV10	HRA			200x ⁽³⁾	1500x
RC-631 pristine	13.36	933	85.5	94	139	A02	-
RC-631 treated	14.88	1609	92.3	228	92	A04	η -phase

(1): Coercive force; (2): magnetic moment at saturation; (3) magnification according to ISO 4499-4.

The MQC of bars obtained by the treated powder satisfactorily show these artifacts possess all the metallurgical features, i.e. density, hardness, coercitive force and magnetic moment saturation, typical for HM materials containing around the 6% of Co. Besides, optical

microscopy highlighted the presence of a small unwanted but expected amount of η -phase (see Fig. 5.13) relating to the previously cited little excess of C and O into the powder.

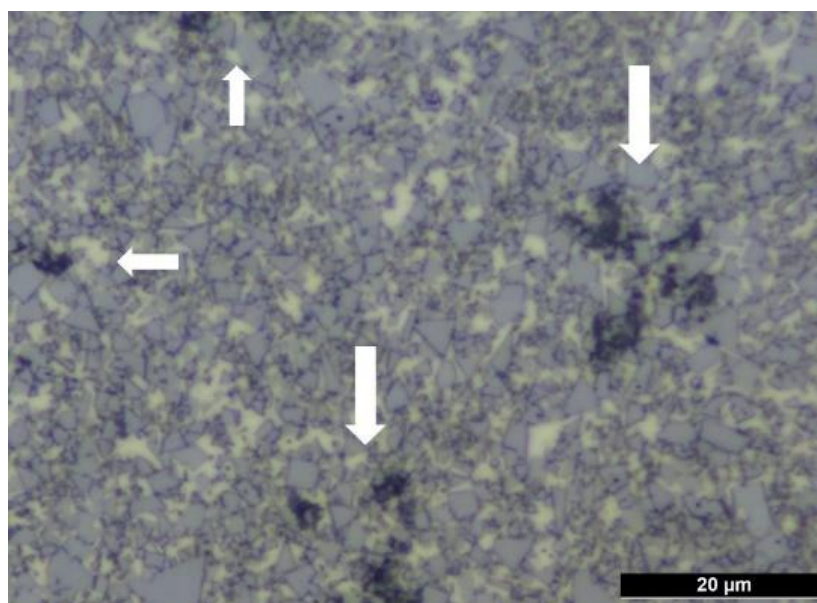


Figure 5.13: Optical microscopy image (1500x) of a sintered artifact obtained by RC-631L powder after leaching. The darkest areas pointed out by the arrows represent the η -phase.

When a small excess of O is present in the recovered powder, a correction of the powder composition during blending process, through the addition of C as high purity carbon black, can overcome the occurrence of undesired η -phase. Thus, it can be definitely stated that recovered powders obtained applying the proposed solvometallurgy method fully meet the requirements for HM manufacturing.

5.2.6 Cobalt recovery from the leaching solution

Following the leaching phase, that is one of the most critical aspects on the whole recovery process, the enhancement of Co in a form suitable for application is a further issue of industrial interest. Besides the possible applications of the complex as it is,⁹ a series of separation & recovery processes for achieving Co metal and Co-oxide (CoO/Co₃O₄), were approached.

⁹ A research activity developed in collaboration with Imperial College London, Wilton-Ely group, Dept. of Chemistry, demonstrated the [Co(Lat)₂(H₂O)₂] and [Co(Mal)₂(H₂O)₄] display significant catalytic activity in the esterification reaction of alcohols with acetic anhydride, under solvent-free conditions and low catalytic loading.[4]

The first approach is the selective complex crystallization from the leachate (see Experimental, Chapters 2 and 3) providing the solid-state compound which can undergo following thermal or electrochemical treatments.

Very interesting preliminary results were also obtained, at the Green Chemistry Center of Excellence, Dept. of Chemistry, University of York, in the selective Liquid-to-Solid extraction of Co-complexes from the solvometallurgy leachates by using Starbon®. Starbon® is a family of carbonaceous mesoporous materials derived from waste polysaccharides (HACS) after carbonization in the range 100-800°C which have been used for adsorption in a low cost process requiring no templates or hazardous chemicals.[5] It is considered to be *green* and sustainable because it is made from renewable materials using a clean production process, as detailed in Appendix A7 Specifically, Starbon® mesoporous materials with various surface functionalities, were prepared by expanded starch through carbonization in furnace at different temperatures (350, 400 and 800°C). Among the synthesized Starbons®, the one prepared at 350° (called S350) the richest in terms of functional groups, was checked for solid-phase extraction of cobalt from HLat and H₂Mal leaching solutions. Specifically, for each case study, a 1:4 diluted solution was prepared from the leachate and passed through 100mg of S350 in a solid-phase extraction apparatus (see **Fig. 5.14**).

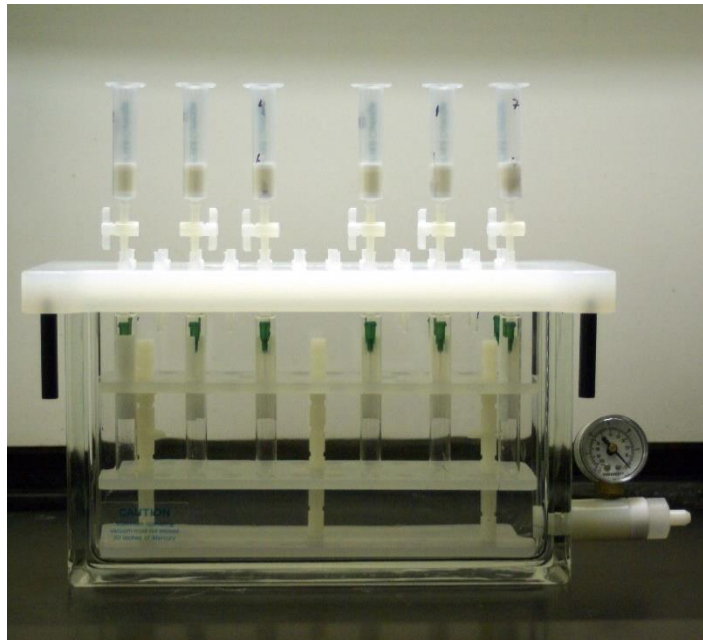


Figure 5.14: Solid-phase extraction apparatus.

Extraction efficiency was determined by UV/Vis spectrophotometry through a colorimetric method based on the comparison of the absorbance of the diluted solution before and after extraction with a calibration curve at the specific wavelength of the complex absorption (both around 520nm).

The preliminary results showed that, while no cobalt being extracted from H₂Mal ethanolic solution, about 10% of [Co(Lat)₂(H₂O)₂] was extracted from the HLat aqueous solution in a single experiment. Experiments can be, in principle, re-run several times for improving the extraction yield. Carbonaceous materials like Starbon® enriched with the metal value, can be sent to oxidative thermal degradation, returning the extracted metal, presumably, in form of metal oxide. On the bases of these preliminary results, further experiments are in progress for improving extraction conditions and yields, the final recovery of the metal as well as for functionalizing Starbons®' surfaces with *soft*-donors for increasing extraction efficiency and selectivity. Appendix A7 describes the preliminary functionalization attempts.

Electrowinning was checked as a suitable technique for cobalt metal recovery from the leaching solution. Preliminary experiments were performed directly on HLat and H₂Suc aqueous leachates into a two-electrode cell with 12 mm graphite rods under galvanostatic conditions, as detailed in Experimental (5.4.2 section). Differently, for the H₂Mal process, a 0.5M water solution of the recovered [Co(HMal)₂(H₂O)₄] complex was prepared starting from the isolated complex and treated in the described cell. Two current values, 300mA and 100mA for 10 and 30 minutes respectively, were investigated resulting in 51.7 mA/cm² and 17.2 mA/cm² current density figures at the cathode, respectively. In all cases, Co-metal deposition to the cathode was observed and energy efficiency spanning from 74 to 87% - specifically, 74% for HLat, 87% for HMal and 77% for H₂Suc solutions - calculated as the ratio between the theoretical charge to get the amount of metallic Co at the cathode and the total amount of charge transferred through the cell, were found. The loss of efficiency is reasonably attributed to the expected cathodic by-process $2\text{H}^+ + 2\text{e}^- \rightarrow \text{H}_2$ occurring in water, in agreement with the experimental evidence of gas evolution to the cathode during the electrowinning. Figs. 5.15 and 5.16 show the SEM/EDS characterization of the Co-metal deposits to the cathode in the two sets of reported conditions, obtained from the [Co(HMal)₂(H₂O)₄] solution as a case study.

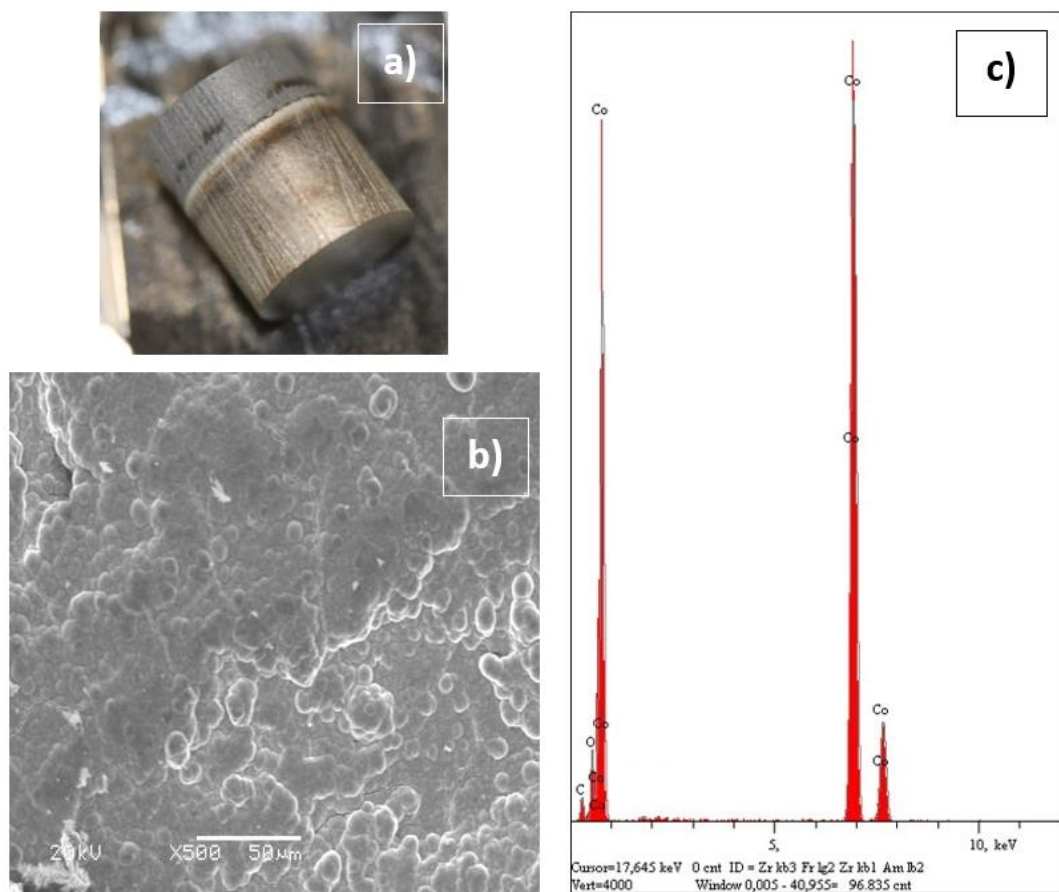


Figure 5.15: Picture (a), SEM micrograph (b) and EDS characterization (c) of the metal deposit obtained to the cathode under 100mA, 30 min, conditions. No peaks were detected up to 30 keV (the corresponding part of the spectrum has been omitted).

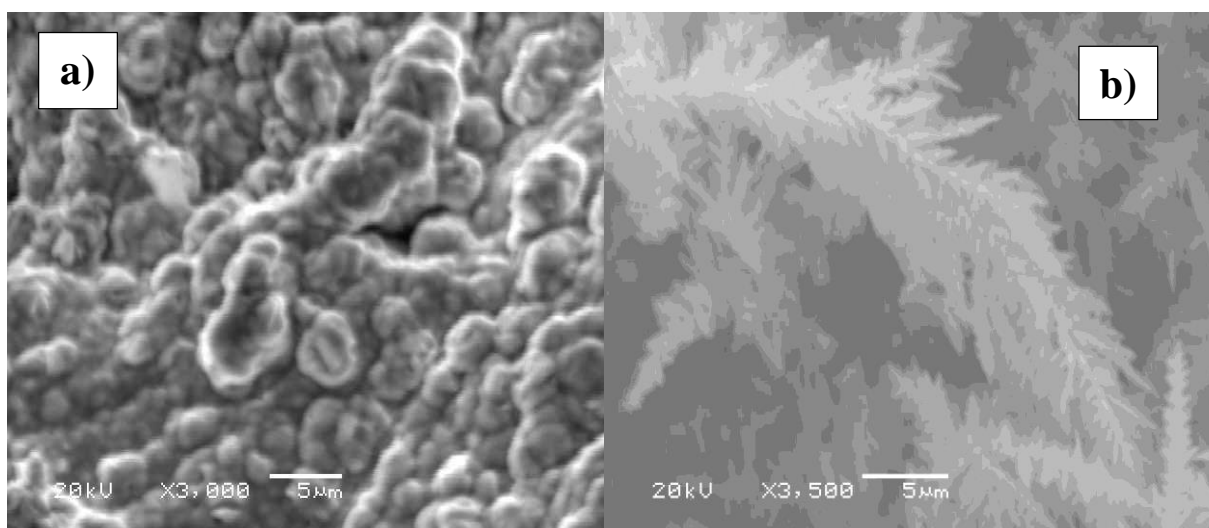


Figure 5.16: Comparison of the morphology, by SEM images, of the two metal cobalt deposits obtained to the cathode at: a) 100 mA, 30 min; b) 300 mA, 10 min.

These results are still at an early stage and the optimization of the electrowinning process exceeds the focus of this work, but they demonstrate the capability of the metal complexes to work as valued precursors for Co-metal by electrochemical reduction. The further benefit related to the use of electrowinning is the contemporary restoration of the leaching solution.

Finally, cobalt recovery was also investigated by thermal treatment of the solid Co-complexes in oxidizing and reducing environment. Specifically, heating ramps ($3^{\circ}\text{C}/\text{min}$) up to 500 and 1000°C , were applied to 5g aliquots of the different complexes in a horizontal oven (see **Fig. 5.17**), as detailed in Experimental (5.4.3 section), with the view to recover cobalt in form of oxide, when heating in O_2 atmosphere, or as a metal powder, by heating under H_2 . As shown in **Fig. 5.18**, a series of red-brown, grey and black powders were obtained by treatment of the different pink Co-complexes in oxidizing and reducing atmosphere. The characterization of these recovered powders is still in progress.

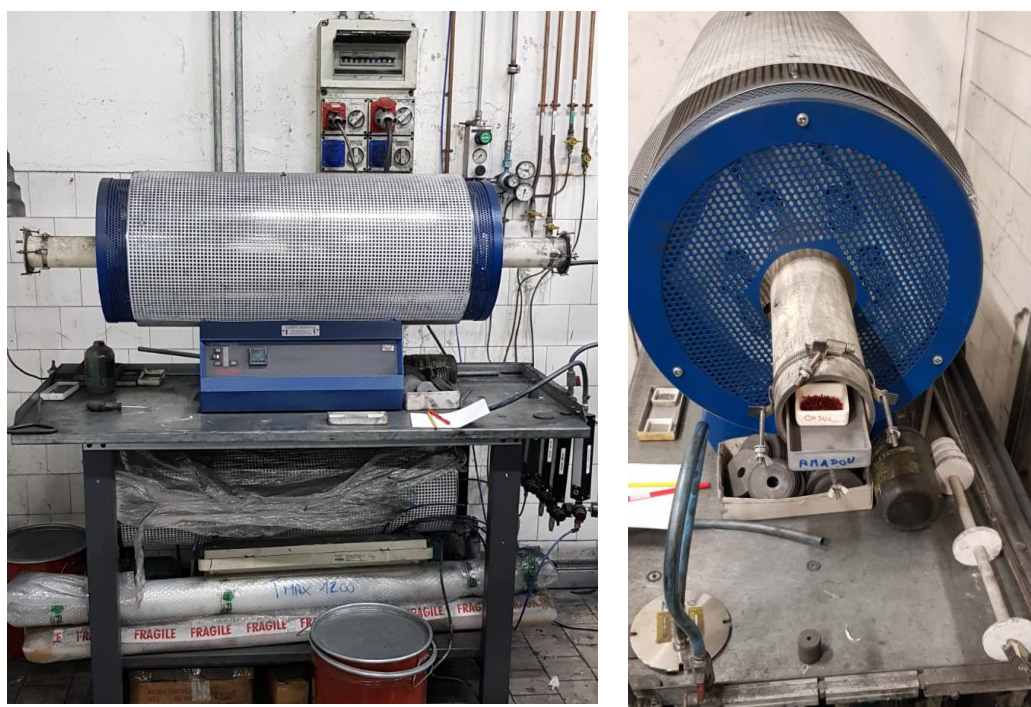


Figure 5.17: Lenton's oven for thermal treatments under controlled conditions and environment.

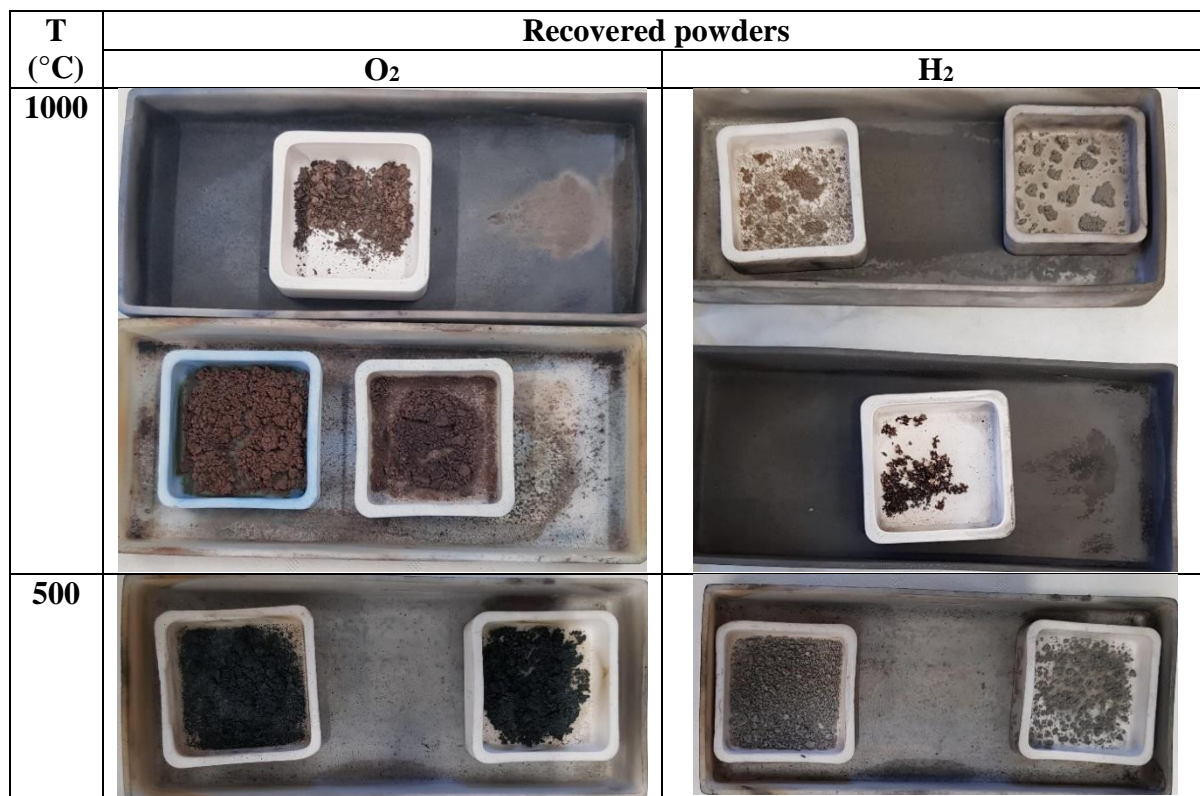


Figure 5.18: Recovered powders by thermal treatments of $[\text{Co}(\text{HMal})_2(\text{H}_2\text{O})_4]$, $[\text{Co}(\text{Lat})_2(\text{H}_2\text{O})_2]$ and $[\text{Co}(\text{Suc})(\text{H}_2\text{O})_4]$ at 500 and 1000°C under oxidizing (O₂) and reducing (H₂) environment.

5.3 Conclusions

In this chapter a focus on the Co-leaching process set-up and scalability for pursuing industrial application were pointed out with specific reference to three representative and interesting cases of Class 1-3 acids: HLat and H₂Suc in water in the presence of O₂, H₂Mal in ethanol. The performed experiments allowed to strongly support the role of oxygen in HLat and H₂Suc action in water and in finding the best operative conditions, in terms of L/S ratio and Co:Acid molar ratio as well as pH values, for moving to the scale-up process. Under these premises, HLat and H₂Suc water solutions demonstrated to achieve satisfactory Co-leaching dissolution on larger scale within 24h at room conditions under forced aeration, providing respectively WC-(5.7%)Co and WC-(3.1%)Co recovered powders, which can be made suitable for use in HM manufacturing after undergoing a 2h thermal treatment at 1000°C for removing the excess of C and O. On the other hand, H₂Mal solvometallurgy demonstrated very high efficiency reaching WC-(6%)Co in just 6h on the larger scale without addition of any external oxidizing specie and preventing oxidizing/hydrating phenomena on the material. Finally, several ways for Co enhancement were approached with more than satisfactory preliminary results, specifically in

the case of the electrowinning process on the leachates, which allow, at one time, to recover Co metal and to restore the leaching solution. On the bases of the obtained results, a TRL 5 - technology validation in relevant environment – seems to be reached at least for the leaching phase of these processes.

5.4 Experimental¹⁰

5.4.1 Physical, mechanical and magnetic characterization

The metallurgical quality control was investigated on the sintered materials. Recovery powders before/after treatment were homogenized by lab-scale ball milling for 72 h in ethanol and with a 3:1 HM balls to powder ratio in a stainless-steel jar. Samples in forms of bars (according to ISO 3327:2009) were sintered at 1500 °C under Ar (35 bar) in a standard sinterHIP (Hot Isostatic Pressing) process.[6] The sintered test specimens underwent density, hardness (HV10 and HRA), coercitive force (Hc) and magnetic moment saturation (σ) measurements, under conventional protocols and operative conditions.[7][8][9]

5.4.2 Electrowinning experiments

The electrowinning experiments were investigated on the leaching solutions obtained after scale-up process. However, 200mL aliquots of leachate, were employed in a two-electrode cell with 12 mm graphite rods as the electrode at room temperature. The electrowinning process was carried out in galvanostatic conditions using an AMEL Instruments Mod. 7050 Potentiostat/Galvanostat. 300 mA and 100 mA current values were applied to the cell for 10 min and 30 min respectively that resulted in 51.7 mA/cm² and 17.2 mA/cm² current density figures at the cathode. At the end of each experiment, the amount of deposited metallic cobalt was estimated by a mass increase of the cathodic electrode and the current efficiency calculated by dividing the charge needed to get the amount of metal Co at the cathode and the total amount of charge that was transferred through the cell.

5.4.3 Thermal treatments on cobalt complexes

Cobalt recovery from cobalt complexes was investigated by thermal treatment in oxidizing, reducing and neutral environment on a Lenton's oven. A pre-weighted amount of material (ca. 2-5g) underwent a heating ramp up to 500 or to 1000°C with a heating rate of 3°C/min, 0.5 atm,

¹⁰ This part of the work has been carried out at FILMS corp.

and left at the reached temperature for 2h before cooling down to room temperature.

5.5 References

- [1] Stefano Trudu, Research Thesis in MSci "Ingegneria per l'Ambiente e il Territorio" titled "Economia circolare: approccio sostenibile alla valorizzazione degli scarti di produzione del metallo duro", University of Cagliari, 2019.
- [2] Martina Cera, Research Thesis in MSci "Ingegneria per l'Ambiente e il Territorio" titled "Valorizzazione di scarti agroindustriali in idrometallurgia", University of Cagliari, 2019.
- [3] W. A. Badawy, F. M. Al-Kharafi, and J. R. Al-Ajmi, "Electrochemical behaviour of cobalt in aqueous solutions of different pH," *J. Appl. Electrochem.*, vol. 30, no. 6, pp. 693–704, 2000.
- [4] Dilan Al, Research Thesis in MRes "Catalysis: Chemistry and Engineering" titled "Utilising Cobalt Waste as a Feedstock for New Cobalt (II) Catalysts", Imperial College London, 2019.
- [5] A. M. García, A. J. Hunt, V. L. Budarin, H. L. Parker, P. S. Shuttleworth, G. J. Ellis, J. H. Clark, "Starch-derived carbonaceous mesoporous materials (Starbon®) for the selective adsorption and recovery of critical metals", *Green Chem.*, vol. 17, pp. 2146–2149, 2015.
- [6] D. Milligan, U. Engström, N.A. Höganäs, S. Smith, G. Products, S.C.I.H. Division, Presented at PM²TEC2005 in Montréal, Canada , in June 2005 Presented at PM²TEC2005 in Montréal , Canada , in June 2005, 1–5.
- [7] B. Roebuck, M. Gee, E.G. Bennett, R. Morrell, A National Measurement Good Practice Guide No. 20 - Mechanical Tests for Hardmetals, Ceramics. (1999) 1–74.
- [8] M. Lattemann, R. Xie, R. Lizárraga, L. Vitos, E. Holmström, Magnetic Saturation: Understanding Quality Control of Hard Metals in Industry - A Quantum Mechanics Approach (Adv. Theory Simul. 6/2019), *Adv. Theory Simulations*. 2 (2019) 1970021. doi:10.1002/adts.201970021.
- [9] B. Roebuck, Magnetic moment (saturation) measurements on hardmetals, *Int. J. Refract. Met. Hard Mater.* 14 (1996) 419–424. doi:10.1016/S0263-4368(96)00035-2.

Chapter 6

Agroindustrial secondary sources of lactic acid for HM waste enhancement

6.1 Introduction

On the basis of its demonstrated remarkable reactivity towards Co in very mild conditions, the high quality of the recovered products when its solutions are applied on complex wastes like HM recovery powders, its low cost and environmental impact, as well as the possibility of its production starting from agroindustrial wastes, lactic acid was identified as the most intriguing and appealing case study for industrial purposes among the several leaching systems here proposed. Among agroindustrial wastes, dairy wastes are attracting specific attention due to the key role they play in the European economy, especially in the Mediterranean countries, where activities such as livestock farming are considered relevant in economic, social and environmental terms, due to the global wide and spread production of milk and milk derivatives (170 million tons of milk were produced in 2017 in EU and transformed into a wide range of dairy products).[1] In this framework, wide knowledge has been grown up by the environmental sanitary engineering research group of the DICAAR (University of Cagliari) in the valorization of the residues of the dairy industry producing organic acids and hydrogen through fermentative processes.[2][3][4][5] Cheese whey and *scotta* are the main residues of dairy industry with a specific production of 0.8-0.9L per liter of processed milk. They are also the ones earning the highest concerns in terms of environmental impact, due to their high organic substances loading (quantified through the most common environmental parameters such as the COD and BOD - Chemical Oxygen and Biochemical Oxygen Demand, respectively - equal to 50-102 and 27-60 g/L). In the past, agricultural land spreading and/or direct use for animal feeding were the most widely applied solutions for cheese whey management. Nowadays, these practices are no longer considered sustainable due to concerns about the potential adverse effects on the environment and animal health conditions,[4] so more appropriate alternatives need to be explored. In a circular economy perspective, efforts at looking for efficient reuse or recovery of materials/energy from any valuable waste stream originated by the production cycles need to be boosted. To this respect, ambitious valorization options aiming at producing biochemical from organic wastes streams addressed to answer the need of raw material preservation and waste prevention, are highly desirable and included in the waste management aims of EU regulations.[6] With this view, recently, controlled dark fermentation processes of these secondary materials for direct production of HLa^t leaching solutions with the desired features for selective metals dissolution, were performed and here applied to HM waste material for implementing a really sustainable circular economy model appealing for industry.[7][8]

All the mentioned above, together with the strict EU regulations on toxic materials management, namely REACH and SEVESO III directives,[9] make the design of sustainable circular economy models in HM manufacturing based on the use of enhanced dairy wastes, appealing both for industrial and environmental purposes.

6.2 Results and discussion

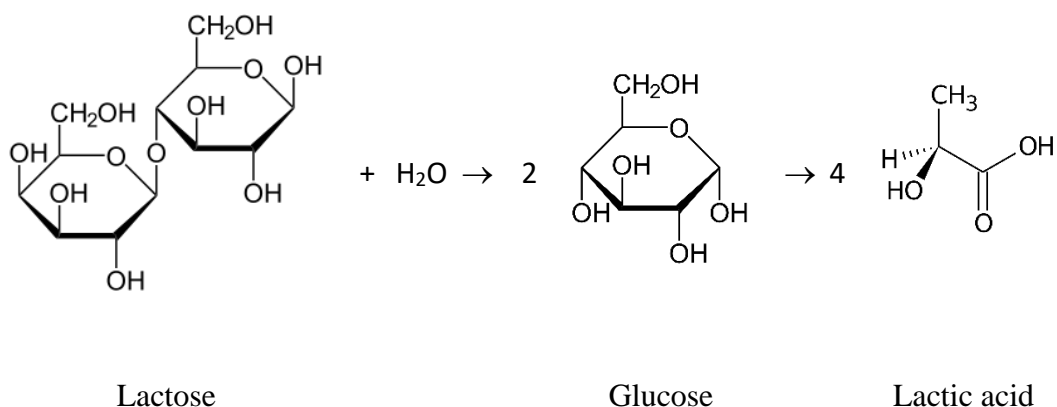
6.2.1 Controlled dark fermentation processes for HLat-based hydrometallurgy⁷

Dark fermentation process is a versatile tool which can be carried out in a controlled mode for achieving selectively the desired products.[5] Specifically, HLat-based aqueous leaching solutions, with the view to promote the highest rates of high-quality recovered materials (Co and WC) directly employable in HM manufacturing, require the following optimal features:

- low residual carbohydrates, proteins and fats content;
- high lactic acid concentration (between 0.1 and 1M);
- pH ≤ 4.

From a biochemical point of view, dark fermentation involves a phase of conversion of carbohydrates, initially present in the form of lactose, into lactic acid, as in the following reaction:

Eq. 6.1:



Conventional dark fermentation processes addressed to favor lactic acid production, are carried out at pH between 5-7, in order to guarantee lacto-bacteria a reaction environment suitable for

their survival, as the accumulation of lactic acid determines their inhibition related to the lowering of the pH. Nevertheless, this approach provides a fermented solution which does not meet the criteria required for working as a metal leaching solution, due to the high pH (around 6) that favors Co oxides and hydroxides precipitation, as well-known and observed in the experiments described in 5.2.2 section.

To simultaneously achieve the three objectives mentioned above, two consecutive phases were investigated:

– Phase I: involved a strict pH control to 6 (by dosing NaOH), as it guaranteed the most favorable conditions for the production of lactic acid (present mainly in form of lactate, at this pH value)¹¹;^[5]

– Phase II: pH was kept uncontrolled and fermentation continued with the production of lactic acid until the substrate exhausted or the solution reached an acid pH that inhibits bacteria. In this phase, the pH spontaneously lowers as a result of the production of lactic acid by fermentation and not neutralized by the addition of the base.

The relative duration of the two phases is a key point for achieving solutions with the desired properties. Phase I is crucial for the efficient conversion of carbohydrates into lactic acid, while Phase II, to spontaneously carrying the fermentation out to the desired pH, limiting the costs of any pH-regulating reagents. For finding the right balance between the two phases able to provide a simultaneous almost complete consumption of the carbohydrates and final $\text{pH} \leq 4$, a monitorable parameter related to the system conditions which highlights Phase I to Phase II switch point, needed to be identified.

Duration times of the two phases demonstrated to be a hardly reproducible parameter on these materials where no specific inoculation was made. Satisfactory results were instead obtained by monitoring the $[\text{HLat}]/[\text{carbo}]$ ratio during controlled fermentation (where $[\text{HLat}]$ and $[\text{carbo}]$ are the molar concentration of produced lactic acid and residual carbohydrates, respectively).

¹¹ For the sake of simplicity, throughout this Chapter, wherever not specified differently, the terms “lactic acid” and “HLat” are used with the widest meaning of product of the lactose conversion by bacteria according with the Eq. 6.1, the real form of the existing specie in solution (undissociated HLat or Lat^- ion) depending on the pH and/or competitive equilibria.

Fig. 6.1 shows the molar fractions of HLat (χ_{HLat}) and carbohydrates (χ_{carbo}) along the fermentation profile vs [HLat]/[carbo] ratio as well as the final pH value achievable by the solution if Phase II would start in those [HLat]/[carbo] ratio conditions (see Appendix 8 for methods). This graph was obtained by monitoring the three parameters, [HLat], [carbo] and final fermentation pH, of aliquots subsampled during the time by a single cheese whey fermentation run at pH 6 (see fermentation reaction in **Fig. 6.2**) and underwent Phase II (with no pH control) in separate reactors thermostated at 39°C.

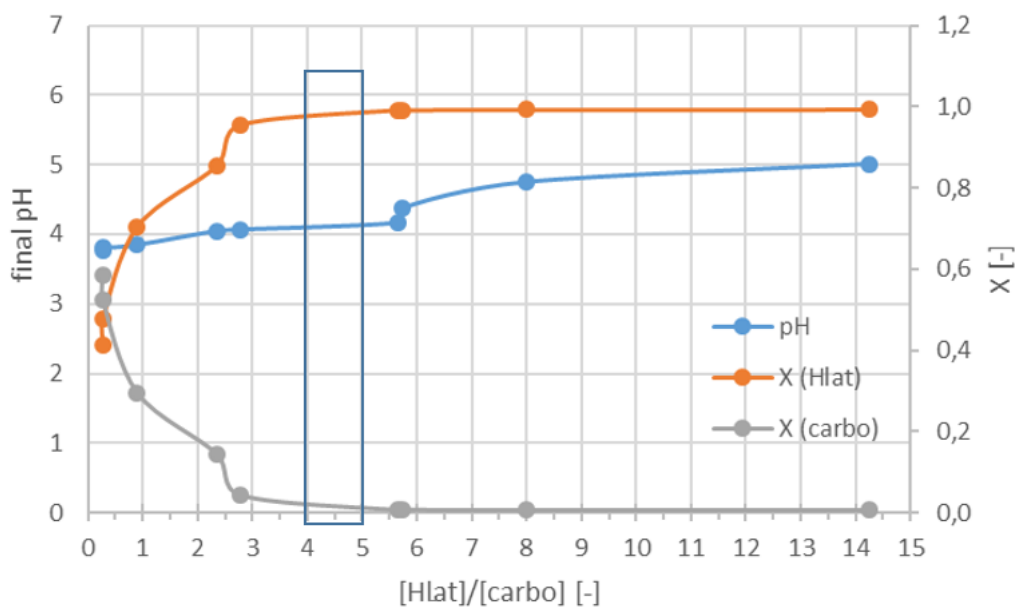


Figure 6.1: HLat and carbohydrates molar fraction (χ) curves vs [HLat]/[carbo] parameter and pH values of the final solutions obtained when Phase II starts in those [HLat]/[carbo] ratio conditions. The rectangle indicates the Phase I-to-Phase II switch zone. See Appendix 8 for methods.

As shown in **Fig. 6.1**, a final pH in the desired range (around 4) can be reached by setting the [HLat]/[carbo] parameter between 4 and 5, obtaining at the same time high carbohydrates conversion yields to HLat which results in high χ_{HLat} and, correspondingly, low χ_{carbo} . Noteworthy, this parameter showed to be completely independent from the duration time of the two phases, being highly reproducible on different kind of dairy waste samples (either whey or *scotta*), depending just on the starting amount of carbohydrates.



Figure 6.2: BIOFLO 110 reactor for dark fermentation (New Brunswick Scientific; Bio Command Lite software).

For the leaching experiments described in this chapter, the fermentation was carried out on a cheese whey sampled by a dairy in Southern Sardinia (**Table 6.1** for details) by the two phases proposed approach, as detailed in Appendix 8. In Phase I the pH was kept constant at the value of 6 by suitably dosing a solution of NaOH 2.5 M. The Phase II was started after reaching a value of [HLat]/[carbo] of 5.6 and was completed with the stabilization of the pH (final pH: 4.09; [HLat]=0.35M; [carbo]=0.02M).

In the view of the specific field of HM waste valorization, despite the optimal composition in terms of HLat and residual carbohydrates concentration of the obtained solution, the residual amount of proteins and fats should be taken into account because they may represent undesired impurities which can affect the quality of the recovered WC powder. An approach based on the use of ethanol as anti-solvent for precipitating hydro-soluble proteins, demonstrated to be suitable to purify the fermented solution allowing, at the same time, the recovery of valuable proteins, namely α -lactalbumin, β -lactoglobulin, serum albumin and immunoglobulin and ethanol recycling.

For these reasons, the fermented cheese whey underwent three pre-treatments:

1. Preliminary settling and separation

2. addition of ethanol with an ethanol:fermented whey volume ratio 3:5 to precipitate the part of hydro-soluble substances insoluble in EtOH
3. Centrifugation and recovery of ethanol.

The purified fermented solution was then sent to the leaching phase on recovery powders.

6.2.2 Hydrometallurgy with fermented cheese whey solutions

Preliminary experiments on recovery powders were performed on the RC-631L test specimen.

The experiment was carried out using a fine bubble aeration system and a mechanical stirring system for 4 hours, using 0.400L of fermented whey 0.35M and 5.18g of test specimen according to a 1:8 acid:Co molar ratio, in agreement with the previous set-up when using commercial HLat solutions (see Chapter 5). In these conditions, the 4h leaching yielded the 50% Co dissolution on the real material. Despite the found leaching yield was lower than expected, it is reasonable as it can be related to the lower HLat concentration in the fermented whey with respect to the commercial HLat solution, depending on the starting amount of carbohydrates in the cheese whey. This result seems, instead, very promising pointing out the direct applicability of the fermented whey to WC-Co-based powders for the selective Co dissolution and suggests that, on the one hand, longer leaching times may improve dissolution yields and, on the other hand, concentration processes of the solution may provide a more effective leaching and improve L/S ratio for industrial purposes.

6.2.3 Circular economy model for bioderived HLat-based hydrometallurgy on HM wastes

On the basis of the really satisfactory results of the scale-up process (5.2.4 section) and the preliminary results related to the direct application of aqueous leaching solutions obtained by controlled dark fermentation of cheese whey, an attempted design of a fully closed-loop circular economy model in HM manufacturing is here proposed and outlined in **Fig. 6.3**.

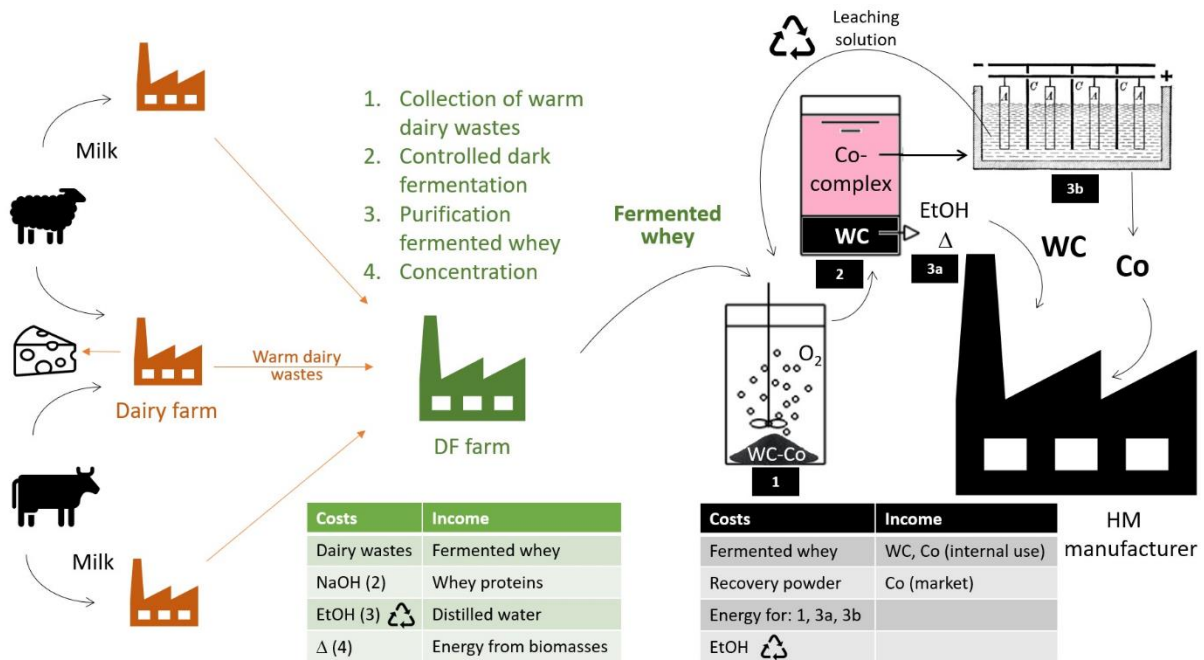


Figure 6.3: Outline of a possible circular economy model in HM manufacturing based on the use of dairy wastes as precursors of Co-leaching solution. DF: Dark Fermentation; ❶ Aerobic leaching in water solution; ❷ decantation; ❸a washing and drying; ❸b electro-winning.

The proposed outline is based on the hypothesis of three main stakeholders: dairy industries, Dark Fermentation (DF) farms and HM manufacturing industries. Alternative models may entrust DF activity directly to dairy or HM manufacturing industries. Anyway, the first phase of activities is related to the cheese whey valorization, which involves collection, controlled two-phase DF, as well as purification & recovery of the most part of valued substances for limiting waste production and marketing the products. The output of this phase is a customized leaching solution that would represent the input stream of the HM hydrometallurgy process which consists of three main phases:

- Phase 1: selective leaching in forced aerobic environment
- Phase 2: decantation and liquid to solid separation
- Phase 3: metal value recovery (3a: washing and drying of WC for re-employment; 3b: electro-winning of the leachate which obtains Co metal, restoring the leaching solution for a new run).

In principle, this is an almost closed-cycle process with relatively low environmental and financial costs. Indeed, cheese whey is valorized preventing irregular disposal or employ in low

value fields and it represents a low-cost input for the process. Controlled DF does not require specific inoculation and use a negligible amount of chemicals (NaOH). It can benefit of the warmth of cheese whey, if it is ready fermented after production and EtOH used for compound purification can be recycled (as well as water obtained by concentration). Fermented whey, hence, represents a low cost and sustainable material for hydrometallurgy. For its part, the proposed hydrometallurgical process does not require further reactants, except for the oxygen which can be furnished to the reaction by forced aeration. The leaching times can be also finely tuned in order to obtain the desired Co-amount in the recovered WC powders to be sent to the following HM production phases. The most critical aspects are related to:

- **washing and drying of the WC powder obtained after leaching (phase 3a)** for removal of interfering species like residual organic substances (which can ingenerate an excess of C and O in the material) as well as water molecules (which can increase the content of O), nevertheless EtOH used for washing can be recycled and residual organic substances can be valorized as energy as well as the heat typically developed by HM plants can be valorized in the part of hydrometallurgical process where heating is necessary;

- **electrowinning (phase 3b)**, where the energy efficiency is around 75% in water due to the H^+/H_2 by-process to the cathode besides Co deposition, **and recovery of leaching solution**, which is expected will limit wastewater production, even if a strict assessment of the quality of the recycled solution is still in progress.

6.2.4 Perspectives in the use of bioderived lactate salt/ I_2 solvometallurgy⁷

Non-acid ligand/ I_2 solvometallurgy demonstrated to be a powerful but gentle tool for the selective Co-leaching from HM wastes. Despite S-donor organic ligands showed the highest efficiency in metal dissolution when in the presence of the oxidizing specie, great interest is attracting the Lat⁻/ I_2 (EtOH) system because, beside the more than satisfying Co-dissolution rates, lactate species can be suitably produced from dairy wastes through DF. Indeed, as anticipated previously, DF can be carried out in a controlled manner for pursuing a final solution with the desired characteristics. Recent results by the environmental sanitary engineering group of DICAAR,[5] demonstrated that high concentration lactate solutions with negligible amount of undissociated HLat and residue carbohydrates can be obtained by carrying out DF at 39°C, under pH control at 6 by dosing NaOH. In order to be used in solvometallurgy, the fermented whey must be deprived of water. Appendix 8 reports details on applied DF processes.

The fermented whey prepared for the present study was treated under fully controlled pH 6 conditions and then underwent a first decantation/separation of the insoluble organic matter, then it was dried in an oven at 50-60°C (see **Fig. 6.4a**). Ethanol washing of the dried fermented whey allowed to extract lactate salts from the whole solid mass to the solution, leaving back the organic substance insoluble in ethanol (see **Fig. 6.4b**).

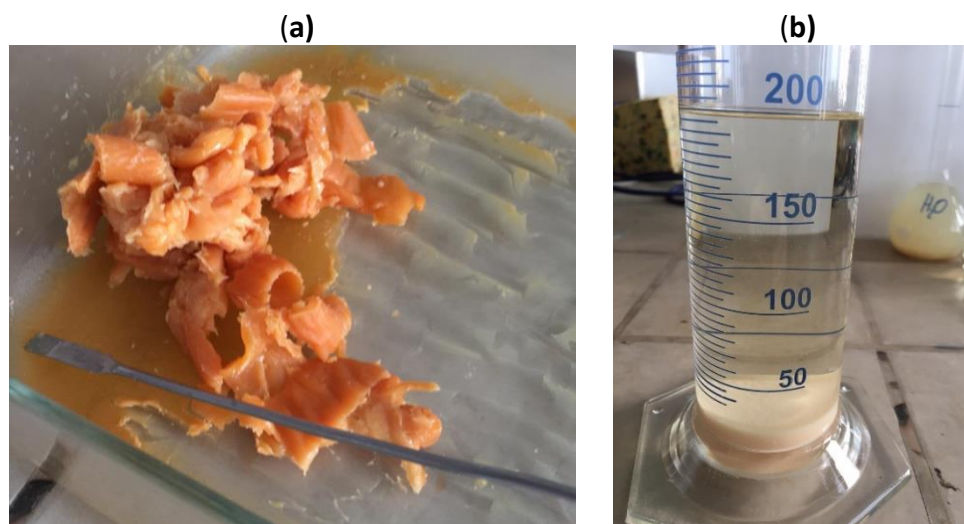


Figure 6.4: Fermented cheese whey after drying (a) and following extraction with EtOH (b).

The main advantages of this approach are related to the possibility to achieve, in one stage, a purified lactate solution of the desired concentration. For leaching purposes, a 1M lactate solution was prepared.

The leaching experiment was carried out on 32.5g the RC-627C recovery powder with 440mL of the prepared solution. The powder was reacted under magnetic bar stirring for 24 hours and using I_2 as the oxidant. The Co:HLat: I_2 molar ratio was 1:4:1. Despite the leachate and the recovered powder are still under characterization, the initial dark brown solution turned to pink when the reaction went off, assessing the effective occurrence of the leaching.

On the bases of these preliminary but satisfactory results and the results recorded on Co-powder (4.2.3 section), an attempted design of a fully closed-loop circular economy model in HM manufacturing based on this new process is here proposed and outlined in **Fig. 6.5**.

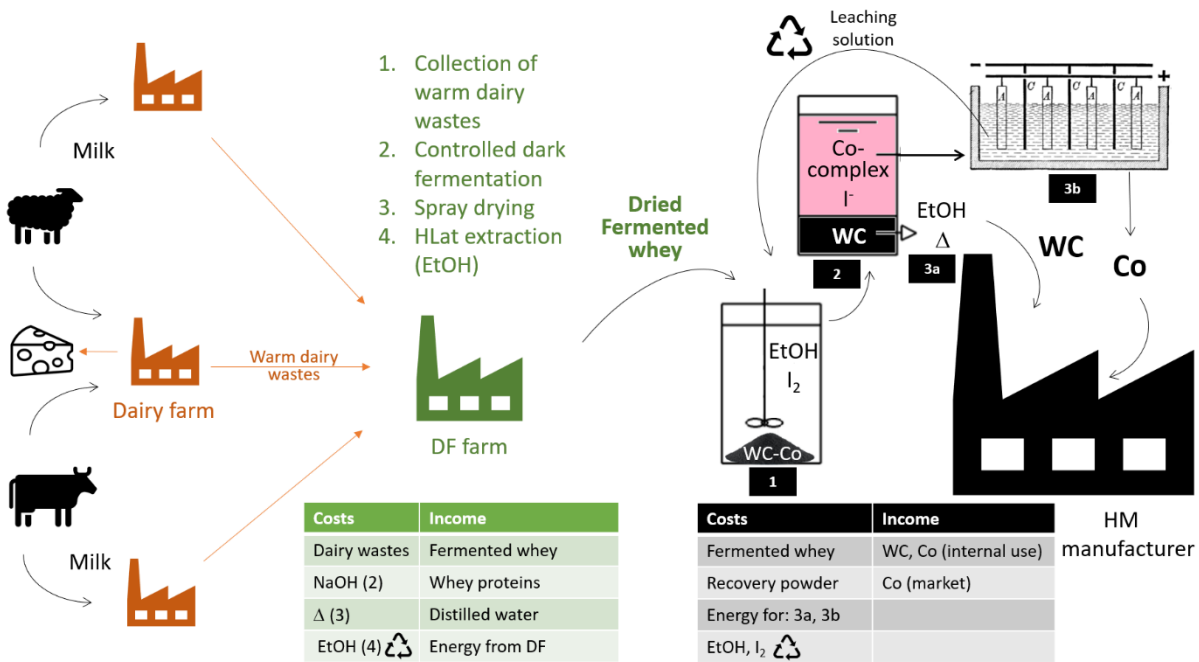


Figure 6.5: Outline of a possible circular economy model in HM manufacturing based on the use of dairy wastes as precursors of Co-leaching solution. DF: Dark Fermentation; ❶ leaching reaction in ethanol; ❷ decantation; ❸a washing and drying; ❸b electrowinning.

Also in this case, the proposed outline exploits dairy industries, Dark Fermentation (DF) farms, and HM manufacturing industries, as main stakeholders. The cheese whey valorization phase now involves collection, controlled DF at pH=6, drying (spray drying seems to be an appealing solution), lactate extraction in ethanol. The extraction solvent can be recycled in order to store and put on the market an easier to handle solid powder, which can be suitably reconstituted adding ethanol directly in the leaching plant. The residue organic substances, primarily whey proteins, can also be valorized. The ethanol leaching solution would represent, together with I₂, the input stream of this HM solvometallurgy process which consists of three main phases:

- Phase 1: selective leaching at room conditions
- Phase 2: decantation and liquid to solid separation
- Phase 3: metal value recovery (3a: washing and drying of WC for re-employment; 3b: electrowinning of the leachate which obtains Co metal, restoring the leaching solution for a new run).

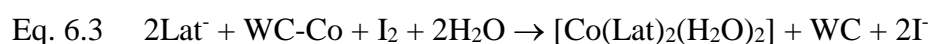
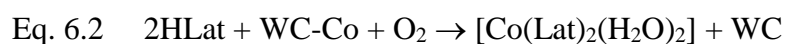
With respect to the previously proposed hydrometallurgical system, in the present process, leaching requires the addition of I₂ as oxidizing agent. Iodine is a costly but very powerful and

recyclable reagent. It makes the reaction more efficient than low solubility oxygen does in water. Moreover, ethanol is a more costly and flammable solvent respect to water but highly recyclable and *green*. The third phase of metal value enhancement promises to be particularly appealing. Indeed, recovered WC (or composition tuned WC-Co) powders should be cleaner than found in the hydrometallurgical process, both in terms of residual organic residues and hydration (negligible in non-water solvents), requiring less washing as well as thermal treatments before re-employment for industrial purposes. Electrowinning is expected to deposit Co by reduction at the cathode and obtain I₂ by oxidation from I⁻ to the anode, restoring the leaching solution.

6.2.5 Comparing the leaching systems in terms of green chemistry

Green chemistry metrics [10] represent a suitable tool for comparing the environmental impact expected for different reactions addressed to obtain the same products or for similar reactions with the same focus and this can be helpful for comparing the proposed processes with respect to the more conventional hydrometallurgy systems.

Table 6.1 summarizes the metrics calculated for the two leaching reactions discussed in this chapter and reported in Eq. 6.1 and 6.2:



The first consideration is that both these reactions occurs almost quantitatively, in a single stage and selectively, so they can be graded as high step-economy reactions. Besides, considering [Co(Lat)₂(H₂O)₂] and WC as the desired products, Atom Economy (AE) is calculated to be 100% and 64.7% for Eq. 6.2 and Eq. 6.3, respectively. These values suggest an almost full conversion of the reactants into the valued products, for the Eq. 6.2, while lower grade of conversion is found for Eq. 6.3, given the I⁻ species are not involved in the valued products. The impact of this parameter can be assessed differently thinking the role of I⁻ at the end of the recovery process, being the specie that restore I₂ by electrowinning. Further important information comes from Mass Productivity (MP). This parameter points out the percentage of valorized material in the process. This parameter also seems favour Eq. 6.2, with a 52.3% MP, with respect Eq. 6.3, with a significantly lower 10.8% MP. These values are calculated taking into account a 100% yield of the main Co-complex. MP calculated for solvometallurgy is heavily affected by the non-aqueous solvent – EtOH – who's mass is added at the denominator of the fraction. Noteworthy, EtOH is an environmentally sustainable solvent (listed among the

most sustainable solvents) and it is fully recyclable preventing wastewater production. On the other end, water is not included in the MP calculation of the hydrometallurgy process, as well as gaseous O₂ which is provided to the reaction blowing air. These very important aspects can be pointed out by calculating the E Factor, which puts in relationship the amount of desired products with the amount of generated wastes and represents a good connection between the laboratory and the industrial scale. Despite a strict evaluation of the E Factor is hard to be done and would come from an industrial application of the process, this is expected to approach zero if all the fractions generated by the reaction are treated under a Circular Economy vision. Indeed, E Factor may assume very different values depending on the rate of reagents and solvents recycling at the end of the process. Approximated E Factor values found for Eq. 6.2 and 6.3 are 16 and 8.7, respectively, if no recycling of solvents and leaching agents is applied, approaching to zero if all the fractions are well managed. In the case of solvometallurgy, recycling procedures and wastewater prevention seem easily to be pursued.

Table 6.1. Selection of *green chemistry* metrics applied to the hydrometallurgical and the solvometallurgical processes.

	Metrics	Mathematic expression	Calculated value	
			Eq. 6.2	Eq. 6.3
AE	Atom Economy [11]	$\frac{\sum \text{m.w. desired products}}{\sum \text{m.w. reagents}} \times 100$	100%	64.7%
MP	Mass Productivity[10]	$\frac{\text{Mass desired products}}{\text{Total mass used in the process}}$	52.3%	10.8%
EF	E Factor [12][13]	$\frac{\text{Total waste}}{\text{Mass of product}}$	16 (WC, Co metal recovery; no recycling of leac. solutions) Towards 0 (WC, Co metal recovery; coordinated and free reagents, solvents recycling)	8,7 (WC, Co metal recovery; no recycling of leac. solutions) Towards 0 (WC, Co metal recovery; coordinated and free reagents, solvents recycling)

With respect to the use of more conventional strong inorganic acids in water, the applications of both these two leaching processes seems more sustainable. Inorganic acids like HNO₃ and

H₂SO₄ are efficient leaching agents for cobalt. Nevertheless, they are not selective leading to a deep transformation of the WC-matrix (formation of H₂WO₄) which requires following treatments for obtaining back the desired WC for HM manufacturing. Besides, they are harmful to operators and their action is accompanied by undesired toxic gases evolution (NO_x and SO_x, respectively) in large amounts. For these reasons, the step economy and AE of the reactions involved, are expected to be lower than those calculated for the proposed HLat-based systems. The expected higher MP of these systems is counter-balanced by higher values for the E factors due to lower rates of reagents recyclability and strongly acidic wastewater production.

6.3 Conclusions

On the basis of the previous results of leaching methods based on the use of bio-derived lactic acid, two possible approaches for the implementation of profitable and sustainable circular economy models have been proposed pointing out their advantages and disadvantages. A comparison of molecular scale sustainability through the application of green chemistry metrics, also compared with conventional hydrometallurgical methods, was discussed. Despite the final assessment of the whole technical-environmental-financial sustainability on industrial scale would come only by a full configuration pilot-scale application, the preliminary results discussed above seem promising and appealing. In this framework, dairy wastes demonstrated to be a valued substrate and dark fermentation an intriguing and versatile tool for producing leaching solutions for both hydro- and solvo-metallurgy. The DF controlling strategy proposed here for producing lixivants with the desired features for hydrometallurgy represents a unique solution that optimizes the quality and quantity of the products obtained as well as the efficient use of resources and chemicals. The valorization at one time of two relevant wastes, cheese whey and WC-Co recovery powders, which to date represent environmental concerns, is the key point that suggested us to select HLat-based methods as our case study for both hydro-acidic- and solvo-non-acid-metallurgy and inspired the two circular economy models proposed here.

6.4 References

- [1] H. Strandell and P. Wolff, *The EU in the world - 2018 Edition*. Luxembourg: 160pp 2018.
- [2] G. De Gioannis, A. Muntoni, A. Poletini, and R. Pomi, "A review of dark fermentative hydrogen production from biodegradable municipal waste fractions," *Waste Manag.*, vol. 33, no. 6, pp. 1345–1361, 2013.
- [3] G. De Gioannis *et al.*, "Biohydrogen production from dark fermentation of cheese whey: Influence of pH," *Int. J. Hydrogen Energy*, vol. 39, no. 36, pp. 20930–20941, 2014.
- [4] M. Akhlaghi *et al.*, "A parametric response surface study of fermentative hydrogen production from cheese whey," *Bioresour. Technol.*, vol. 244, no. July, pp. 473–483, 2017.
- [5] F. Asunis *et al.*, "Control of fermentation duration and pH to orient biochemicals and biofuels production from cheese whey," *Bioresour. Technol.*, vol. 289, no. May, p. 121722, 2019.
- [6] European Parliament and Council, "Directive (EU) 2018/851 of the European Parliament and of the Council of 30 May 2018 amending Directive 2008/98/EC on waste," *Off. J. Eur. Union*, no. 1907, pp. 109–140, 2018.
- [7] Stefano Trudu, *Economia circolare: approccio sostenibile alla valorizzazione degli scarti di produzione del metallo duro*, M.Sc. thesis, 2019.
- [8] Martina Cera, *Valorizzazione di scarti agroindustriali in idrometallurgia*, M.Sc. thesis, 2019.
- [9] European Union, "Seveso III Directive: DIRECTIVE 2012/18/EU OF THE EUROPEAN PARLIAMENT AND OF THE COUNCIL of 4 July 2012 on the control of major-accident hazards involving dangerous substances, amending and subsequently repealing Council Directive 96/82/EC," *Off. J. Eur. Union*, pp. 1–37, 2012.
- [10] D. J. C. Constable, A. D. Curzons, and V. L. Cunningham, "Metrics to 'green' chemistry - Which are the best," *Green Chem.*, vol. 4, no. 6, pp. 521–527, 2002.
- [11] B. M. Trost, "The atom economy - A search for synthetic efficiency," *Science (80-.)*, vol. 254, no. 5037, pp. 1471–1477, 1991.
- [12] M. Peron, S. C. de Sousa, R. L. Fernandes Oliveira, and L. C. Mandarino Freire, "Green chemistry," *PCI-Paint Coatings Ind.*, no. MAR 2014, 2014.
- [13] I. Arends, R. Sheldon, and U. Hanefeld, *1. Introduction to E Factors and Atom Efficiency*, pp 48 2007.

Conclusions and perspectives

7.1 Overall conclusions

Starting from scope this thesis wanted to pursue, i.e. the design and application of new solvometallurgical methods for a sustainable, effective and selective metals recovery from the complex matrix of HM recovery powders, hazardous wastes of HM manufacturing with the aim of implementing a circular economy model CEM of industrial interest, the following primary results have been obtained:

In PART I

- 1) a series of bio-derived organic acids, namely HLat, H₂Suc, HLB, HMB, H₂It and HArg were found to be effective leaching agents for cobalt from WC-Co wastes through hydrometallurgy, dissolving almost quantitatively Co in aqueous solutions at low concentration level (0.5M) and room conditions in very short times (4-6h for treating 0.1-0.5g of recovery powder) and leaving the residual WC unreacted;
- 2) an attempted classification that discriminate organic acids on the basis of the specie involved as oxidant in the leaching process in water (H⁺ or O₂) - where Class 1 acids behave as oxidants through H⁺, Class 2 need O₂ for leaching, Class 3 follow the two pathways - allowed to properly set-up the experimental conditions for practical application;
- 3) two new compounds, i.e. [Co(It)(H₂O)₂]₃ and [Co(MB)₂(H₂O)₂], were firstly isolated in this work by leaching reaction and the former also characterized by single crystal X-Ray diffraction;
- 4) among the organic acids selected for solvometallurgy in non-water solvent, H₂Mal ethanolic solutions demonstrated to be the most promising for practical application dissolving almost quantitatively and selectively Co from HM-wastes in a short time without the addition of external oxidizing agents and leaving the residual WC unreacted;
- 5) H₂Suc/MeOH demonstrated to be a promising alternative to H₂Mal/EtOH solutions, when solvometallurgy would be preferred to hydrometallurgy;
- 6) Tu, DTO and PhDTMA/I₂ mixtures in EtOH and acetone demonstrated to be powerful S-donor ligands leaching systems for cobalt, being specifically PhDTMA/I₂ the most powerful dissolving almost quantitatively and selective Co from 0.5g of WC-Co powders within 20’;

- 7) Lat⁻/I₂ mixture in EtOH seemed to couple eco-friendliness (bio-derived) and efficiency (45' leaching time) and benefits of the easy recyclability of reagents and solvent of solvometallurgy, key point for highly sustainable and profitable potentially wastewater-free processes.

On the bases of PART I results, in PART II

- 8) experimental set-up addressed to move towards industrial application was obtained for HLat and H₂Suc in water in the presence of O₂ and H₂Mal in ethanol, optimizing oxygenation conditions for the formers and reagent/solvent economy (optimal L/S ratio and Co:Acid molar ratio) for all the selected systems;
- 9) scale-up experiments for HLat/O₂ and H₂Suc/O₂ hydrometallurgy on 650g and 1500g of WC-Co powders, respectively, obtained WC-(5.7%)Co and WC-(3.1%)Co recovered powders within 24h at room conditions under forced aeration, which can be made suitable for use in HM manufacturing after undergoing a 2h thermal treatment at 1000°C for removing the excess of C and O;
- 10) scale-up experiment for H₂Mal (EtOH) solvometallurgy on 300g WC-Co powders demonstrated very high efficiency reaching WC-(6%)Co within 6h without addition of any external oxidizing specie and preventing oxidizing/hydrating phenomena on the material, very promising for industrial purposes;
- 11) Starbon® solid-phase extraction seemed promising for cobalt recovery from the HLat leachate, as well as the precipitation of Co-complexes from the solution by solvent evaporation and washing with acetone or Et₂O;
- 12) electrowinning demonstrated to be a suitable tool for depositing Co metal and restoring the leaching solution;
- 13) a TRL 5 - technology validation in relevant environment – seems to be reached at least for the leaching phase of the latter three processes;
- 14) dairy waste underwent dark fermentation in controlled conditions providing, on the one hand, a hydrometallurgical leaching solution based on high HLat and low carbohydrates contents and, on the other hand, a semi-finished dry product rich in lactate salts which

can be used as precursor of ethanolic lactate solutions for solvometallurgy in the presence of iodine;

15) On the bases of the satisfactory preliminary leaching results of these two fermented cheese whey solutions, two innovative CEMs for HM manufacturing were proposed and tentatively assessed for sustainability by green chemistry metrics on the leaching process. The valorization at one time of two relevant wastes, cheese whey and WC-Co recovery powders, which to date represent environmental concerns, is the key point that suggested us to select HLat-based methods as our case study for both hydro-acidic- and solvo-non-acid-metallurgy and inspired the two proposed CEMs.

7.2 Work in progress and perspectives

The satisfactory results obtained by this work and the commitment of the partners involved in the project, stimulate further studies.

Among all the experiments in progress, such as the isolation and characterization of the leaching products with S-donor ligands/I₂ mixtures, recovered Co by complexes by thermal degradation, etc.,

With the view of fully implement the proposed CEMs moving on a pilot-scale, experiments regarding:

- the effect of residual organic substances (proteins and fats) present in the fermented cheese whey solutions on the recovered WC powder;
- the systematic study on leaching conditions *vs* leaching results for performing a multivariate analysis addressed to predict the leaching times for achieving the desired final WC-Co composition given the characteristics of the input recovery powder and, specifically for the Lat⁻/I₂ (EtOH) system,
- the efficiency study on WC-Co powders;
- the metallurgical quality assessment of the recovery powders;
- the electrowinning recovery of Co metal from EtOH solutions by restoring the leaching solutions; are in progress and rise great interest.

Further challenges will be faced in the next future, primarily:

- the application of these findings to other kind of HM wastes, like scraps and regenerated powders, widening the industrial interest and the environmental impact of the proposed approach;
- the study of selective leaching systems, based on the knowledge of this work, for other Co-containing scraps such as Li-ion batteries, or more complex multimetallic systems like waste electric and electronic equipment.

APPENDICES

A1 Test specimen characterization and metallurgical quality control (MQC)

1. Test specimen characterization

1.1 Sample digestion and ICP-OES chemical analysis

0.5 g WC-based powder aliquots were reacted with 1L of H₂O₂ 30%_{v/v} in the presence of 10 mL of concentrated nitric acid and fluoric acid by heating at around 150°C for 15 min since the reaction became vigorous, then left to react at room temperature. 15 mL of tartaric acid solution was added to the mixture for preventing tungstic acid precipitation. [1] 10 mL of H₂O₂ were also added before making a proper dilution with deionized water. The freshly prepared solutions were analyzed for Co, Fe, Ni, Ta, Ti, Nb, Cr, Cu, Mo, V, via Inductively Coupled Plasma-Optical Emission Spectrometry (ICP-OES, Horiba Jobin Yvon JY 2000 series, Thermo Scientific) after appropriate dilutions.

Table 1: Metal composition (wt. %) of the recovery powders (RC-631L and RC-627C) used throughout the present study.

	Elements	W	Co	Fe	Ni	Ta	Ti	Nb
RC-631L	Wt. %	78.26	20.40	0.08	0.32	0.27	0.40	0.27
RC-67C	Wt. %	79.4	19.55	0.05	0.22	0.25	0.40	0.13

1.2 Powders oxygen and carbon analysis

The amount of oxygen present in the powder was determined using an LECO RO400 infrared spectrometry, with calibration standard (0.0366 ± 0.0006) %, Oxygen-Nitrogen analyser in a helium atmosphere. Firstly, a graphite crucible was placed in the instrument, and was out-gassed to ensure there was no oxygen present. About 0.05 mg of powder was weighed and placed in the loading head and once the instrument was closed, the powders were dropped into the crucible. The crucible was heated to 200°C at a pressure of 1.5 bar for 5 minutes. The contents were then analysed to determine the amount of oxygen present in the powder. Whereas, the carbon contain was determined by infrared spectrometry, using LECO WC 230, with calibration standard (6.26 ± 0.05) % carbon analyzer.

Table 1: C and O content (wt. %) of RC-631L and RC-627C.

Sample	Elemental analysis (wt. %)	
	C	O
RC-631L	4.94	0.58
RC-627C	4.93	0.59

2. Mechanical properties of sintered cemented carbides

The metallurgical quality control was investigated on the sintered materials. Hence, the recovery powders before/after treatment, were homogenized by lab-scale ball milling for 72h in ethanol and with a 3:1 HM balls to powder ratio in a stainless-steel jar. Samples in forms of bars (according to ISO 3327) were sintered at 1500 °C under Ar (35 bar) in a standard sinterHIP (Hot Isostatic Pressing) process. The sintered test specimens underwent density, hardness (HV10 and HRA), coercitive force (H_c) and magnetic moment saturation (σ) measurements, under conventional protocols and operative conditions.[2]

2.1 Transverse rupture strength (TRS)

Transverse rupture strength is a standard measurement in cemented carbides. It is a combination of shear strength, compressive strength, and tensile strength, and hence is used as a general measure of the strength of WC-cemented carbide.[3] The principle is breaking a test piece lying freely on two supports by application of a force at the midpoint of the span, under conditions of short-term dynamic application of the force.[4] The fixture for testing shall have two freely lying support cylinders (rollers) with a fixed distance between them and a freely lying force cylinder (roller). The three cylinders shall be of equal diameter between 3, 2 and 6 mm. alternatively, the force may be applied by a ball having a diameter of 10 mm. The support cylinders and the force cylinder or ball shall be made of tungsten carbide hard metal which will not be visibly deformed by the applied force.

The procedure involves placing a test piece flat and centrally on the support cylinders so that its length is perpendicular to the lengths of the support cylinders. Then, bring the force cylinder or ball gradually into contact within the test piece. A typical TRS test set up and measurement results for cemented carbides are illustrated in **Fig 1.11**. According to Norm ISO 3327 – 1982, the TRS value (R_{bm}) of the samples is calculated using the equation:

$$R_{bm} = \frac{3 \times F \times L}{2 \times b \times h^2}$$

Where: F = force required to fracture the test piece (N)

L = distance between supports (mm)

b = width of test piece perpendicular to its height (mm)

h = height of test piece parallel to the direction of application of the test force (mm)

R_{bm} = transverse rupture strength value in N/mm^2

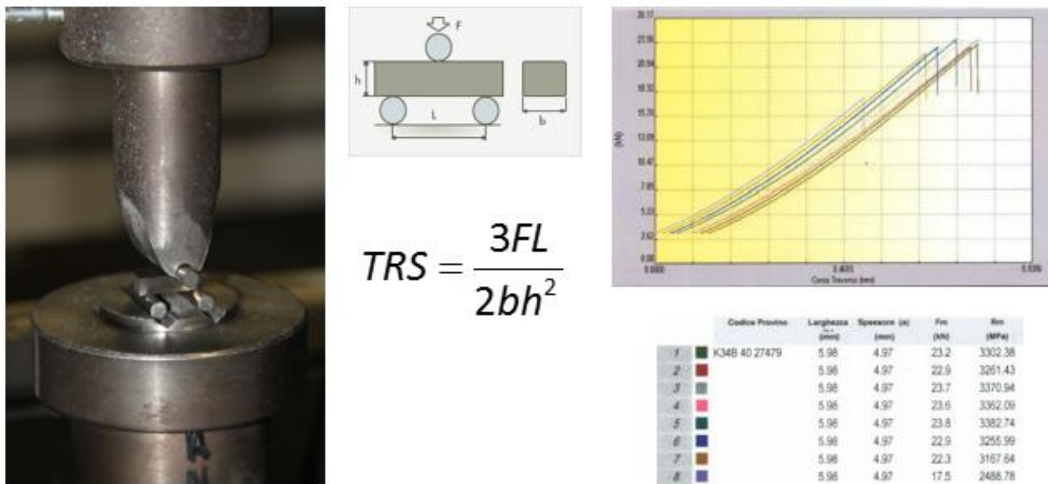


Figure 1. Schematic illustration of the TRS process according to Norm ISO 3327 – 1982.

2.2 Hardness

Hardness is the resistance to plastic deformation. It is one of the most important requirements for cemented carbide applications. As reported above, hardness is related to the nature of the composition and microstructure of the WC-cemented carbide since it varies with the amount and distribution of the binder, WC grain size and degree of porosity.[5][4] Factors with the most profound influence on apparent hardness are the volume fraction and particle size of the carbide phase: the hardness is higher and higher with increasing carbide volume fraction and decreasing carbide grain size.[4] All the WC-Co composite grades are characterized by extremely high hardness values, generally expressed in terms of Vickers (HV) hardness or Rockwell (HRA) hardness, although the widely accepted model is the Vickers (HV). [6][7] According to norm ISO 3878 (Hardmetal – Vickers hardness test), the Vickers hardness was designed in the 1920s by engineers from the Vickers Company in England. It is characterized by the imprint made by an indenter under a given load for 15 seconds. The indenter is formed of

a square-based diamond pyramid whose opposite faces make an angle of 136°. The applied load is between 9.807 N (HV 1) and 490.3 N (HV 50), with preferred force 294.2 N (HV 30). The diagonal of the impression is of the order of 0.5 mm, the measurement is carried out using a microscope. The Rockwell hardness standard dates from 1932 and the test consists to apply a charge of 60 N and measuring the penetrating depth of the indentation. According to Lee and Gurland, [6] the hardness of cemented carbide can be related to microstructural properties according to the following equation:

$$H_{cc} = H_{wc} V_{wc} C + H_{Co} (1 - V_{wc} C)$$

Where H_{cc} is the hardness of cemented carbide, H_{wc} is the in situ hardness of WC, H_c is the in situ hardness of the binder phase, V_{wc} is the volume fraction of the WC phase, C is the WC contiguity and H_{wc} & H_{Co} are expressed respectively by:

$$H_{wc} = 13.5 + 7.2 / d^{1/2} \quad \text{and} \quad H_{Co} = 2.98 + 3.9 / \lambda^{1/2}$$

Where d is the carbide grain size and λ is binder mean free path. Both grain size and binder mean free path are expressed in μm , while the obtained hardness value is expressed in GPa.

2.3 Fracture Toughness K_{IC}

Fracture toughness is the resistance of the material to crack propagation and is independent of specimen size, geometry and finish. Fracture toughness is a measure of the energy required for mechanical failure. Since the binder phase is ductile, it can absorb energy and go under plastic deformation. Low carbide volume fraction and large grain size of WC enhance toughness, which means it shows the inverse relationship concerning hardness. As fracture toughness is not an intrinsic material property, it depends not only on the material itself but also on the size of the defects in the material being fractured. Fracture toughness is usually reported in terms of K_{IC} , which is known as critical stress intensity factor. [8][9]

The fracture toughness can be estimated through the formula:

$$K_{IC} = \sigma_F (\alpha \pi c)^{1/2}$$

Where K_{IC} is in (MPa), σ_F is the stress required to propagate an interior crack of length $2c$, α is a constant dependent on the precise crack shape (close to unity) i.e. 1.[8][9] In the hardmetal field, the stress intensity factor is often evaluated according to the Palmqvist toughness methodology (ISO 28079).

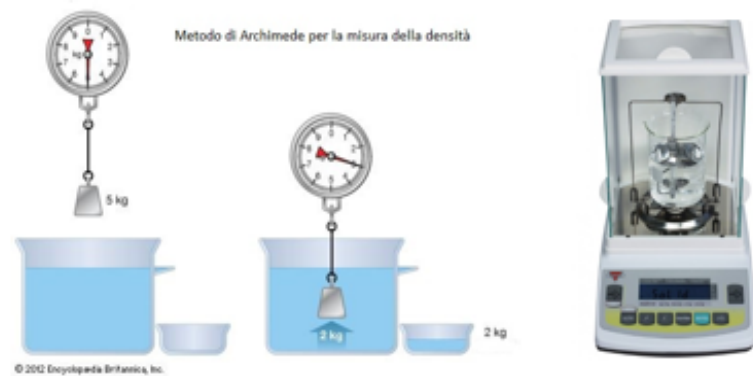
2.4 Density measurements

The density of the samples is usually determined by Archimedes' principle. After sintering, the samples are grounded to remove the Co-rich surface layer and to clean from the graphite residual from the sintering process. However, the density of a correctly sintered sample will be close to the theoretical density (the density that the sample would have if no voids were present). [10] **Fig 1.12** describes the Archimedes' principle according to Norm ISO 3369 – 1975.

Componente	D (g/cm ³)
Co	8.9
Ni	8.9
Fe	7.8
WC	15.56
TiC	4.92
TaC	14.40
TiN	5.44
Mo2C	9.04
Cr3C2	6.74
VC	5.48

$$d_{MD} \geq 99.7\%d_{th}$$

Metodo di Archimede



$$d = \frac{P_{aria}}{P_{aria} - P_{liq}} \cdot d_{liq}$$

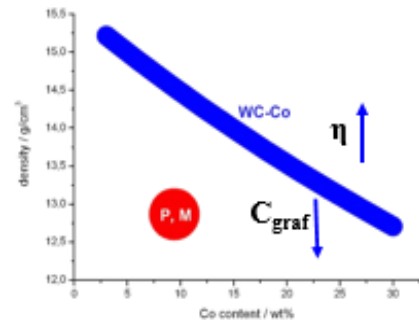


Figure 2: Density measurement according to ISO 3369 – 1975

2.5 Magnetic properties

The measurement of the binder phase's ferromagnetic properties, such as coercivity and magnetic saturation, in cemented carbides make it possible to perform quick non-destructive quality control tests. The coercivity and magnetic saturation tests give information about the effectiveness of the sintering process and some information about the microstructure.[5][11]

2.6 The Coercivity (Hc)

Coercivity is the value of the magnetic field required to demagnetize the samples after it has been magnetized up to saturation. It has rather a complex meaning, as it is related at the same time to (a) the WC grain size, (b) the amount of W solved in the metallic binder and (c) the

homogeneity character of distribution of the metallic binder, i.e. the status reached by sintering. In spite of such complexity, the coercivity value is very useful to MQC when an acceptable range is defined for each grade, on an experimental basis. As an example, it is used to compare the size of WC grains of different materials after sintering to detect whether there has been an unexpected grain growth or not.[5] According to ISO Norm 3326 – 1975, the coercivity is high when the Co content is low and/or WC grain size is fine, and low when the Co content is high and/or the WC grain size is coarse. Free carbon, which also leads to increased WC grain growth also reduces the value of coercivity. The measurement instrument consists of two sections: a magnetic field generator and a magnetic field measuring unit. For performing the measures, the sample is attached to a wooden sample holder and placed in the magnetic field generated by the magnetic coil.[12]

2.7 Magnetic saturation (Ms)

Magnetic saturation is used as an indirect, quick and reliable method of measuring the carbon content of sintered cemented carbide. The advantage of this method is the linear relationship between the tungsten content in the metallic binder and the values of the magnetic saturation in the region of interest. In particular, the magnetic moment at saturation of the Co-base metallic binder reduces with an increasing amount of tungsten solved in alloy. As at equilibrium that value is a function of the material total carbon content, this parameter can be accurately estimated by magnetic saturation measurements. There are exceptions for this rule, i.e. when high carbon alloys are quickly cooled from the sintering temperature.[13]

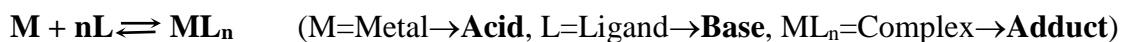
References

- [1] D. hyo Yang, R. R. Srivastava, M. seuk Kim, D. D. Nam, J. chun Lee, and H. T. Huynh, “Efficient recycling of WC-Co hardmetal sludge by oxidation followed by alkali and sulfuric acid treatments,” *Met. Mater. Int.*, vol. 22, no. 5, pp. 897–906, 2016.
- [2] B. Roebuck, “Magnetic moment (saturation) measurements on hardmetals,” *Int. J. Refract. Met. Hard Mater.*, vol. 14, no. 5–6, pp. 419–424, 1996.
- [3] J. Gurland and P. Bardzil, “Relation of Strength, Composition, and Grain Size of Sintered WC-Co Alloys,” *Jom*, vol. 7, no. 2, pp. 311–315, 1955.
- [4] Z. Z. Fang, X. Wang, T. Ryu, K. S. Hwang, and H. Y. Sohn, “Synthesis, sintering, and mechanical properties of nanocrystalline cemented tungsten carbide - A review,” *Int. J. Refract. Met. Hard Mater.*, vol. 27, no. 2, pp. 288–299, 2009.
- [5] R. M. Genga, “Microstructure and Properties of Selected Wc-Cemented Carbides

- Manufactured By Sps Method,” no. September, 2014.
- [6] H. C. Lee and J. Gurland, “Hardness and deformation of cemented tungsten carbide,” *Mater. Sci. Eng.*, vol. 33, no. 1, pp. 125–133, 1978.
- [7] L. J. Prakash, “Application of fine grained tungsten carbide based cemented carbides,” *Int. J. Refract. Met. Hard Mater.*, vol. 13, no. 5, pp. 257–264, 1995.
- [8] S. Nahak, S. Dewangan, and S. Chattopadhyaya, “Discussion on Wear Phenomenain Cemented Carbide,” *Procedia Earth Planet. Sci.*, vol. 11, pp. 284–293, 2015.
- [9] H. C. Kim, D. Y. Oh, and I. J. Shon, “Sintering of nanophase WC-15vol.%Co hard metals by rapid sintering process,” *Int. J. Refract. Met. Hard Mater.*, vol. 22, no. 4–5, pp. 197–203, 2004.
- [10] F. J. J. Kellner, H. Hildebrand, and S. Virtanen, “Effect of WC grain size on the corrosion behavior of WC-Co based hardmetals in alkaline solutions,” *Int. J. Refract. Met. Hard Mater.*, vol. 27, no. 4, pp. 806–812, 2009.
- [11] S. Sundin and S. Haglund, “Comparison between magnetic properties and grain size for WC/Co hard materials containing additives of Cr and V,” *Int. J. Refract. Met. Hard Mater.*, vol. 18, no. 6, pp. 297–300, 2000.
- [12] J. García, V. Collado Ciprés, A. Blomqvist, and B. Kaplan, “Cemented carbide microstructures: a review,” *Int. J. Refract. Met. Hard Mater.*, vol. 80, no. August 2018, pp. 40–68, 2019.
- [13] J. Garcia and W. Strelsky, “Process development and scale up of cemented carbide production,” no. May, pp. 1–31, 2017.

A2 Hard-Soft acid-base theory

Complex formation can be described as a Lewis acid-base reaction:



HSAB Theory is a qualitative concept introduced by Ralph Pearson to explain the stability of metal complexes.

Hard acids and bases are typically small and relatively non-polarisable, whereas *Soft* acids and bases are larger and more polarisable, as described in the table:

	Hard species	Soft species
Acids	Small ionic radii, high positive charge, strongly solvated, empty orbitals in the valence shell, high energy LUMOs ^a (e.g. alkaline and alkaline earth metal cations, light transition metals in high oxidation state)	Large ionic radii, low positive charge, completely filled atomic orbitals and with low energy LUMOs ^a (e.g. zero oxidation state metals, heavy transition metals in low oxidation state)
Basis*	Small ionic radii, strongly solvated, highly electronegative, weakly polarisable and with high energy HOMOs ^b (e.g. F ⁻ , Cl ⁻ , H ₂ O, OH ⁻ , RO ⁻ , NO ₃ ⁻ , SO ₄ ²⁻ , ClO ₄ ⁻ , ox ²⁻ , NH ₃)	Large ionic radii, intermediate electronegativity, highly polarisable and with low energy HOMOs ^b (e.g. I ⁻ , H ⁻ , R ⁻ , <u>CN</u> ⁻ , <u>CO</u> , RSH, SR ⁻ , <u>SCN</u> ⁻ , PR ₃ , alkenes)

^aLowest Unoccupied Molecular Orbital (LUMO); ^bHighest Occupied Molecular Orbital (HOMO). *Bolded and underlined species behave as donor atoms towards the metal cation.

Borderline species with intermediate properties are identified as well: Acids → e.g. Sn²⁺, Fe²⁺, Co²⁺, Ni²⁺, Cu²⁺, Zn²⁺, Ru³⁺, Rh³⁺, Ir³⁺; Basis → e.g. Br⁻, py, SCN⁻, NO₂⁻, SO₃²⁻.

HSAB Principle: According to the HSAB concept, *hard* acids prefer binding to *hard* bases to give complexes with main ionic character, whereas *soft* acids prefer binding to *soft* bases to give complexes with main covalent character.

NB: The driving force related to the matching of species with similar H-S nature is additional to other factors that contribute to bond strength between atoms (relative sizes/charges/electronegativity/orbital overlap/acid-base strength).

A3 Materials and methods

1. Materials and chemicals

All chemicals were of reagent grade and used as purchased by Sigma Aldrich (EtOH, 96%; Acetone, technical grade; Et₂O 99%; MeOH 99.8%; maleic acid, 99%; Lactic acid, 99%; Succinic acid, 99.5%; Citric acid, 99.5%; Itaconic acid, 99%; Lactobionic acid, 97%; Maltobionic acid, 97%; L-Arginine acid, 98%; Rubeanic acid 97%; Thiourea 99%; Urea 99%; N,N'-dimethyl-piperazine-2,3-dione 99%) without any purification. Cobalt powder was used as purchased by Umicore (Extrafine, > 99.5 wt%, 1.3 μm). WC-Co recovery powders (RC-627C and RC-631L), were provided by F.I.L.M.S. Corp. (OMCD Group, Anzola d'Ossola (VB), Italy).

2. Solid-state characterization and treatment methods

Wherever not indicated differently, characterization and treatments have been performed at DICAAR.

2.1 CHN-elemental analysis

Elemental analysis was carried out in double for C and H on a dried solid sample of cobalt complex using a LECO CHN628 equipment.

2.2 Thermogravimetric analysis (TGA)

Thermogravimetric analysis was performed at GCCE-University of York, on a Netzsch STA 409 equipment. A pre-weighted amount of material (ca. 50 mg) underwent a heating ramp up to 1300°C, with a heating rate of 5°C min⁻¹ under a mixed atmosphere of air (100 mLmin⁻¹) and pure nitrogen (20 mLmin⁻¹).

2.3 Fourier Transform Infrared Spectroscopy (FT-IR)

Fourier transform-infrared spectroscopy was conducted at GCCE-University of York on a Bruker Vertex 70 FT-IR spectrometer in attenuated total reflectance (ATR) mode. All the spectra were recorded using a resolution of 2 cm⁻¹ and 32 scans each for background and samples.

FT-IR spectra of [Co(HMal)₂(H₂O)₄] and CoDTO-complex (still under characterization), were

recorded by a Jasco FT-IR6300A spectrometer equipped with a ATR PRO ONE (diamond crystal) in the 4000-400 cm^{-1} spectral range, ris. 4.0 cm^{-1} , 50 scans.

2.4 Single-crystal X-Ray diffraction

Well-shaped single-crystals were analyzed by Prof. L. Marchiò, University of Parma, on a Bruker D8 Venture PhotonII diffractometer. The crystal was kept at 160 K during data collection. Using Olex2,⁴ the structure was solved with the ShelXT⁵ structure solution program using Intrinsic Phasing and refined with the ShelXL⁶ refinement package using Least Squares minimization.

2.5 Powder X-Ray diffraction

Powder X-Ray diffraction patterns were recorded by Dr. Stefano Cara, IGAG_CNR Cagliari, by a Rigaku Geigerflex D-Max diffractometer operating with Cu tube at 30 kV and 30 mA (mineral identification was carried out by comparison with the JCPDS File 1985).[23]

2.6 SEM/EDS

Scanning Electron Microscopy and Energy Dispersive Spectroscopy were performed at GCCE-University of York, by means of a SEM/EDS JEOL JSM-7800F equipment.

SEM/EDS characterization of WC-Co materials described in Chapter 5 was performed at FILMS, by a JEOL JSM 5500LV equipment.

2.7 Thermal treatment of cobalt complexes

Cobalt recovery from cobalt complexes was investigated at FILMS by thermal treatment in oxidizing, reducing and neutral environment on a Lenton's oven. A pre-weighted amount of material (ca. 2-5g) underwent a heating ramp up to 500 or to 1000°C with a heating rate of 3°C/min, 0.5 atm, and left at the reached temperature for 2h before cooling down to room temperature.

A4 Thermogravimetric Analysis of Co-complexes

1. General discussion

The thermal analysis profiles recorded for cobalt complexes ($[\text{Co}(\text{Lat})_2(\text{H}_2\text{O})_2]$; $[\text{Co}(\text{HMal})_2(\text{H}_2\text{O})_4]$; $[\text{Co}_3(\text{Cit})_2(\text{H}_2\text{O})_2]$; $[\text{Co}(\text{LB})_2(\text{H}_2\text{O})_2]$; $[\text{Co}(\text{MB})_2(\text{H}_2\text{O})_2]$; $[\text{Co}(\text{Suc})(\text{H}_2\text{O})_4]$; $[\text{Co}(\text{It})(\text{H}_2\text{O})_2]_3$), under mixed atmosphere of air (100 mLmin^{-1}) and pure nitrogen (20 mLmin^{-1}) (heating ramp up to 1300°C , rates of 5°C min^{-1}), are reported below. The behavior shown by the different compounds is very similar, showing a first decomposition stage, occurring approximately at 200°C , reasonably associated with the loss of the coordinated water molecules. The second decomposition observed in the range ($230\text{-}300^\circ\text{C}$) is related to the organic ligand decomposition and suggests the formation of an intermediate product, reasonably a non-stoichiometric metal oxide like Co_3O_4 , as observed previously for similar compounds. [1] Such an assumption is proved by the existence of the third decomposition step, where a continuous mass loss attributed to oxygen evolving is registered with the expected formation of CoO . [1]

References

- [1] M. Bîrzescu, M. Niculescu, Raluca Dumitru, Oana Carp, E. Segal, *J Therm Anal Calorim* (2009) 96:979–986, DOI 10.1007/s10973-009-0054-z.

2. Thermal degradation profiles

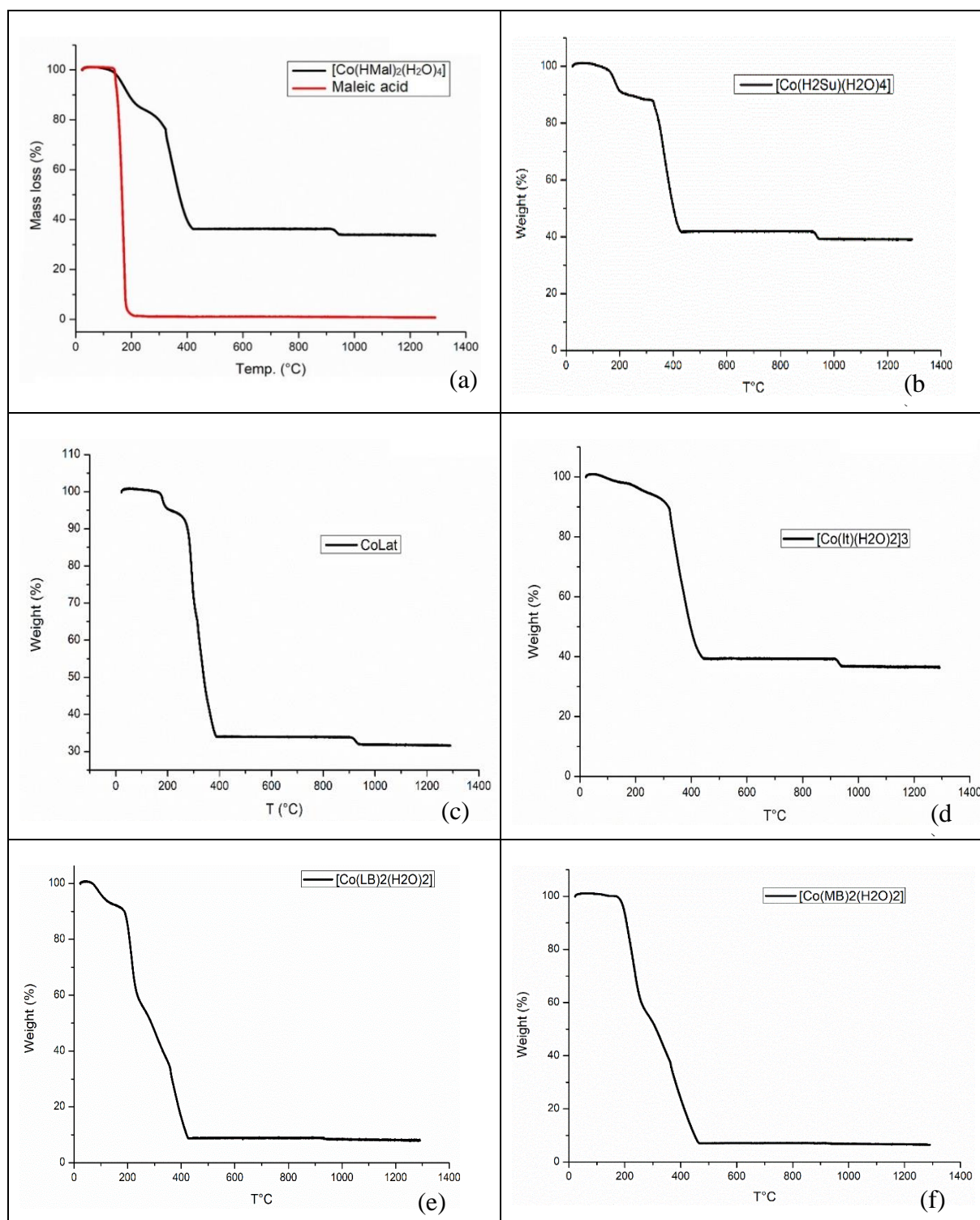


Figure 1: Thermal decomposition curve (TG) for (a) $[\text{Co}(\text{HMal})_2(\text{H}_2\text{O})_4]$, (b) $[\text{Co}(\text{H}_2\text{Su})(\text{H}_2\text{O})_4]$, (c) $[\text{CoLat}_2(\text{H}_2\text{O})_2]$, (d) $[\text{Co}(\text{It})(\text{H}_2\text{O})_2]_3$, (e) $[\text{Co}(\text{LB})_2(\text{H}_2\text{O})_2]$ and (f) $[\text{Co}(\text{MB})_2(\text{H}_2\text{O})_2]$.

A5 Single-crystal X-Ray diffraction characterization of [Co(It)(H₂O)₂]₃

X-Ray diffraction measurements performed by Prof. L. Marchiò, University of Parma (IT).

1. Molecular structure of [Co(It)(H₂O)₂]₃

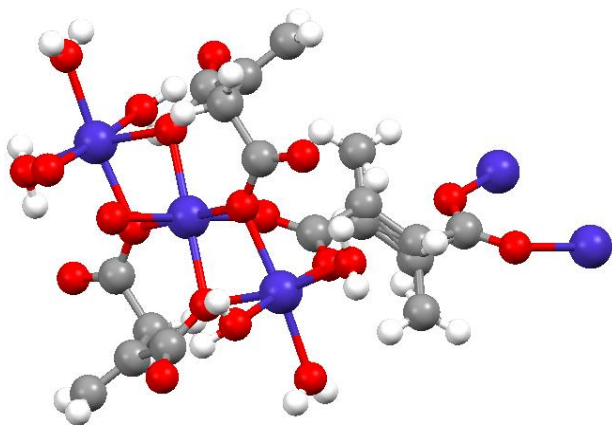


Figure 1. Molecular structure [Co(It)(H₂O)₂]₃ complex.¹² Color legend: blue, Co; red, O; grey, C; white, H.

2. Tables

Table 1 Crystal data and structure refinement for CoIt2_0m_a.	
Identification code	CoIt2_0m_a
Empirical formula	C ₁₅ H ₂₄ Co ₃ O ₁₈
Formula weight	668.12
Temperature/K	200.0
Crystal system	orthorhombic
Space group	Pbca
a/Å	9.9809(13)
b/Å	14.5548(14)
c/Å	15.3513(19)
α/°	90
β/°	90
γ/°	90
Volume/Å ³	2230.1(5)
Z	4
ρ _{calc} /cm ³	1.990
μ/mm ⁻¹	2.296

¹² Single crystal X-ray diffractometric studies were performed by Prof. Luciano Marchiò, Dipartimento di Scienze Chimiche, della Vita e della Sostenibilità Ambientale, University of Parma (IT).

F(000)	1352.0
Crystal size/mm ³	0.05 × 0.04 × 0.03
Radiation	MoK α ($\lambda = 0.71073$)
2 Θ range for data collection/ $^\circ$	5.598 to 51.694
Index ranges	-12 \leq h \leq 12, -17 \leq k \leq 17, -18 \leq l \leq 18
Reflections collected	73713
Independent reflections	2145 [R _{int} = 0.1107, R _{sigma} = 0.0274]
Data/restraints/parameters	2145/18/192
Goodness-of-fit on F ²	1.051
Final R indexes [I > 2 σ (I)]	R ₁ = 0.0274, wR ₂ = 0.0776
Final R indexes [all data]	R ₁ = 0.0363, wR ₂ = 0.0800
Largest diff. peak/hole / e \AA^{-3}	0.70/-0.57

Table 2 Fractional Atomic Coordinates ($\times 10^4$) and Equivalent Isotropic Displacement Parameters ($\text{\AA}^2 \times 10^3$) for Colt2_0m_a. U_{eq} is defined as 1/3 of of the trace of the orthogonalised U_{ij} tensor.				
Atom	x	y	z	U(eq)
Co2	5000	5000	5000	13.48(14)
Co1	6438.0(3)	6858.3(2)	5603.5(2)	16.09(13)
O1A	5496.0(18)	6300.1(12)	4472.8(12)	19.2(4)
O1A1	7044.7(18)	4677.7(12)	4977.4(14)	22.1(4)
O4A	4680.8(18)	4236.9(12)	3868.4(12)	19.5(4)
O3W	7432.8(19)	7822.8(13)	4861.0(14)	25.0(4)
O2A1	8025.2(18)	6008.4(12)	5329.1(14)	23.4(4)
O1W	4886(2)	7777.1(14)	5928.7(16)	26.9(5)
O2W	7272(3)	7253.7(16)	6789.1(16)	27.6(5)
O3A	5909(2)	3504.4(14)	2891.8(15)	35.9(5)
O2A	6211(3)	7233.1(15)	3429.8(15)	41.5(6)
C1A	5580(3)	6545.5(18)	3674(2)	23.9(6)
C4A	5452(3)	4223.6(18)	3195.6(19)	25.1(6)
C2A	4865(4)	5954(2)	3013(2)	37.5(8)
C3A	5720(4)	5137(2)	2769(2)	42.1(9)
C5A	6610(5)	5217(3)	2168(3)	71.7(15)
C1A1	8052(3)	5197.6(17)	5057.3(19)	20.4(6)
C2A1	9370(20)	4813(15)	4660(8)	21(2)
C4A1	9310(6)	4306(5)	3978(5)	38.5(16)
C3A1	9410(20)	4793(15)	4914(9)	23(2)

Table 3 Anisotropic Displacement Parameters ($\text{\AA}^2 \times 10^3$) for CoIt2_0m_a. The Anisotropic displacement factor exponent takes the form: $-2\pi^2[h^2a^{*2}U_{11}+2hka^*b^*U_{12}+\dots]$.

Atom	U ₁₁	U ₂₂	U ₃₃	U ₂₃	U ₁₃	U ₁₂
Co2	10.5(3)	12.9(2)	17.0(3)	-0.71(18)	0.83(19)	-0.58(16)
Co1	13.3(2)	14.17(19)	20.8(2)	-2.08(13)	0.58(14)	-0.18(12)
O1A	20.1(10)	17.9(8)	19.6(11)	1.7(7)	-1.1(8)	-2.1(7)
O1A1	14.5(10)	15.7(9)	36.2(12)	-3.1(8)	3.7(8)	0.5(7)
O4A	21.6(9)	19.3(9)	17.6(10)	-3.0(7)	3.6(8)	-4.1(7)
O3W	25.3(10)	17.6(9)	32.2(12)	-1.8(8)	4.9(9)	-5.6(7)
O2A1	13.5(9)	19.2(9)	37.4(12)	-7.2(8)	0.7(8)	1.6(7)
O1W	19.3(11)	28.3(11)	33.2(13)	-1.6(9)	-0.9(10)	4.8(8)
O2W	28.3(12)	31.5(11)	23.1(12)	-8.7(10)	-8.4(11)	10.9(9)
O3A	42.3(13)	30.5(11)	34.9(13)	-1.9(10)	19.2(11)	4.4(9)
O2A	67.8(16)	31.5(11)	25.2(13)	4.9(10)	0.2(11)	-23.7(11)
C1A	29.3(15)	18.5(12)	23.9(16)	3.5(11)	-2.6(12)	-2.3(10)
C4A	25.2(14)	27.9(14)	22.2(15)	-6.4(12)	3.3(12)	-5.7(11)
C2A	61(2)	26.5(14)	25.4(17)	6.2(13)	-8.8(15)	-10.7(14)
C3A	65(2)	32.9(16)	28.6(19)	-6.6(14)	16.6(18)	-16.5(16)
C5A	100(4)	45(2)	70(3)	-3(2)	43(3)	-10(2)
C1A1	14.8(13)	16.6(12)	29.8(16)	0.1(11)	0.0(12)	1.7(10)
C2A1	12(3)	27(2)	24(6)	-8(5)	5(5)	1(2)
C4A1	16(3)	54(4)	46(4)	-14(3)	6(3)	-1(3)
C3A1	16(3)	25(2)	28(7)	-12(5)	4(5)	0(2)

Table 4 Bond Lengths for CoIt2_0m_a.

Atom	Atom	Length/ \AA	Atom	Atom	Length/ \AA
Co2	O1A ¹	2.1168(17)	O4A	Co1 ¹	2.1083(17)
Co2	O1A	2.1168(17)	O4A	C4A	1.288(3)
Co2	O1A1	2.0943(18)	O2A1	C1A1	1.252(3)
Co2	O1A1 ¹	2.0943(18)	O3A	C4A	1.234(3)
Co2	O4A	2.0863(18)	O2A	C1A	1.241(3)
Co2	O4A ¹	2.0863(18)	C1A	C2A	1.510(4)
Co1	O1A	2.1348(19)	C4A	C3A	1.506(4)
Co1	O4A ¹	2.1084(18)	C2A	C3A	1.511(5)
Co1	O3W	2.0630(19)	C3A	C5A	1.286(6)
Co1	O2A1	2.0536(18)	C1A1	C2A1	1.55(2)
Co1	O1W	2.106(2)	C1A1	C3A1	1.50(2)
Co1	O2W	2.083(2)	C2A1	C4A1	1.282(19)

O1A	C1A	1.279(4)	C2A1	C3A1 ²	1.495(8)
O1A1	C1A1	1.264(3)	C3A1	C2A1 ²	1.495(8)

¹1-X,1-Y,1-Z; ²2-X,1-Y,1-Z

Table 5 Bond Angles for CoIt2_0m_a.							
Atom	Atom	Atom	Angle/°	Atom	Atom	Atom	Angle/°
O1A	Co2	O1A ¹	180.0	O2W	Co1	O1W	84.93(10)
O1A1 ¹	Co2	O1A	91.95(7)	Co2	O1A	Co1	97.61(8)
O1A1	Co2	O1A	88.05(7)	C1A	O1A	Co2	129.13(17)
O1A1	Co2	O1A ¹	91.95(7)	C1A	O1A	Co1	130.09(17)
O1A1 ¹	Co2	O1A ¹	88.05(7)	C1A1	O1A1	Co2	129.74(16)
O1A1 ¹	Co2	O1A1	180.0	Co2	O4A	Co1 ¹	99.40(8)
O4A ¹	Co2	O1A	78.86(7)	C4A	O4A	Co2	125.76(16)
O4A ¹	Co2	O1A ¹	101.14(7)	C4A	O4A	Co1 ¹	127.83(16)
O4A	Co2	O1A ¹	78.86(7)	C1A1	O2A1	Co1	130.75(18)
O4A	Co2	O1A	101.14(7)	O1A	C1A	C2A	117.0(2)
O4A	Co2	O1A1	90.90(7)	O2A	C1A	O1A	123.3(3)
O4A ¹	Co2	O1A1 ¹	90.90(7)	O2A	C1A	C2A	119.7(3)
O4A	Co2	O1A1 ¹	89.10(7)	O4A	C4A	C3A	116.2(2)
O4A ¹	Co2	O1A1	89.10(7)	O3A	C4A	O4A	122.5(3)
O4A ¹	Co2	O4A	180.0	O3A	C4A	C3A	121.2(3)
O4A ¹	Co1	O1A	77.97(7)	C1A	C2A	C3A	110.4(3)
O3W	Co1	O1A	91.24(8)	C4A	C3A	C2A	119.1(3)
O3W	Co1	O4A ¹	169.07(8)	C5A	C3A	C4A	121.0(4)
O3W	Co1	O1W	93.03(8)	C5A	C3A	C2A	119.8(3)
O3W	Co1	O2W	95.87(9)	O1A1	C1A1	C2A1	114.8(8)
O2A1	Co1	O1A	86.77(7)	O1A1	C1A1	C3A1	118.2(8)
O2A1	Co1	O4A ¹	91.84(7)	O2A1	C1A1	O1A1	125.4(2)
O2A1	Co1	O3W	85.71(8)	O2A1	C1A1	C2A1	119.2(8)
O2A1	Co1	O1W	176.68(9)	O2A1	C1A1	C3A1	116.1(8)
O2A1	Co1	O2W	92.13(9)	C3A1	C1A1	C2A1	14.7(9)
O1W	Co1	O1A	96.34(9)	C4A1	C2A1	C1A1	119.3(15)
O1W	Co1	O4A ¹	89.96(8)	C4A1	C2A1	C3A1 ²	128.0(10)
O2W	Co1	O1A	172.70(8)	C3A1 ²	C2A1	C1A1	112.2(8)
O2W	Co1	O4A ¹	94.86(9)	C2A1 ²	C3A1	C1A1	121.5(8)

¹1-X,1-Y,1-Z; ²2-X,1-Y,1-Z

Table 6 Hydrogen Atom Coordinates ($\text{\AA} \times 10^4$) and Isotropic Displacement Parameters ($\text{\AA}^2 \times 10^3$) for CoIt2_0m_a.				
Atom	x	y	z	U(eq)
H3WA	7343	8380	5090	38
H3WB	7048	7875	4342	38
H1WA	4310	7544	6339	40
H2AA	4667	6322	2486	45
H2AB	4004	5738	3259	45
H5AA	7109	4696	1986	86
H5AB	6767	5798	1905	86
H4AA	10109	4138	3682	46
H4AB	8467	4098	3769	46
H3AA	9362	4140	5088	28
H3AB	9578	4802	4278	28
H2WA	7850(40)	6980(20)	7020(30)	33(10)
H2WB	6890(40)	7440(20)	7130(30)	25(10)
H1WB	4340(40)	7810(30)	5600(30)	35(11)

Table 7 Atomic Occupancy for CoIt2_0m_a.					
Atom	Occupancy	Atom	Occupancy	Atom	Occupancy
C2A1	0.5	C4A1	0.5	H4AA	0.5
H4AB	0.5	C3A1	0.5	H3AA	0.5
H3AB	0.5				

Experimental

Single crystals of $\text{C}_{15}\text{H}_{24}\text{Co}_3\text{O}_{18}$ [CoIt2_0m_a] were []. A suitable crystal was selected and [] on a Bruker D8 PhotonII diffractometer. The crystal was kept at 200.0 K during data collection. Using Olex2 [1], the structure was solved with the ShelXT [2] structure solution program using Intrinsic Phasing and refined with the ShelXL [3] refinement package using Least Squares minimisation.

1. Dolomanov, O.V., Bourhis, L.J., Gildea, R.J, Howard, J.A.K. & Puschmann, H. (2009), *J. Appl. Cryst.* 42, 339-341.
2. Sheldrick, G.M. (2015). *Acta Cryst.* A71, 3-8.
3. Sheldrick, G.M. (2015). *Acta Cryst.* C71, 3-8.

Crystal structure determination of [CoIt2_0m_a]

Crystal Data for $C_{15}H_{24}Co_3O_{18}$ ($M = 668.12$ g/mol): orthorhombic, space group *Pbca* (no. 61), $a = 9.9809(13)$ Å, $b = 14.5548(14)$ Å, $c = 15.3513(19)$ Å, $V = 2230.1(5)$ Å³, $Z = 4$, $T = 200.0$ K, $\mu(\text{MoK}\alpha) = 2.296$ mm⁻¹, $D_{\text{calc}} = 1.990$ g/cm³, 73713 reflections measured ($5.598^\circ \leq 2\theta \leq 51.694^\circ$), 2145 unique ($R_{\text{int}} = 0.1107$, $R_{\text{sigma}} = 0.0274$) which were used in all calculations. The final R_1 was 0.0274 ($I > 2\sigma(I)$) and wR_2 was 0.0800 (all data).

Refinement model description

Number of restraints - 18, number of constraints - unknown.

Details:

1. Fixed Uiso

At 1.2 times of:

All C(H,H) groups

At 1.5 times of:

All O(H) groups, All O(H,H) groups

2. Uiso/Uanis restraints and constraints

C2A1 \approx C2A1 \approx C3A1 \approx C3A1: within 1.7Å with sigma of 0.004 and sigma for terminal atoms of 0.008

Uanis(C3A1) \approx Ueq, Uanis(C2A1) \approx Ueq, Uanis(C3A1) \approx Ueq,

Uanis(C2A1) \approx Ueq: with sigma of 0.01 and sigma for terminal atoms of 0.02

3. Others

Fixed Sof: C2A1(0.5) C4A1(0.5) H4AA(0.5) H4AB(0.5) C3A1(0.5) H3AA(0.5) H3AB(0.5)

4.a Rotating group:

O3W(H3WA, H3WB), O1W(H1WA)

4.b Secondary CH2 refined with riding coordinates:

C2A(H2AA, H2AB), C3A1(H3AA, H3AB)

4.c X=CH2 refined with riding coordinates:

C5A(H5AA, H5AB), C4A1(H4AA, H4AB)

This report has been created with Olex2, compiled on 2018.05.29 svn.r3508 for OlexSys. Please [let us know](#) if there are any errors or if you would like to have additional features.

3. CIF file (available in electronic format).

A6 ICP-OES characterization of leachates

1. Sample digestion

From 100 to 5000 μ L of leachate aliquots underwent microwave digestion by a Milestone ETHOS1 apparatus equipped with an HPR1000/10S high-pressure segmented rotor, an ATC-400CE automatic temperature control and a Terminal 640 with easyCONTROL software.

Samples underwent a microwave program consisting of two steps lasting 10 minutes each, at the temperature of 200°C and microwave power up to 1000W. The samples were introduced in TFM vessels and dried. Mixtures of HNO₃ (65%, 4 mL), H₂SO₄ (96%, 4 mL) and H₂O (deionized, 2 mL).

2. ICP-OES characterization

Digested samples were diluted 1:100 or 1:1000 (depending on the sampled aliquot) by a 1% HNO₃ solution in deionized water and analyzed by Inductively Coupled Plasma–Optical Emission Spectroscopy (ICP-OES) with a Perkin Elmer Optima DV 7000 with respect to 5-point calibration plots in the 0.01–10 ppm range for Co. Accuracy was tested by periodical measurement of standard solution samples.

The metal recovery was calculated using the following equation:

$$\text{Eq a}_1 \quad R(\%) = \frac{m_f}{m_i} \times 100$$

where: **R (%)** = metal recovery yield; **m_f** = mass (g) of Co extracted into the leaching solution, and **m_i** = mass (g) Co metal in the starting sample.

A7 Starbon® materials

1. Introduction

This work was performed at GCCE, University of York, UK.

Green Chemistry, which is one of the most important new aspects of chemistry, is defined by Anastas and Warner[1] as a chemical approach that reduce or eliminate the use and generation of hazardous substances in processes, and it is governed by 12 Principles as listed:[1]

- 1- Prevention: it is better to prevent waste than to treat or clean up waste after it has been created;
- 2- Atom Economy: synthetic methods should be designed to maximize the incorporation of all materials used in the process into the final product;
- 3- Less Hazardous Chemical Syntheses: wherever practicable, synthetic methods should be designed to use and generate substances that possess little or no toxicity to human health and the environment;
- 4- Designing Safer Chemicals: chemical products should be designed to affect their desired function while minimizing their toxicity;
- 5- Safer Solvents and Auxiliaries: the use of auxiliary substances (e.g., solvents, separation agents, etc.) should be made unnecessary wherever possible and innocuous when used;
- 6- Design for Energy Efficiency: energy requirements of chemical processes should be recognized for their environmental and economic impacts and should be minimized, conducting synthetic methods at ambient temperature and pressure where possible;
- 7- Use of Renewable Feedstocks: a raw material or feedstock should be renewable rather than depleting whenever technically and economically practicable;
- 8- Reduce Derivatives: unnecessary derivatization (use of blocking groups, protection/ de protection, temporary modification of physical/chemical processes) should be minimized or avoided if possible, because such steps require additional reagents and can generate waste.
- 9- Catalysis: catalytic reagents (as selective as possible) are superior to stoichiometric reagents;
- 10- Design for Degradation: chemical products should be designed so that at the end of their function they break down into innocuous degradation products and do not persist in the environment;

11- Real-time analysis for Pollution Prevention: analytical methodologies need to be further developed to allow for real-time, in process monitoring and control prior to the formation of hazardous substances.

12- Inherently Safer Chemistry for Accident Prevention: substances and the form of a substance used in a chemical process should be chosen to minimize the potential for chemical accidents, including releases, explosions, and fires.

Adoption of green chemistry practices and principles through the use of renewable feedstock can save the chemical industry \$65 billion by 2020.[2][3]

According to the 7 principle (Use of Renewable Feedstocks), waste material from plants or animals have attracted a great interest in view of their availability, inexpensive and sustainability.[4] Thus, Starch (HACS) is one of the most abundant renewable materials which can be easily available from many plants and has a naturally nano-channeled biopolymer structure which can be used as a template.[5] Starch is the major storage carbohydrate in higher plants; it is found primarily in the seeds of cereals and legumes, and in the tubers and roots of potato, yam and cassava.[6] It consists of two major components: amylose, a linear α (1-4) D-glucan polymer; and amylopectin, a branched α (1-4 and 1-6) D-glucan polymer.[6][7] It can be also a carbohydrate extracted from agricultural raw materials which is widely present in literally thousands of everyday food and non-food applications. The starch molecule consists of a large number of glucose units joined by glycosidic bonds. It is produced by all vegetables as an energy store. In Europe it is extracted almost exclusively from potatoes, wheat and maize.[8]

Recently, carbonaceous mesoporous materials (Starbon®) derived from waste polysaccharides (HACS) after carbonization from 100 to 800°C have been used for adsorption, in a low cost process requiring no templates or hazardous chemicals.[9] It is considered to be green and sustainable because it is made from renewable materials using a clean production process. Gracia A.M. *et al.*[9] demonstrated that Starbons® are effective materials for the selective adsorption and separation of metals.

However, in the literature, many analytical separation procedures have been described such as liquid extraction, supercritical fluids, microwave and solid phase extraction (SPE).[10] Among them, SPE seems the most interesting because homely, easy to use and not require any chemical interaction.[9][10]

Due to the diversity of this surface functional group, the expanded starch or Starbon® can be easily chemically modified.[11] Hence, the aim of this study is to synthesize a new material by

using a *soft/hard* donor ligands like dithiooxamide/oxamide to be supported on Starch/Starbons® as potential filter for selective extraction of cobalt from the leachate of hard metals (WC-Co) waste by means of solid phase extraction (SPE).

According to Shuttleworth *et al.*, [5] the synthesis of Starbon® is based on using expanded polysaccharides as precursor negating the need for a templating agent and the method of preparation comprises three key words as described on figure below.

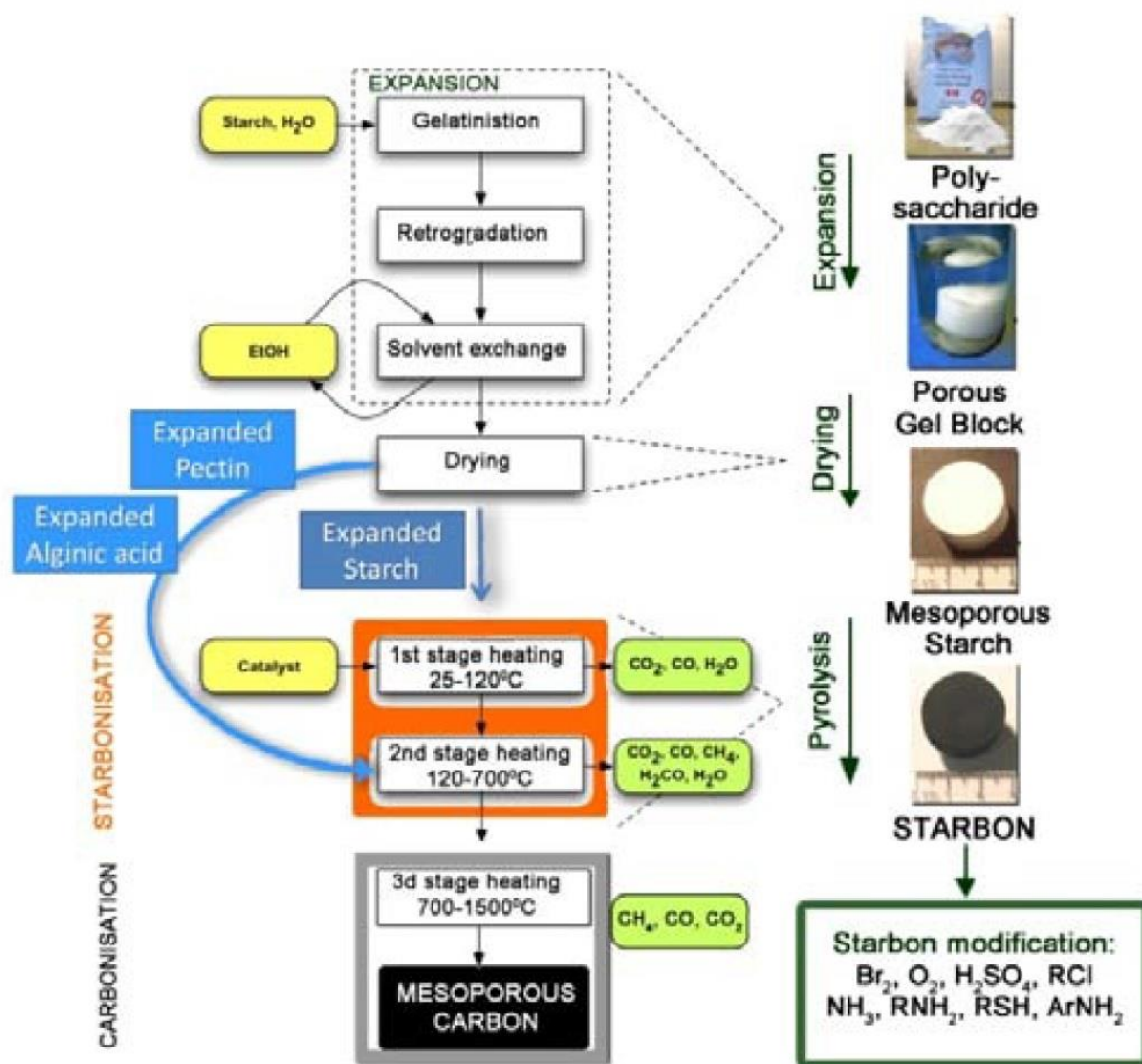


Figure 1: Method of Starbon preparation according to Shuttleworth *et al.* [5]

The principal methodology to produce our Starbon® comprises many different stages. Firstly, Starch (typically from high amylose corn starch) is gelatinized by heating in water under microwaves at a temperature of 45°C for 10 minutes [10g:70 mL (w/v) ratio per vessel]. The resulting viscous solution is cooled in the fridge to 5°C for typically two or three days to yield a porous gel for retrogradation. Then, the water in the gel is subsequently exchanged with the lower surface tension solvent *t*-butanol (30% wt). In the final stage the mesoporous starch is

doped with 5% of *p*-toluene sulfonic acid and dried by freeze-dried. The expanded starch was carbonized in a furnace at different temperatures (350, 400 and 800°C) to obtain a range of mesoporous materials with various surface functionalities (S350, S400 and S800, respectively). Figure 2 shows the occurrence of functional groups on Starbons® with the temperature and relative properties.

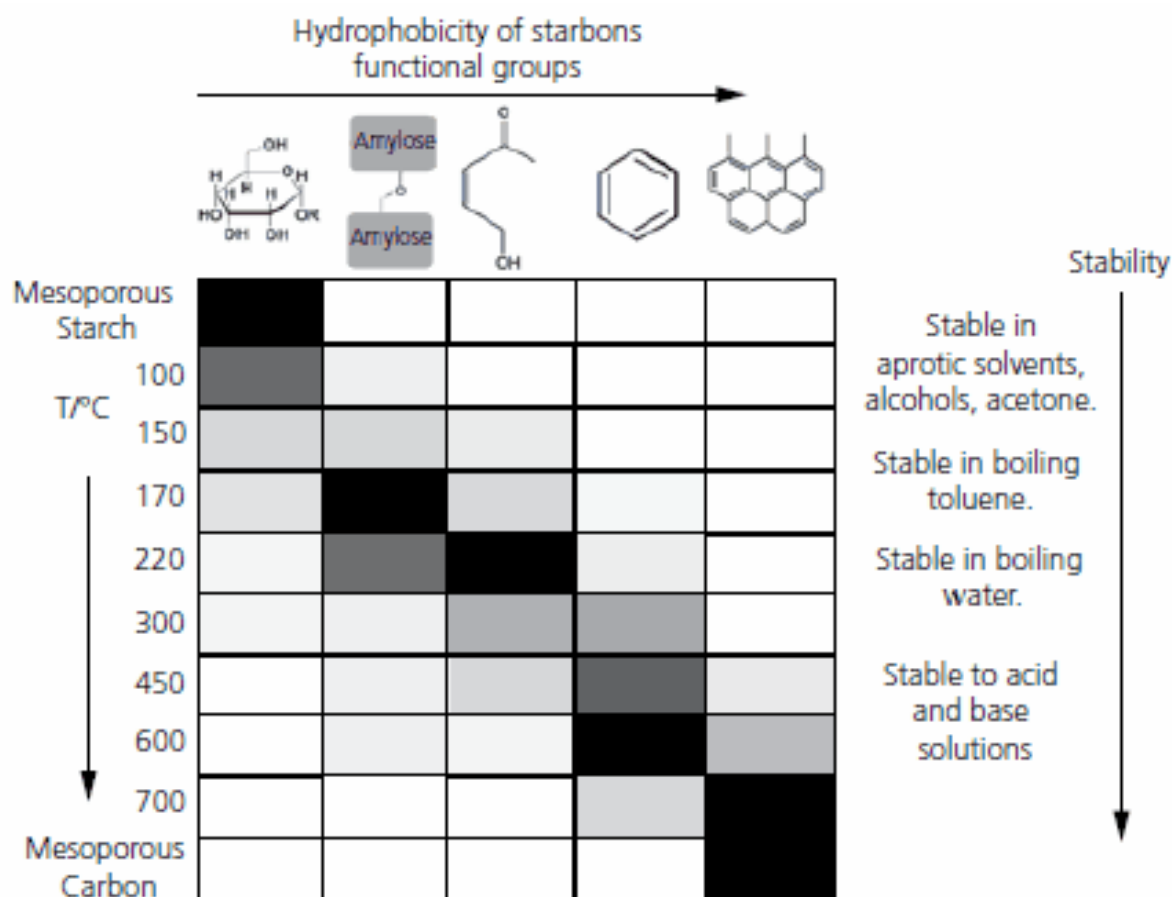


Figure 2: Functional groups occurrence in Starbons® under different thermal conditions as reported by Butarin et al. [5][12]

Starbon® 350 was employed in this study in order to try its functionalization using dithioamide and thiourea ligands. In a typical preparation, 2 g of dry Starbon was mixed together with 20 mL of ethanol and 0.5g of each *soft* sulfur donor organic molecules. Experiments were carried out at reflux (Δ , 78.4°C) for 48h under magnetic bar stirring. Under these conditions, when the reactions went on, the solutions turned from orange and uncolored for DTO and Tu experiments, respectively, to a light red, which suggested a reaction with Starbon occurred in both cases. After cooling, the solid products were collected from the mixture by centrifugation and washed several times with ethanol until the washing solution remained uncolored. The characterization of these solid products is still in progress.

2. Characterization of expanded starch and S350&400

FT-IR

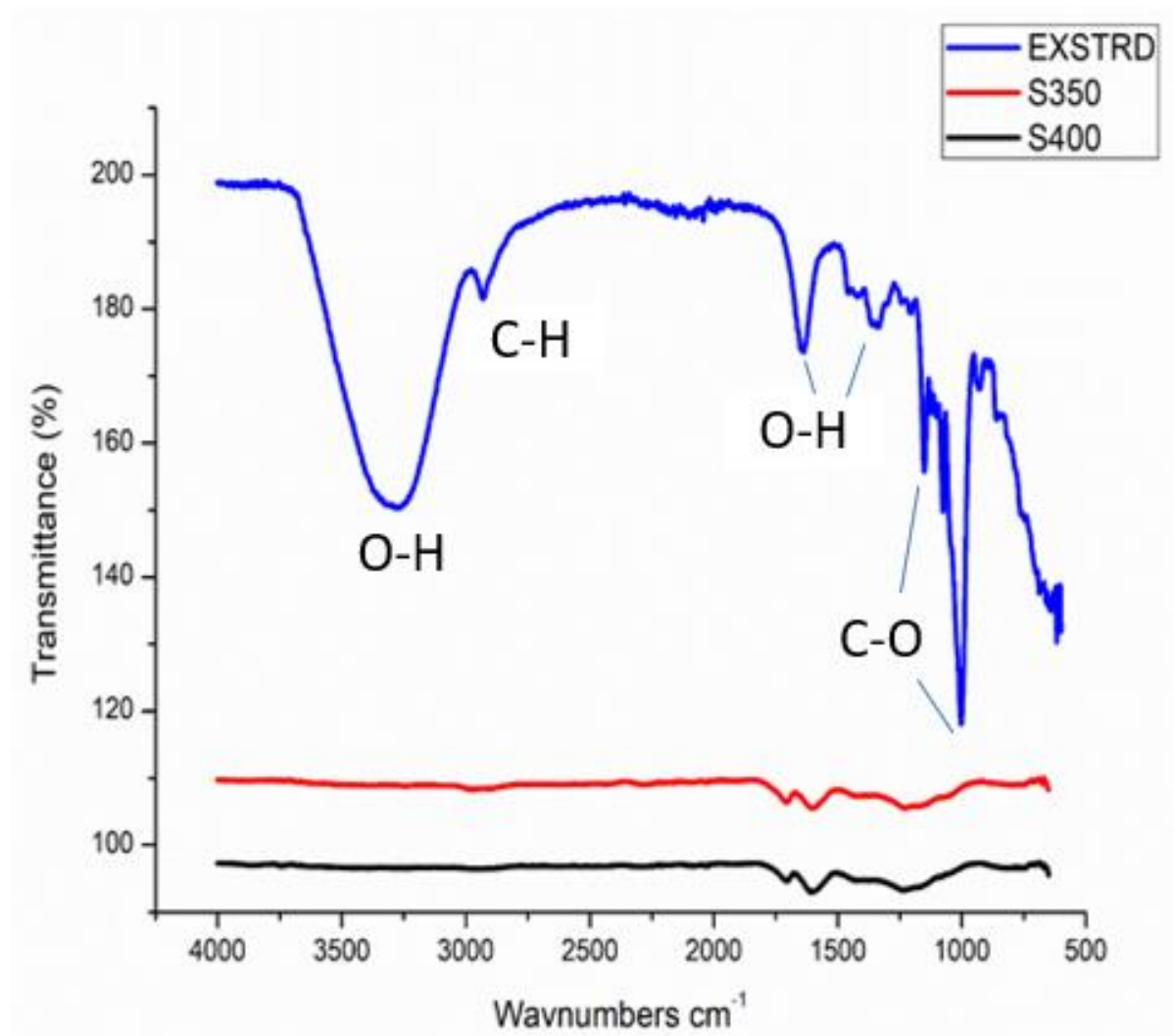


Figure 3: FT-IR OF EXPANDED STARCH, S350 and S400

The characteristic absorbance band centered at 3310cm^{-1} corresponds to O-H stretching vibration. The broadness of bands indicates strong hydrogen bonding. The characteristic peak at 2930cm^{-1} correspond to C-H symmetrical vibration stretching and the peak around 1625cm^{-1} is due to the water tightly bound to the starch. The Characteristic peak at 1150cm^{-1} correspond to C-O stretching vibration. The peak at 1000cm^{-1} correspond to bending and stretching in the expanded starch. The FT-IR spectrum of Starbon® 350&400 shows a narrow O-H stretching vibration centered around 3000cm^{-1} , followed by a carbonyl stretching vibration around 1700cm^{-1} . The characteristic peak around 1200cm^{-1} correspond to C=O stretching vibration.

Simultaneous Thermal Analysis

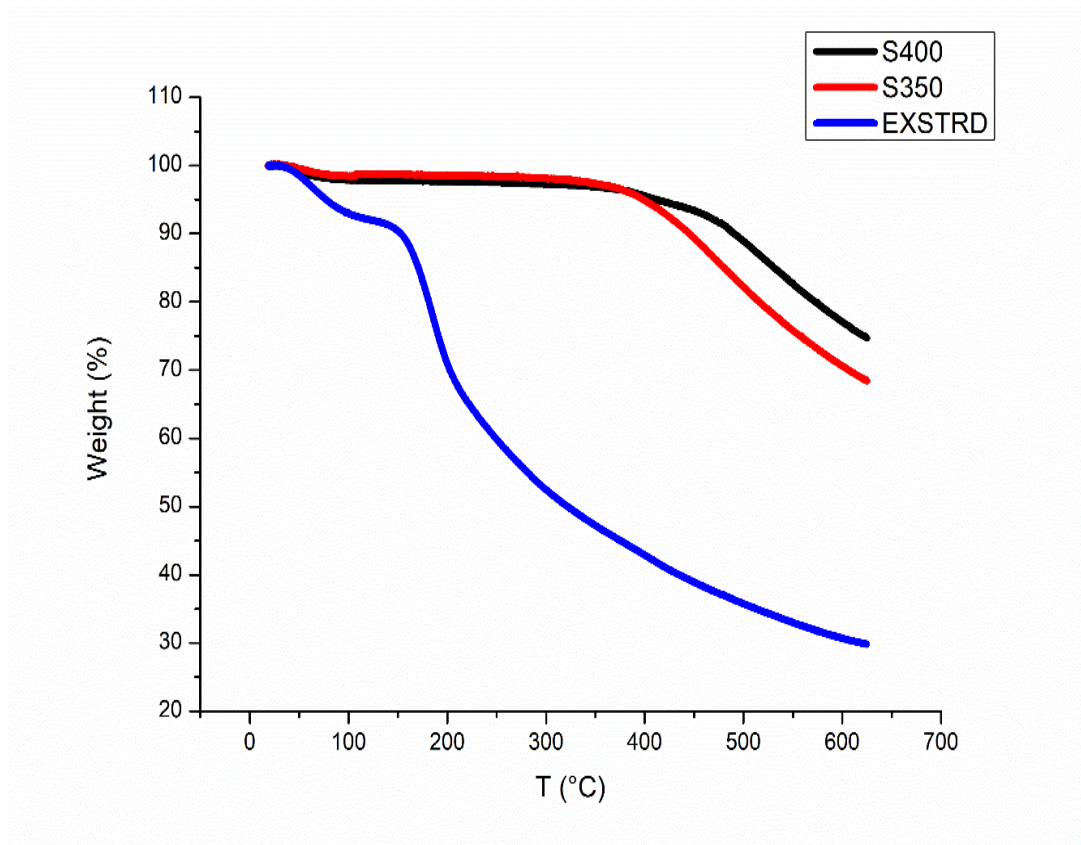


Figure 4: TGA OF EXPANDED STARCH & S350 & S400

The first decomposition stage which occurs at approximately 100°C is associated with loss of water, and any residual solvent in the expanded starch who known to contain approximately 10% bound water in its native state. The major decomposition corresponds to the breakdown of the expanded starch backbone and its point of inflection is around 200°C. The point of inflection who corresponds to the major mass loss temperature, signifying the breakdown of Starbon® is around 400°C.

¹³C NMR Solid state

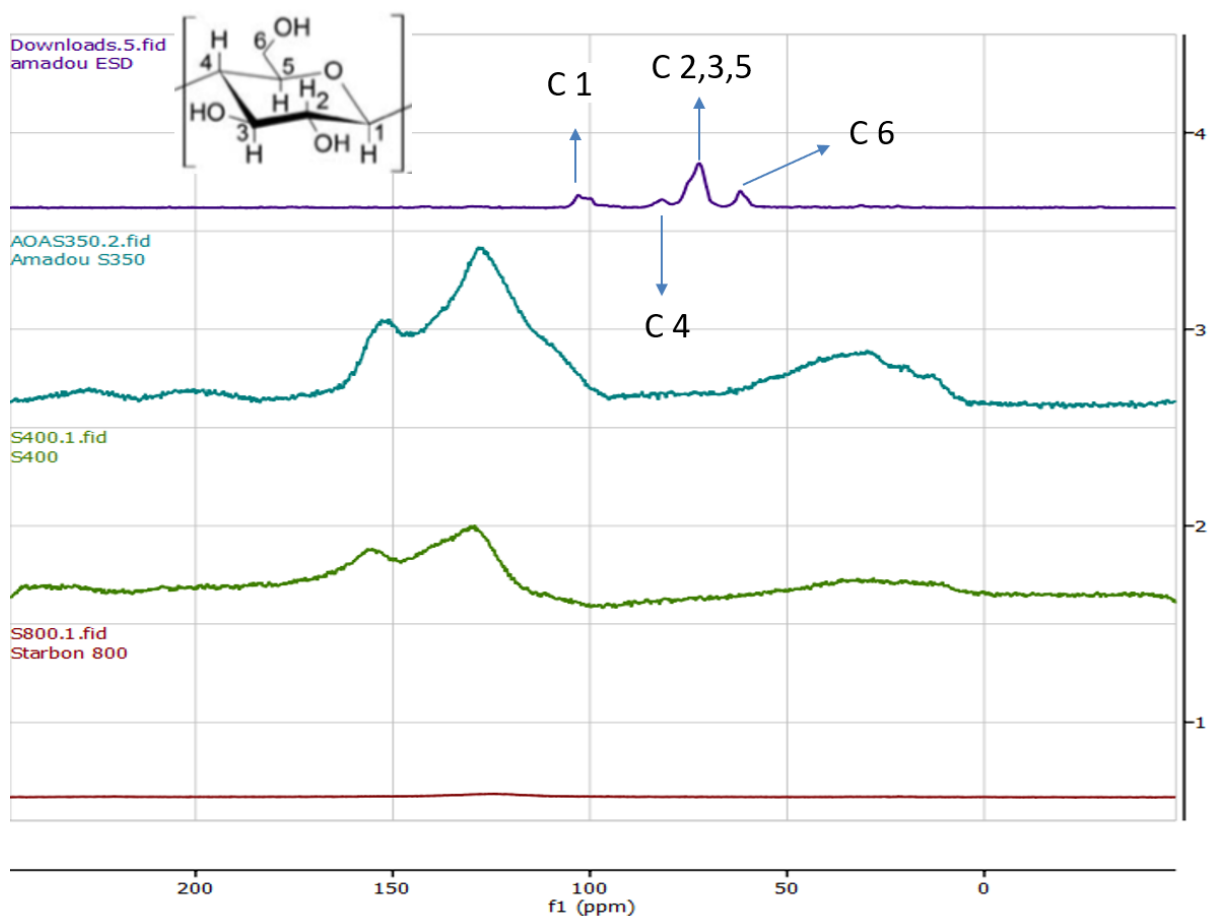


Figure 5: ¹³C CP-MAS NMR spectra of prepared Starbon®.

According to Warren et al,[13] the ¹³C CP-MAS NMR spectra of starch shows the differences in chemical shift displacements due to the change in the conformation of the glucan chain. The signals observed at 61.8, 82.1 and 101 ppm are attributed to C₆, C₄ and C₁ in expanded starch respectively. The signal around 72ppm is assigned to C₂, C₃, and C₅. [7]

3. Solid Phase Extraction (SPE)

The synthesized S350 was used for solid-phase extraction for the Co-containing leaching solutions. A series of diluted solutions (of 500, 400, 300, 200 and 100ppm) were prepared by starting from the leachates of lactic acid in water and maleic acid in ethanol, containing approximately 2000ppm of [Co(Lat)₂(H₂O)₂] and [Co(HMal)₂(H₂O)₄], respectively. These solutions were used for building a calibration plot by UV-Vis spectrometry in order to assess, by colorimetric method at the typical wavelength of absorption of the complex (around 518nm), the lowering of absorbance of a solution undergone S350 solid phase adsorption. On these bases

the absorbance at 518nm of the 500ppm solutions of the two leachates were recorded before and after being passed on to 100mg S350 packed layer in a solid phase extractor (Figure 6).

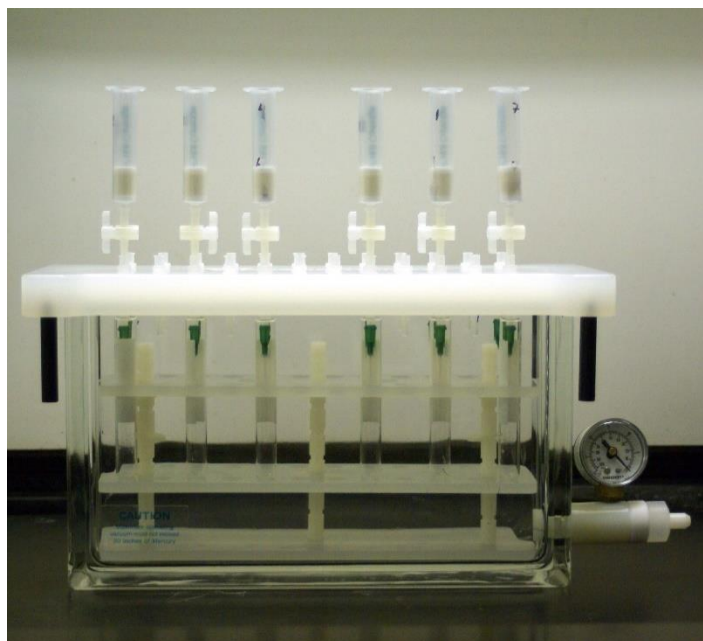


Figure 6: Solid-phase extraction apparatus.

UV-Vis measurements *vs* the calibration plot above, showed that, while no cobalt being extracted from H₂Mal ethanolic solution, about 10% of [Co(Lat)₂(H₂O)₂] was extracted from the HLat aqueous solution about 10% of cobalt in a single experiment.

4. SEM/EDS ANALYSIS S350 after SPE

In order to highlight the presence of the extracted cobalt on the Starbon® material, SEM/EDS measurements were performed on the dried powders after extraction. Unfortunately, the amount of extracted cobalt was below the detection limit of the technique, so no information can be extrapolated by this characterization.

Further experiments are required to clarify efficiency, rates and mechanism of extraction.

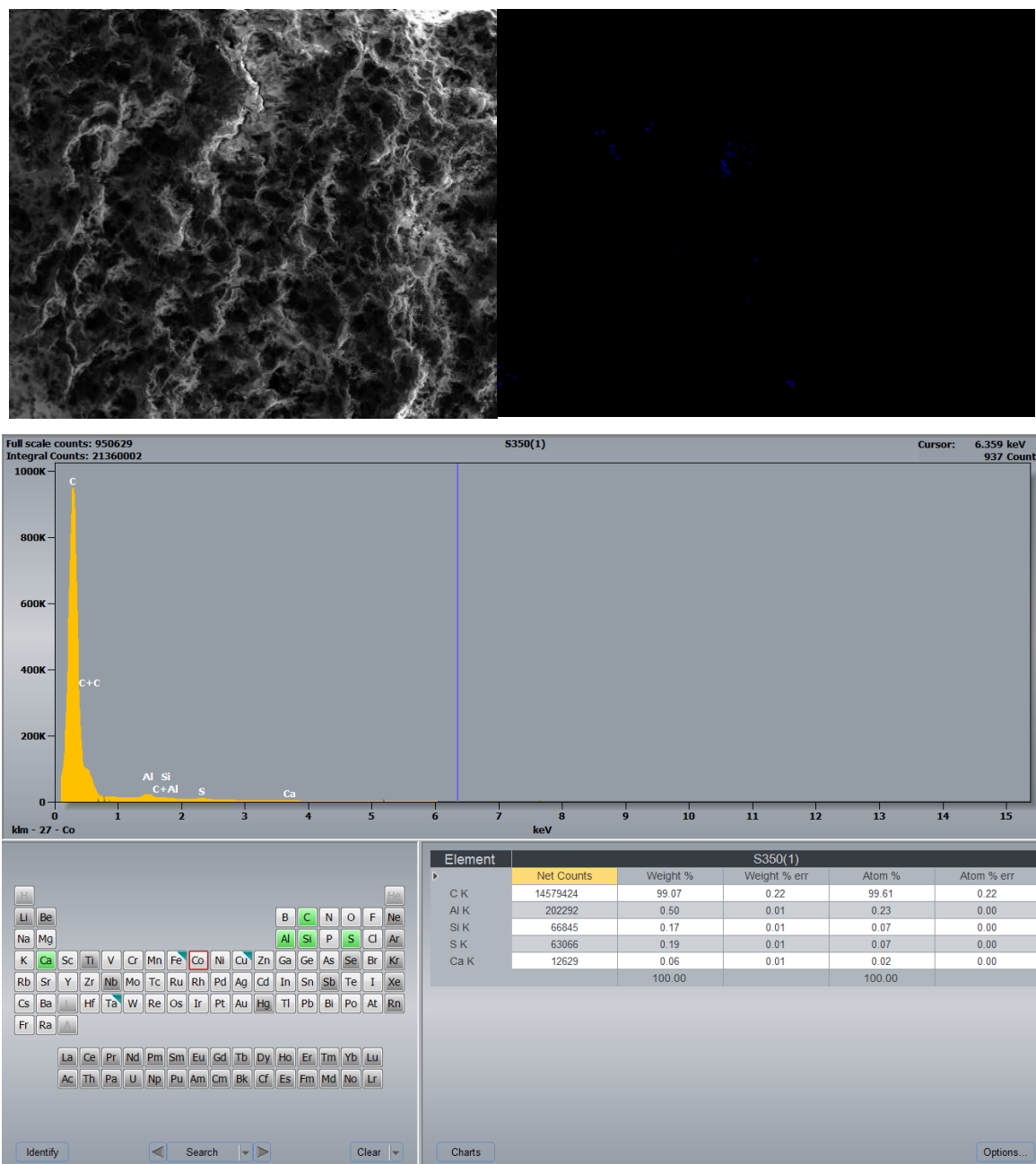


Figure 7: SEM/EDS characterization of S350 used as solid phase extractant for $[\text{Co}(\text{Lat})_2(\text{H}_2\text{O})_2]$ leaching solutions.

References

- [1] J. C. G. C. Theory, “12 Principles of Green Chemistry Design for Energy Efficiency Reduce Derivatives Catalysis Design for Degradation,” 1998.
- [2] R. Feedstocks, G. Polymers, and L. A. C. Formulations, “Industry Report,” vol. 7, no. 6, pp. 431–433, 2011.
- [3] S. Ahmed, “Synthesis, Characterisation and Catalytic Applications of Novel Iron N - Heterocyclic Carbenes immobilised on Renewable Resources,” no. January, 2018.

- [4] S. C. Zeeman, J. Kossmann, and A. M. Smith, “Starch : Its Metabolism , Evolution , and Biotechnological Modification in Plants,” 2010.
- [5] P. S. Shuttleworth *et al.*, “Starbon ® : Preparation , applications and transition from laboratory curiosity to scalable product,” vol. 3, pp. 766–769, 2011.
- [6] R. G. F. Visser and E. Jacobsen, “Towards modifying plants for altered starch content and composition,” vol. 11, no. February, pp. 63–68, 1993.
- [7] F. Zhu, “Food Hydrocolloids NMR spectroscopy of starch systems,” *Food Hydrocoll.*, vol. 63, pp. 611–624, 2017.
- [8] R. Luque, V. Budarin, P. S. Shuttleworth, S. National, and J. H. Clark, “A new star (ch) is born : Starbons ® as biomass-derived mesoporous carbonaceous materials,” no. June, 2012.
- [9] A. M. García *et al.*, “and recovery of critical metals †,” *Green Chem.*, vol. 17, pp. 2146–2149, 2015.
- [10] P. S. Shuttleworth *et al.*, “Polysaccharide-derived mesoporous materials (Starbon ®) for sustainable separation of complex mixtures †,” pp. 451–464, 2017.
- [11] A. S. Matharu, S. Ahmed, B. Almonthery, and D. J. Macquarrie, “Starbon / High-Amylose Corn Starch-Supported N-Heterocyclic Carbene – Iron (III) Catalyst for Conversion of Fructose into 5-Hydroxymethylfurfural,” no. Iii, pp. 716–725, 2018.
- [12] V. L. Budarin, J. H. Clark, R. Luque, and R. J. White, “Starbons®: Cooking up Nanostructured Mesoporous Materials,” *Mater. Matters*, vol. 4, no. 1, pp. 19–22, 2009.
- [13] F. J. Warren, M. J. Gidley, and B. M. Flanagan, “Infrared spectroscopy as a tool to characterise starch ordered structure — a joint FTIR – ATR , NMR , XRD and DSC study,” *Carbohydr. Polym.*, vol. 139, pp. 35–42, 2016.

A8 Dairy waste dark fermentation procedures

1. Cheese whey

The substrate used for the fermentation tests was cheese whey provided by the Sardinian dairy industry "Argiolas Formaggi" which produces cheese and ricotta from sheep's milk. The samples were stored at -15 °C until they were used, for preserving both chemical and biological properties. The tests were carried out without the addition of an external inoculum. Before the tests began, each substrate was characterized.

2. Fermentation tests

The fermentation tests were conducted in 'batch' mode in a glass reactor with a capacity of 2L (BIOFLO 110 - New Brunswick Scientific; BioCom-mand Lite software; 1.8L usable volume). The reactor is equipped with a mechanical stirrer (set at 200 rpm), a sensor for temperature control and a probe for automatic pH control with the addition of sodium hydroxide (NaOH 2.5 M).

The tests for hydrometallurgical leaching experiments were carried out in two steps: a first phase in which the pH is controlled and a subsequent phase in which it is carried out without pH control.

The ones addressed to solvometallurgy, were instead carried out in a single step of controlled pH at 6.

At the beginning of each fermentation test, nitrogen gas (N₂) was flushed for about 5 minutes to eliminate the air present in the head space and ensure anaerobic conditions, while to avoid photo-fermentation phenomena the reactor was covered with a black plastic film.

The fermented substrates were stored at -15°C and, if necessary, were defrosted for leaching tests, after characterization.

3. Analytical methods.

Samples were analyzed after filtering at 0.45 µm.

3.1 Carbohydrate analysis

Soluble carbohydrates (sCARBO, measured on the filtered sample at 0.45 µm) were evaluated using the Dubois method which involves adding 1 mL sample solution to 1 mL of phenol

solution (5%) and 5 mL of concentrated sulfuric acid; a lactose solution was used as standard. After 20 minutes, the concentration was estimated with the Hach Lange spectrophotometer, model DR 2800, with a wavelength of 490 nm.

3.2 Lactic acid analysis

Lactic acid was determined by indirect spectrophotometric method, based on the quantitative measurement of the absorbance at 390 nm of the complex $[\text{Fe}(\text{Lat})_3]$ obtained by reaction between the lactic acid itself and an aqueous Fe(III) nitrate solution.

A calibration curve between 0.5 and 11 gL⁻¹ was constructed by suitably mixing aliquots of pure lactic acid with an aqueous solution of FeNO₃·6H₂O 0.2%, adapting the Borshchevskaya method (Borshchevskaya et al., 2016). The determination of the lactic acid concentration in the unknown concentration solutions was made by comparing the absorbance at 390 nm recorded on the test sample (previously prepared by dilution to meet concentration requirements of the method and mixing 50 μL of the diluted solution with 2 mL of 0.2% solution of Fe(III) nitrate) and the calibration curve.

References:

Borshchevskaya L. N., Gordeeva T. L., Kalinina A.N., Sineokii S.P. 2016. "Spectrophotometric Determination of Lactic Acid" State Research Institute of Genetics and Selection of Industrial Microorganisms, Pervyi Dorozhnyi proezd 1, Moscow, 117545 Russia.

La borsa di dottorato è stata cofinanziata con risorse del
Programma Operativo Nazionale Ricerca e Innovazione 2014-2020 (CCI 2014IT16M2OP005),
Fondo Sociale Europeo, Azione I.1 "Dottorati Innovativi con caratterizzazione Industriale"



UNIONE EUROPEA
Fondo Sociale Europeo



the attached format.